Verres et propriétés optiques en milieu radiatif

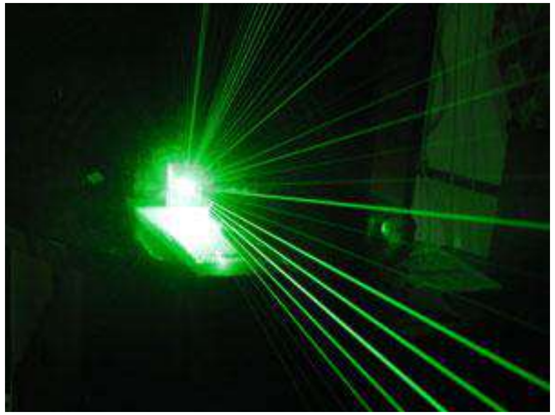

Ollier Nadège

Laboratoire des Solides Irradiés Ecole polytechnique, Palaiseau France
nadege.ollier@polytechnique.edu

Verres en milieu radiatif

Nuclear, medical applications

HLW storage glass
Glass fiber: sensor…
Dosimeters, radiation shielding

Space applications

Optical fibers

Glass structuring

Ion, electron beams
UV, fs laser

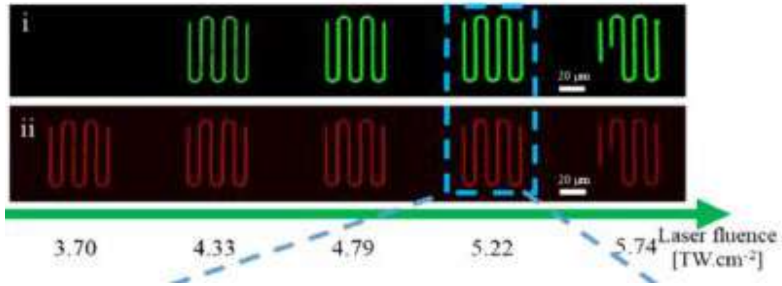

Alassani et al J Phys Chem C 2024

- **Introduction**
  - Quelques éléments sur la tenue du verre nucléaire face aux radiations
  - interaction rayonnement matière
- **Verres pour l'optique** en milieu radiatif
  - **Défauts ponctuels**
  - **Impact des défauts sur les propriétés des verres**
    - Couleur
    - RIA
    - Radiodarkening/Photodarkening
    - Propriétés de luminescence
  - **Evolution de la densité sous irradiation (le cas de la silice)**
    - Tenue des fibres à réseaux de Bragg sous irradiation

Verres nucléaires

Verres simplifiés 4-6 oxydes

oxydes	%
SiO_2	45.12
Al_2O_3	4.87
B_2O_3	13.92
Na_2O	9.78
CaO	4.01
ZnO	2.48
Li_2O	1.97
Fe_2O_3	2.89
P_2O_5	0.28
NiO	0.41
Cr_2O_3	0.5
ZrO_2	0.99
FP	10.35
Act.	0.89
Plati.	1.54

Produits de fission

Se
Rb
Sr
Y
Zr
Nb
Mo
Tc
Ag
Cd
Ln
Sn
Sb
Te
Cs
Ba
La
Ce
Pr
Nd
Pm
Sm
Eu
Gd
Tb
Dy

Actinides

U
Pu
Np
Am
Cm

Platinoides

Ru
Rh
Pd

Verres aluminoborosilicates

- Combustible irradié
  - Stockage en piscine / entreposage (4-5 ans)
  - traitement (procédé PUREX) séparation U/Pu du reste

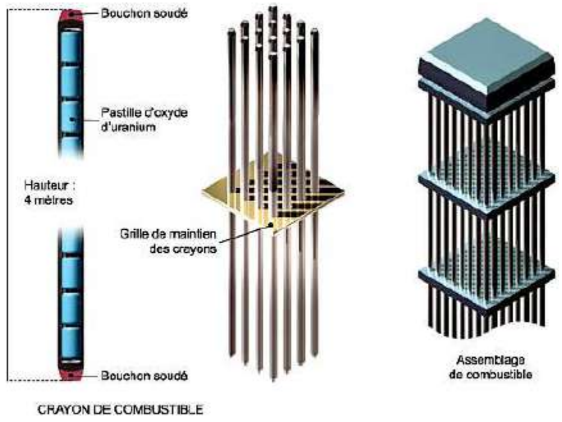

- Obtention d'une « solution de PF »
- Vitrification de la solution de PF
- Entreposage des colis

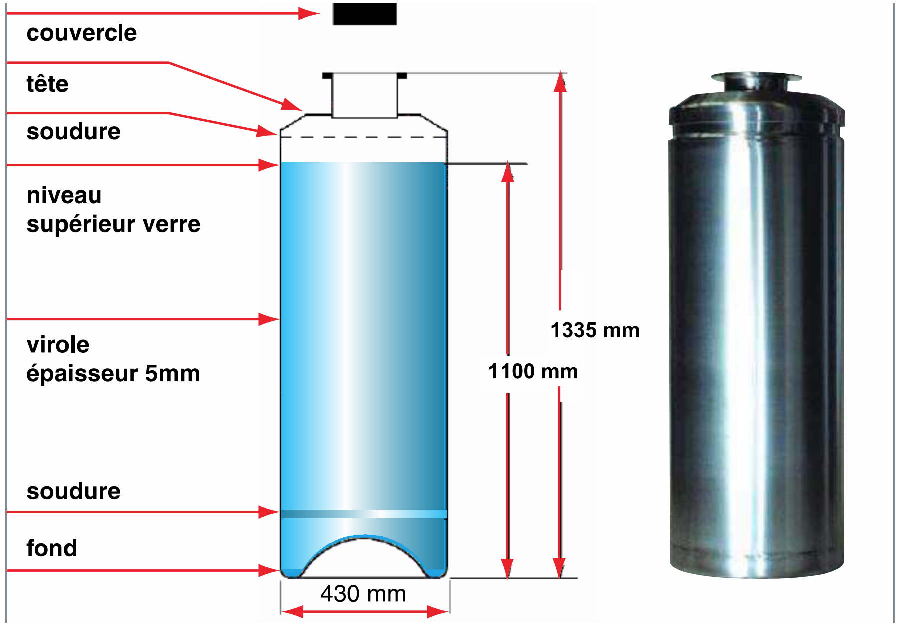

@cea

Fig. 24. L'entreposage des verres à Marcoule et La Hague.

400 kg verre
500-700 litres de PF
1 tonne de combustible irradié

Autoirradiation dans les verres nucléaires

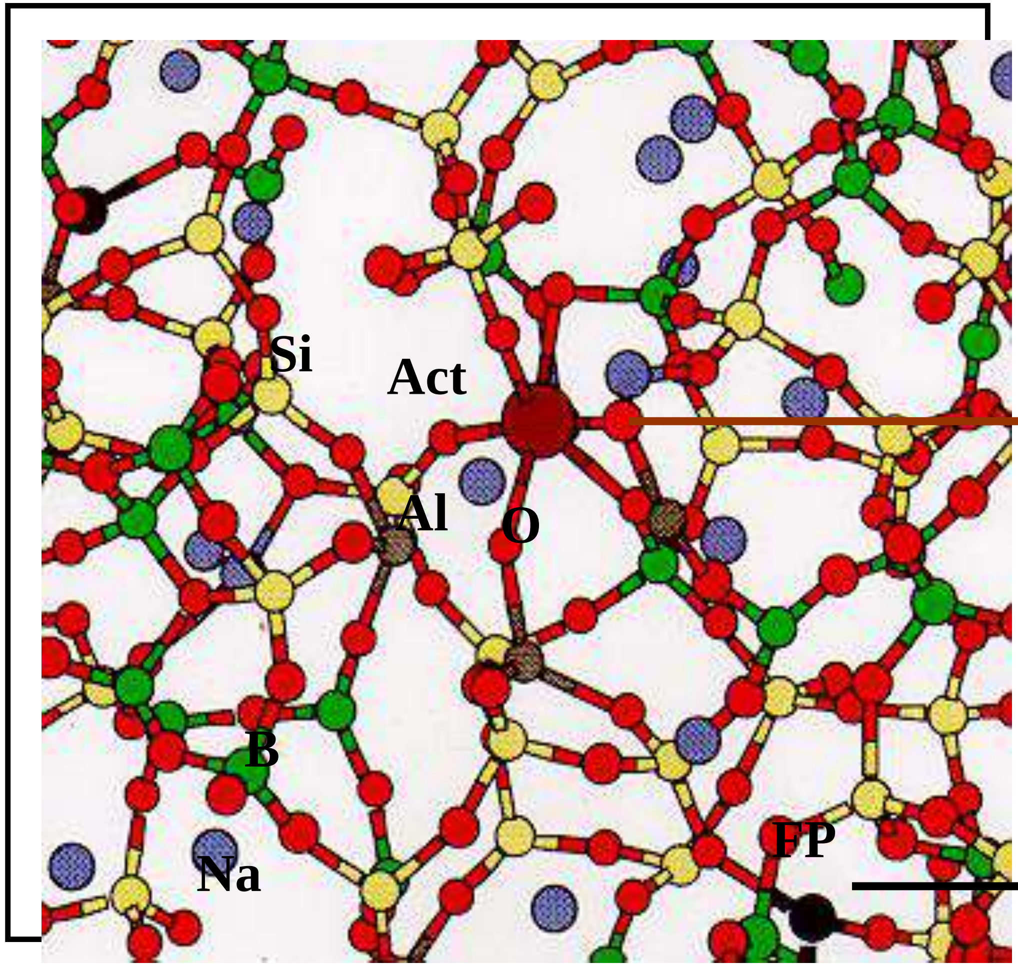

- $\alpha_{-\gamma}$ (Am, Cm , U, Pu, Np, ...)
  - T : Plusieurs milliers d'années
  - Importante à long terme

- $\beta_{-\gamma}$ (PF ^{137}Cs, ^{90}Sr)
  - T = ~ 30 years
  - Prédominance durant les 500 premières années

^{137}Cs emits beta particles of ~514 keV (94%) and ~1.17 MeV (5.6%) and a gamma particle of about ~661 keV mainly. Similarly, ^{90}Sr and ^{90}Y mainly emit beta particles of ~546 keV and ~2.3 MeV respectively.

Désintégration α

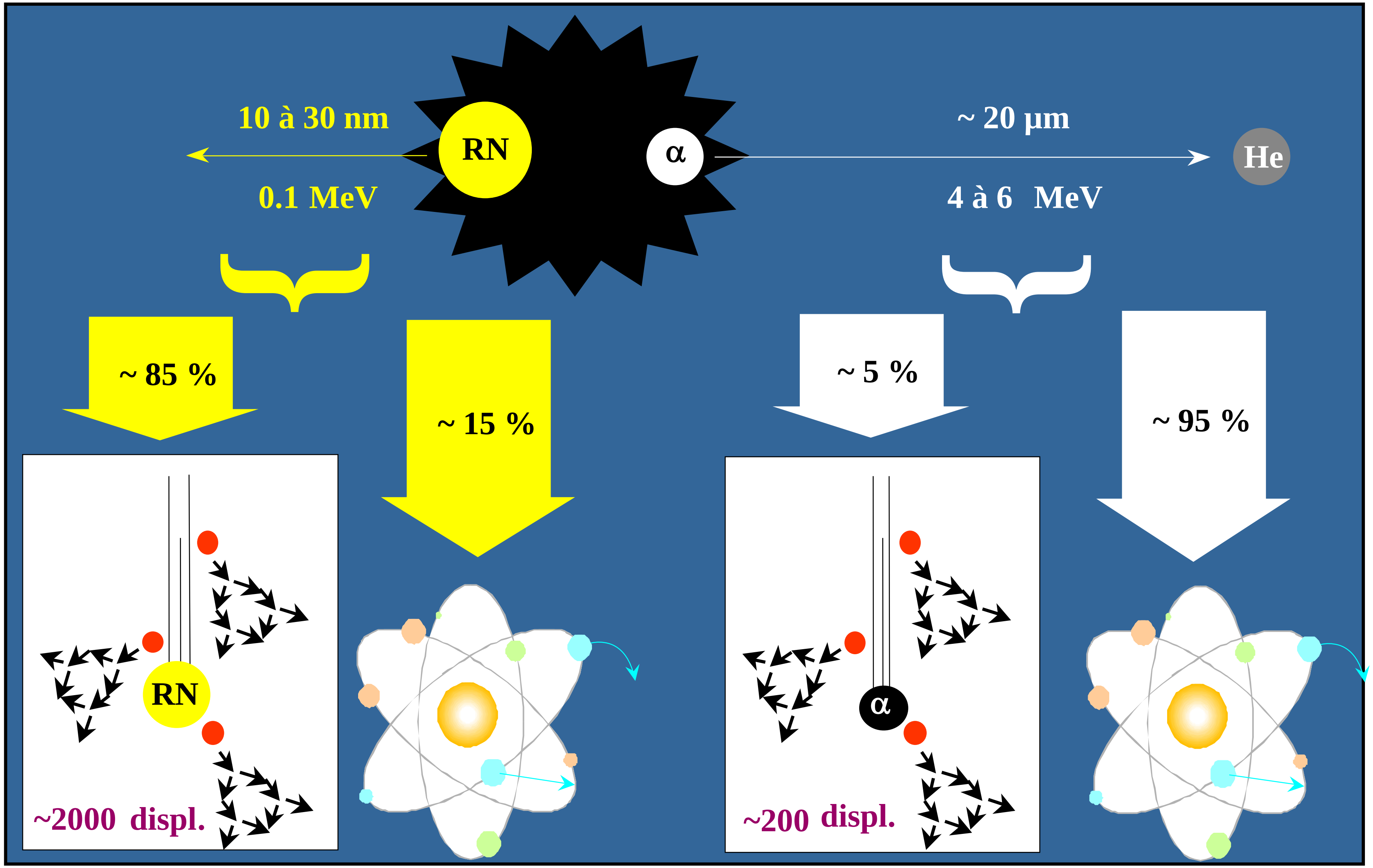

- **Alpha particles** on average lose about 0.2 keV nm^{-1} whereas the beta particles only lose about 10^{-3} times this. **Alpha particles therefore cause more intense ionization compared to electrons**. A typical alpha particle will travel about 25 µm in the glass waste form causing about 200 atomic displacements (**~8 displacements per micrometer**).
- Recoil nuclei due to their large mass, only have energy in the range of 80–120 keV and will interact mainly through elastic interaction (nuclear collisions). They will travel up to about 40 nm causing about 1600 atomic displacements (**$\sim 4 \times 10^4$ displacements per micrometer**).

A. H. Mir, S. Peuget, Journal of Nuclear Materials, Volume 539, 2020,

Désintégration βγ

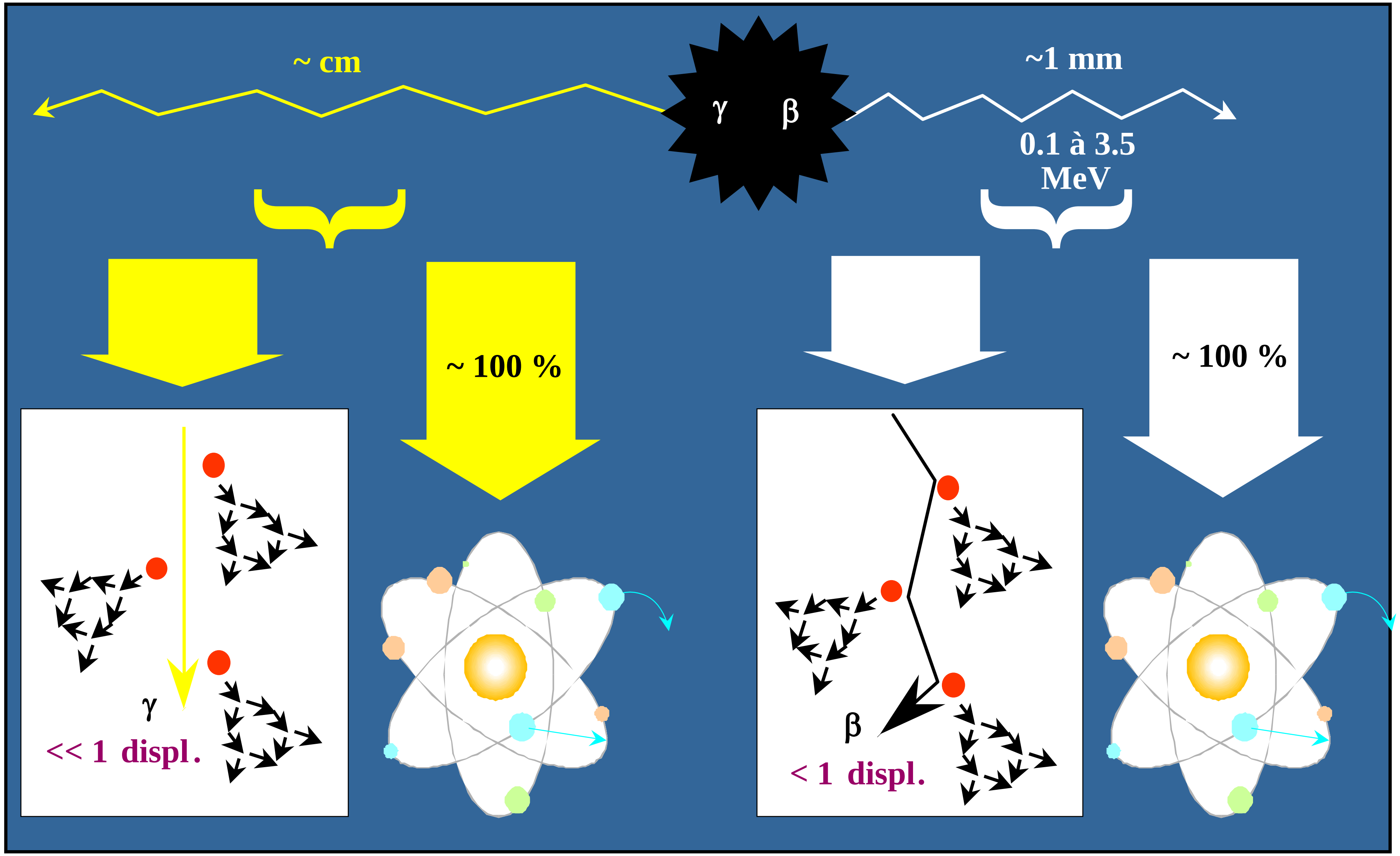

The energy of the gamma particles is mostly in the range of **few hundreds of keV**. **Compton scattering**, in which a gamma particle ejects an electron from the target atom, is the dominant interaction mechanism in this energy range. A gamma particle of 661 keV can transfer a maximum of about 472 keV to the electron and this Compton electron can then take part in further ionization and atomic displacements as a typical electron would**. Therefore, gamma particles indirectly cause the same or similar damage as the beta particles do**.

However, the Compton scattering cross-sections are significantly smaller. 10^{-2} to 10^{-3} times the electron displacement cross-sections (which is $\sim 10^{-23}$ cm^2**). Therefore, the effect of the gamma particle irradiation is essentially similar to the effects of the beta particles of few hundred keV except that the cross-section is significantly small.** For all practical reasons, **the direct atomic displacements from gamma particles can be completely ignored and their ionization effects can essentially be simulated using electrons of few hundreds of keV.**

A. H. Mir, S. Peuget, Journal of Nuclear Materials, Volume 539, 2020,

- Les **neutrons** sont des particules neutres → pas d'interactions coulombiennes comme les particules chargées
- Les neutrons ne vont interagir qu'avec les noyaux via les forces nucléaires → les sections efficaces sont faibles → les neutrons sont des particules très pénétrantes
- **les neutrons sont des particules indirectement ionisantes comme les photons → ils peuvent produire des particules secondaires chargées qui sont directement ionisantes**

2 types d'interactions :

1.Diffusion: Modification de l'énergie et de la trajectoire du neutron mais le noyau conserve un nombre de protons et de neutrons identique

2.Absorption: Modification du noyau cible → émission de rayonnements secondaires

Evolution du verre nucléaire sous désintégration alpha

Verres actifs dopés Cm, DM, irradiations externes ions

Several actinide doping studies have addressed the changes occurring in the mechanical properties (hardness, elastic moduli, fracture toughness), density, stored energy and, structure as a result of the alpha decays.

- Maximum density changes of about ±1% (swelling or densification)
- Hardness and elastic modulus decrease and finally saturate with alpha decay accumulation of about 2×10^{18} to 5×10^{18} alpha decays per gram (nuclear dose of about 3×10^{20} to 7×10^{20} keV cm^{-3}).

Owing to the large number of atomic displacements induced by the recoil nuclei, **it is assumed that nuclear collisions (NC) mainly control the damage formation**. **The role of alpha particles in damage accumulation is believed to be negligible.**

Furthermore, Molecular dynamics (MD) simulations of simple borosilicate glasses subjected to displacement cascades have shown that NCs result **in swelling, modulus decrease, boron coordination change (transformation of BO_4 to BO_3) and network depolymerization -** all of which tend to saturation after about 4×10^{20} keV cm^{-3} (~26 MGy ~ 6 eV/atom) in good agreement with actinide doping studies**.**

Besides these studies, which essentially deal with the effects of homogenous self-irradiation, more recent work on the effects of i**nhomogeneous self-irradiation** (due to nonuniform radionuclide distribution) has provided some new and important insights , **It has been shown that electrostatic charging of waste inclusions can generate high enough fields that can lead to local discharges and fractures/cracks.**

A. H. Mir, S. Peuget, Journal of Nuclear Materials, Volume 539, 2020,

Désintégration beta: formation de défauts ponctuels

Doses > GGy: Evolutions structurales augmentation de polymerisation du verre, BO4/BO3, formation d’O2…..

Verres de protection antiradiation

Radiation Physics and Chemistry 220 (2024) 111701

ELSEVIER

Contents lists available at ScienceDirect

Radiation Physics and Chemistry

journal homepage: www.elsevier.com/locate/radphyschem

Recent developments in radiation shielding glass studies: A mini-review on various glass types

Recep Kurtulus

Afyon Kocatepe University, Faculty of Engineering, Department of Materials Science and Engineering, Afyonkarahisar, Turkiye

Médical, nucléaire

RD 30® et RD 50® Schott

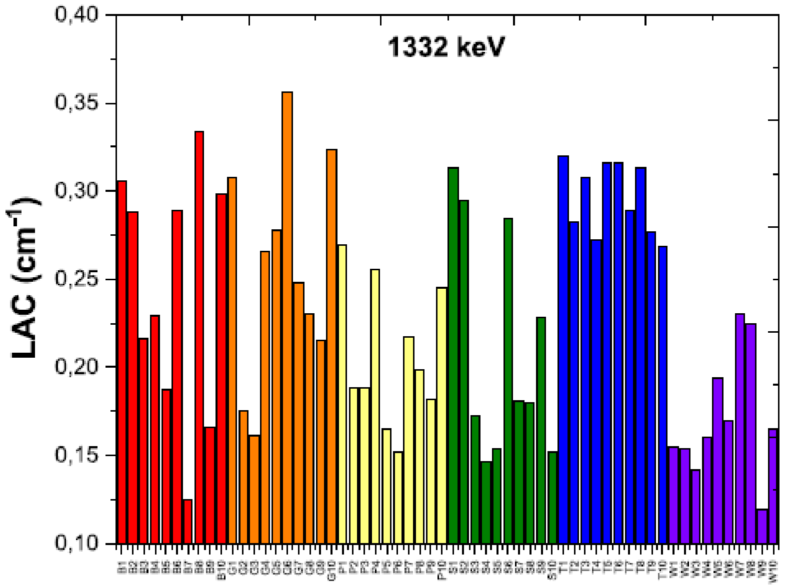

Fig. 6. Linear attenuation coefficient of the glass studies at 1332 keV photon energy.

Borates, germanates, tellures, phosphates « de déchets » BS,
Densité élevée > 3
En évitant Pb – Bi ?

Verres: applications pour l'optique

Silice
Verres phosphates (milieux amplificateur laser puissance)
Verres dopés TR (laser, amplificateurs Er/Yb…)
Tellures, chalcogénures, fluorés (IR)

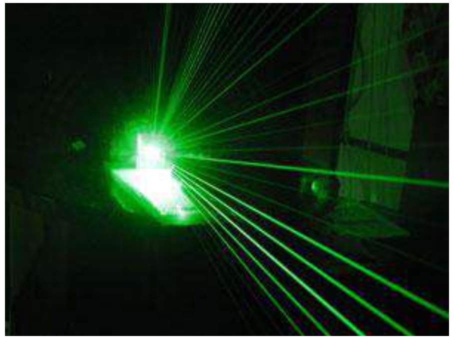

Lasers de forte puissance

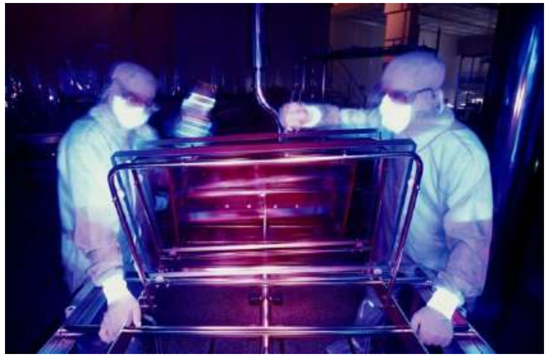

Neutrons
Ions
Electrons
Rayons gamma

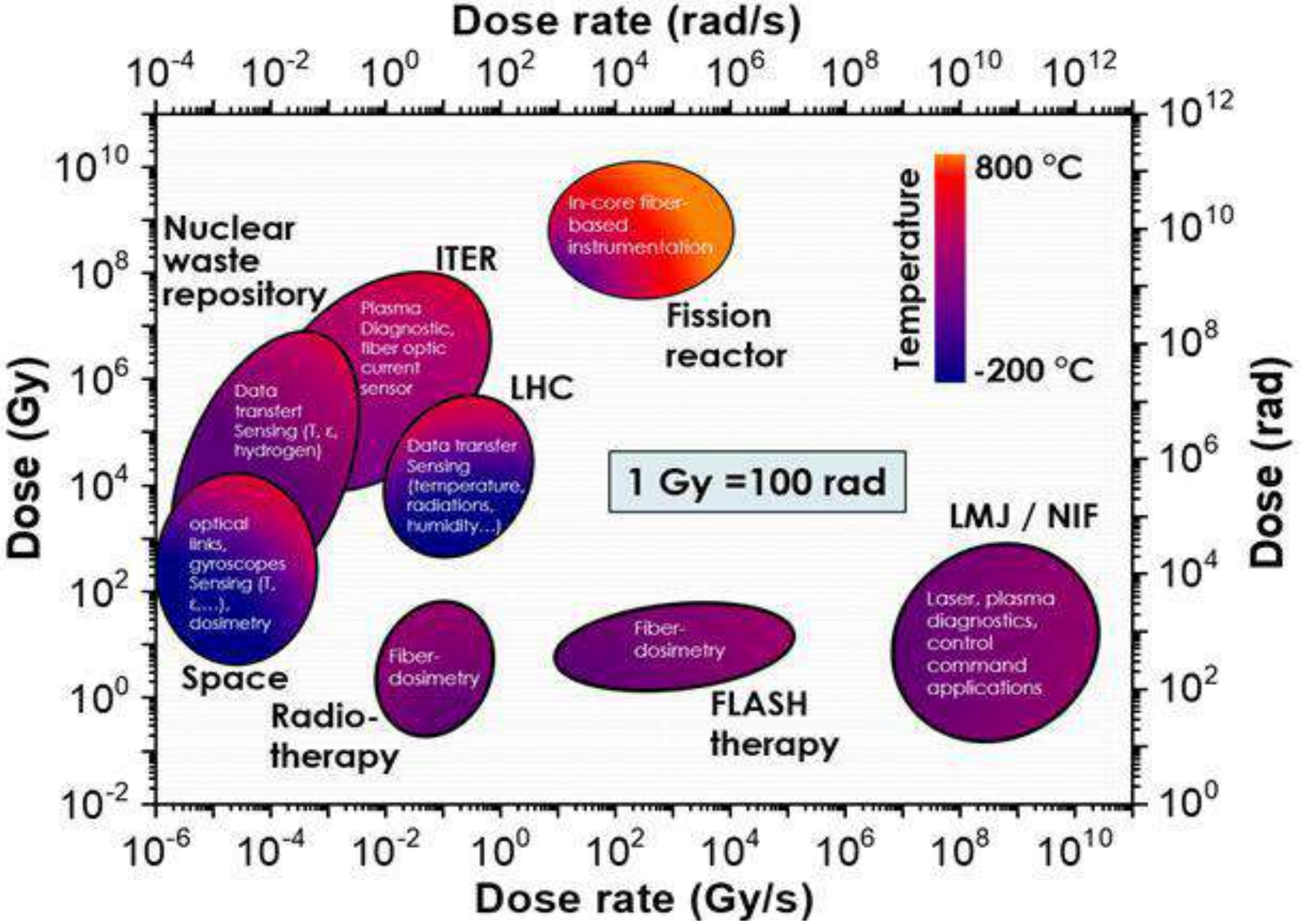

Espace :
89% of protons, 10% of alpha particles and 1% of heavy nuclei

S Girard et al IEEE TRANS. NUCL. SCI. 2024

Properties of silica glass

Two-dimentional silica film

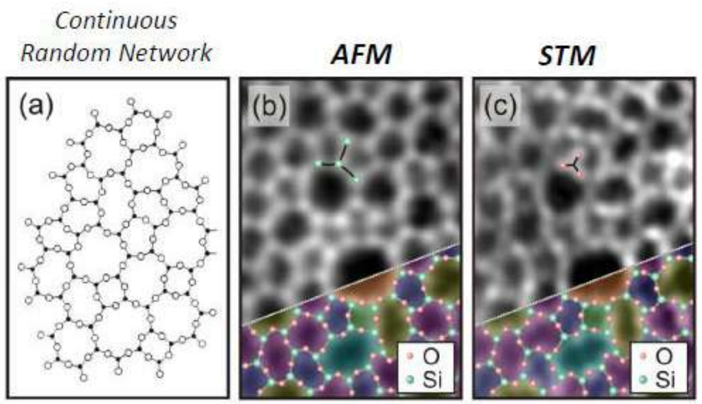

Zachariasen, *JACS* 1932.

Lichtenstein et al., *Angew. Chem.* 2012, *J. Phys. Chem.* C 2012, *Phys. Rev. Lett.* 2012.

- Ultra-transparency in the optical range UV-NIR
- Low thermal expansion
- High mechanical resistance
- Chemical durability

- **Silica-based optical components**: fibers for communications, laser fibers, FBGs sensors, UV optics

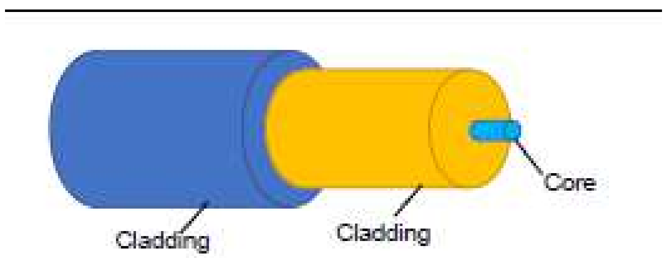

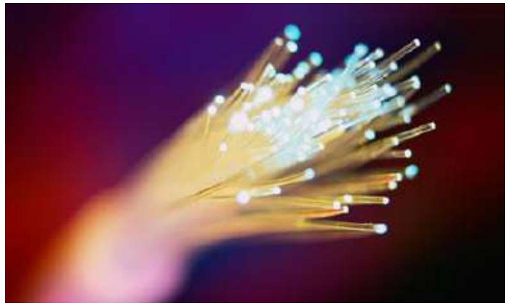

Formation de défauts ponctuels

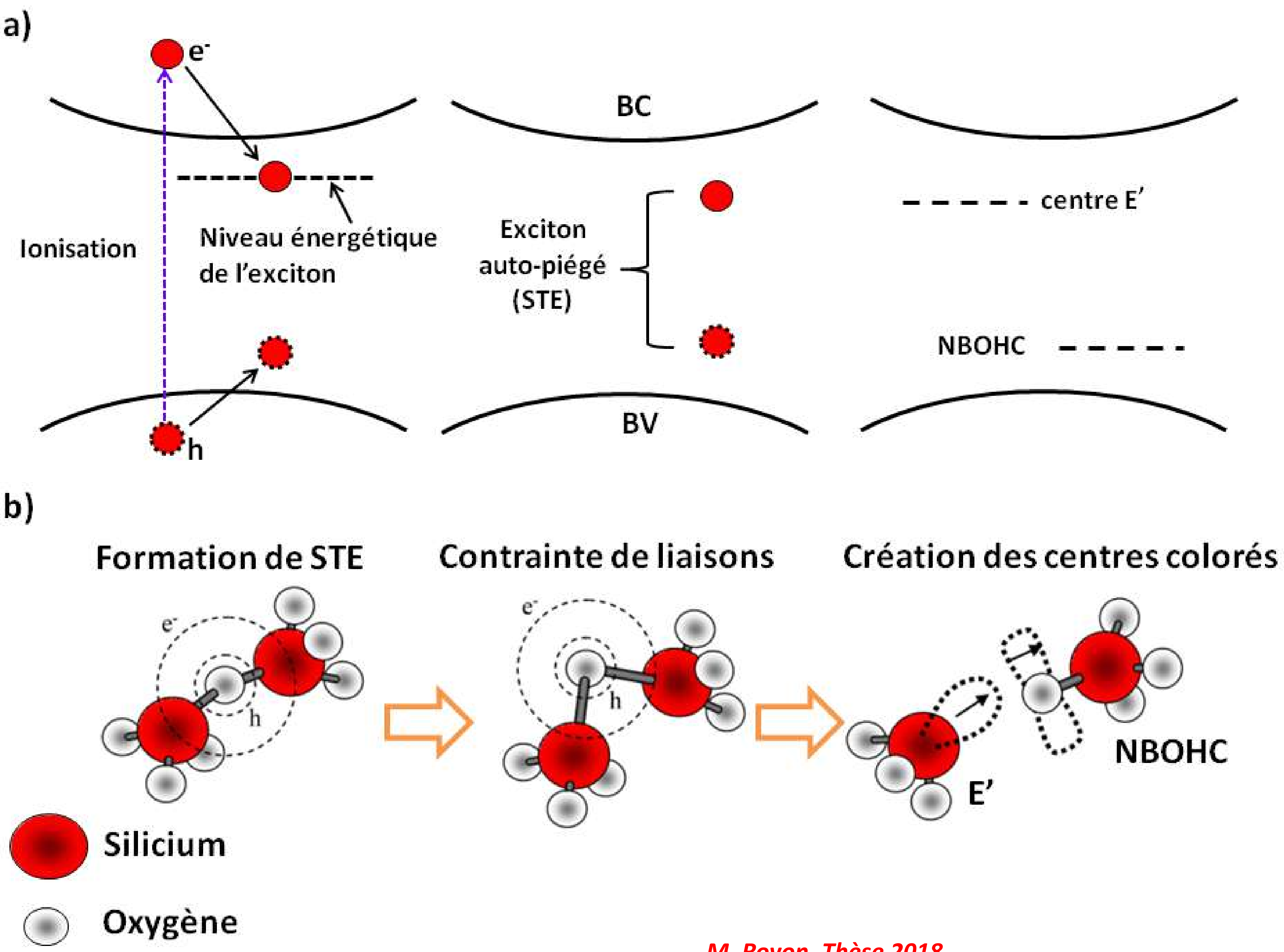

M. Royon, Thèse 2018

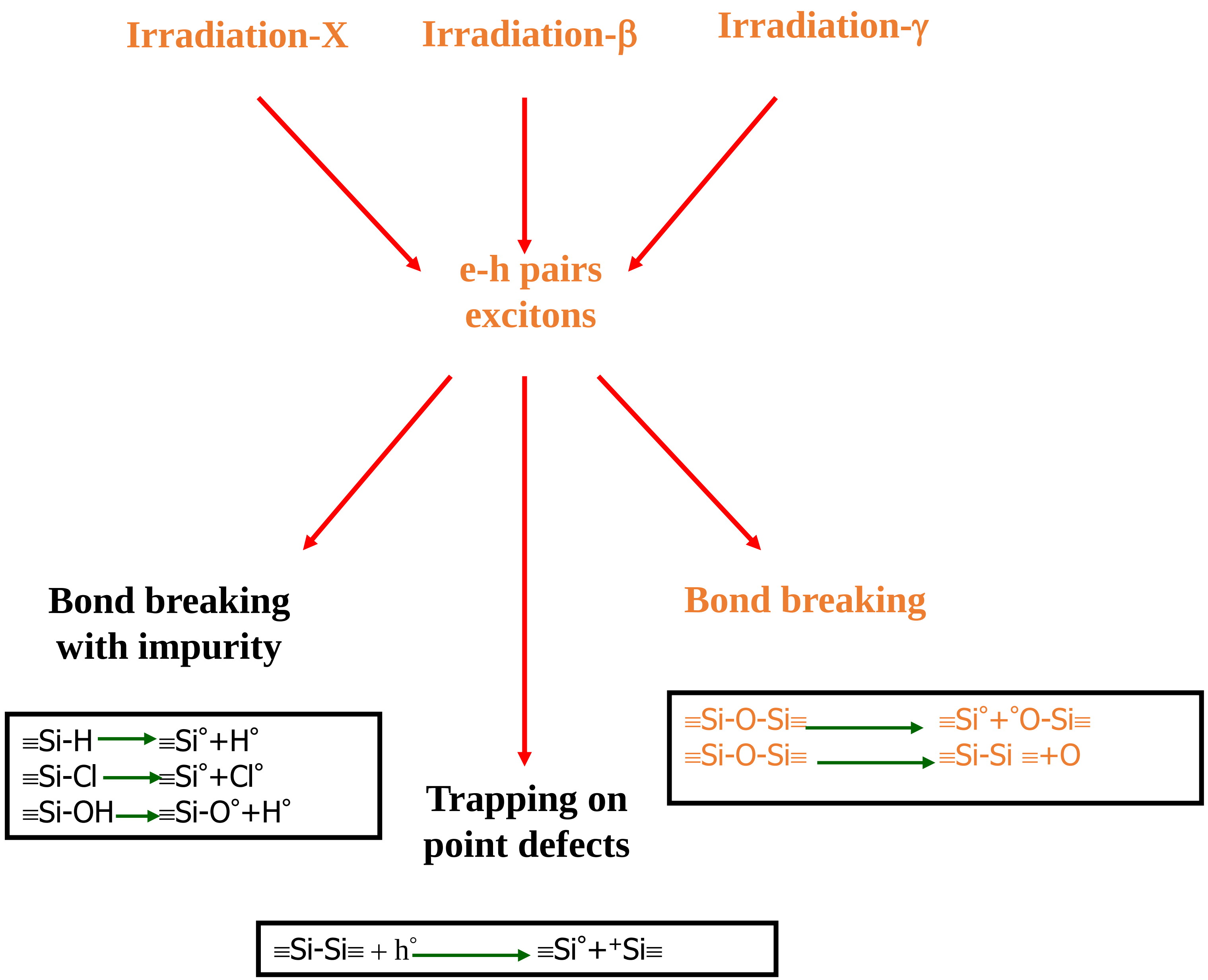
Irradiation-X
Irradiation-β
Irradiation-γ
e-h pairs
excitons
Bond breaking
with impurity
≡Si-H → ≡Si°+H°
≡Si-Cl → ≡Si°+Cl°
≡Si-OH → ≡Si-O°+H°
Trapping on
point defects
≡Si-Si≡ + h° → ≡Si°+⁺Si≡
Bond breaking
≡Si-O-Si≡ → ≡Si°+°O-Si≡
≡Si-O-Si≡ → ≡Si-Si ≡+O

Centre	Defect	Precursor
ODC Oxygen Deficient Center	≡Si-Si≡	≡Si-O-Si≡
E'	$\equiv Si^{-}$	≡Si-Si≡ ≡Si-O-Si≡ ≡Si-H ≡Si-Cl ≡Si-OH
NBOHC	≡Si-O°	≡Si-OH ≡Si-O-Si≡
POR Peroxy radicals	≡Si-O-O°	$\equiv Si^{-}$ ≡Si-O-O-Si≡
STH (self trapped hole)	≡Si-O°-Si≡ ≡Si-O-°O-Si≡	

Methods to characterize point defects

- Optical absorption (quantification)
- Photoluminescence
- **RPE: Résonance Paramagnétique Electronique (identification et quantification)**

Absorption and emission of point defects in silica glass

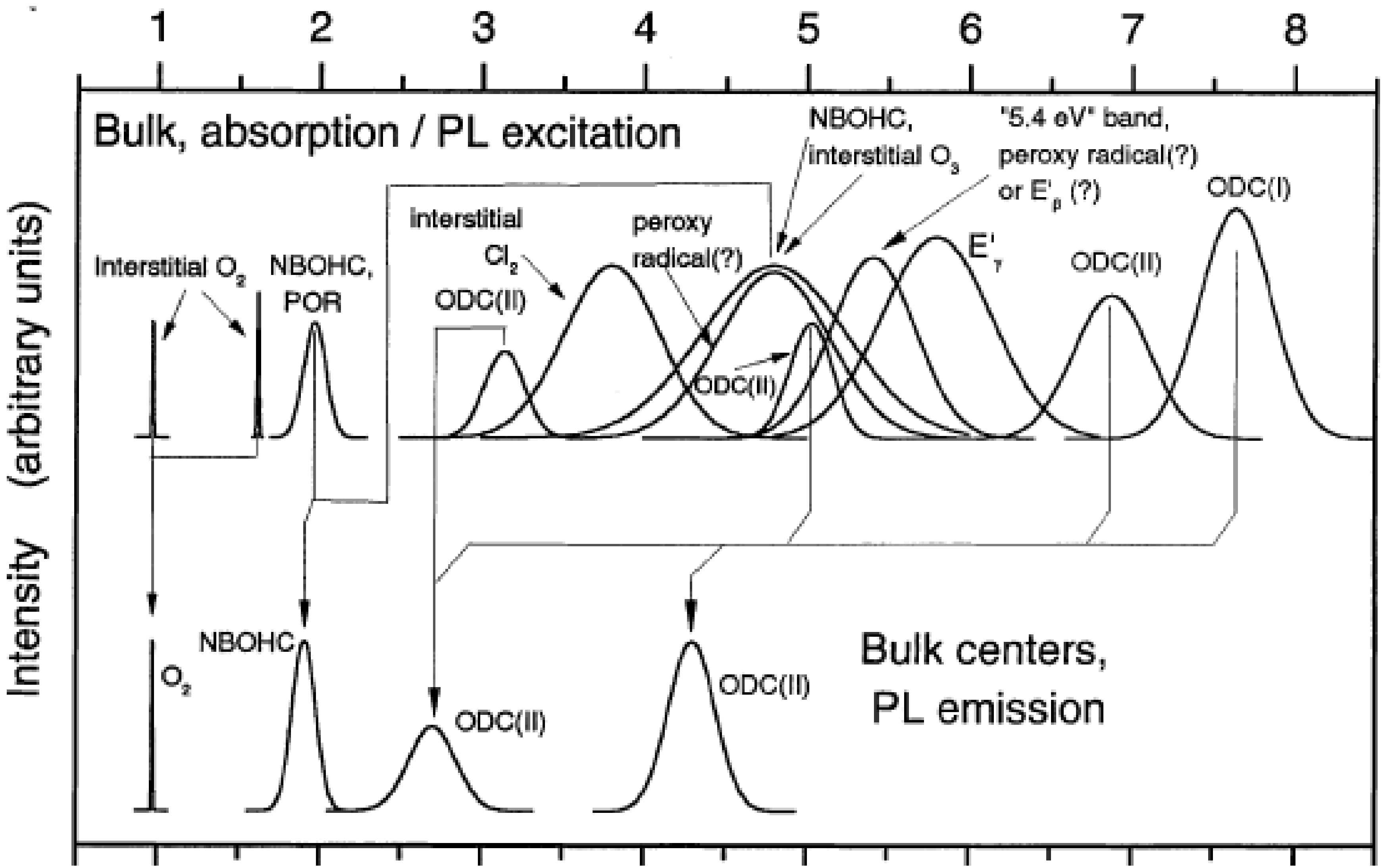

L. Skuja, JNCS 1998

Résonance Paramagnétique Electronique (RPE)

- Radicaux
- Défauts
- Ions de transition ou terres rares

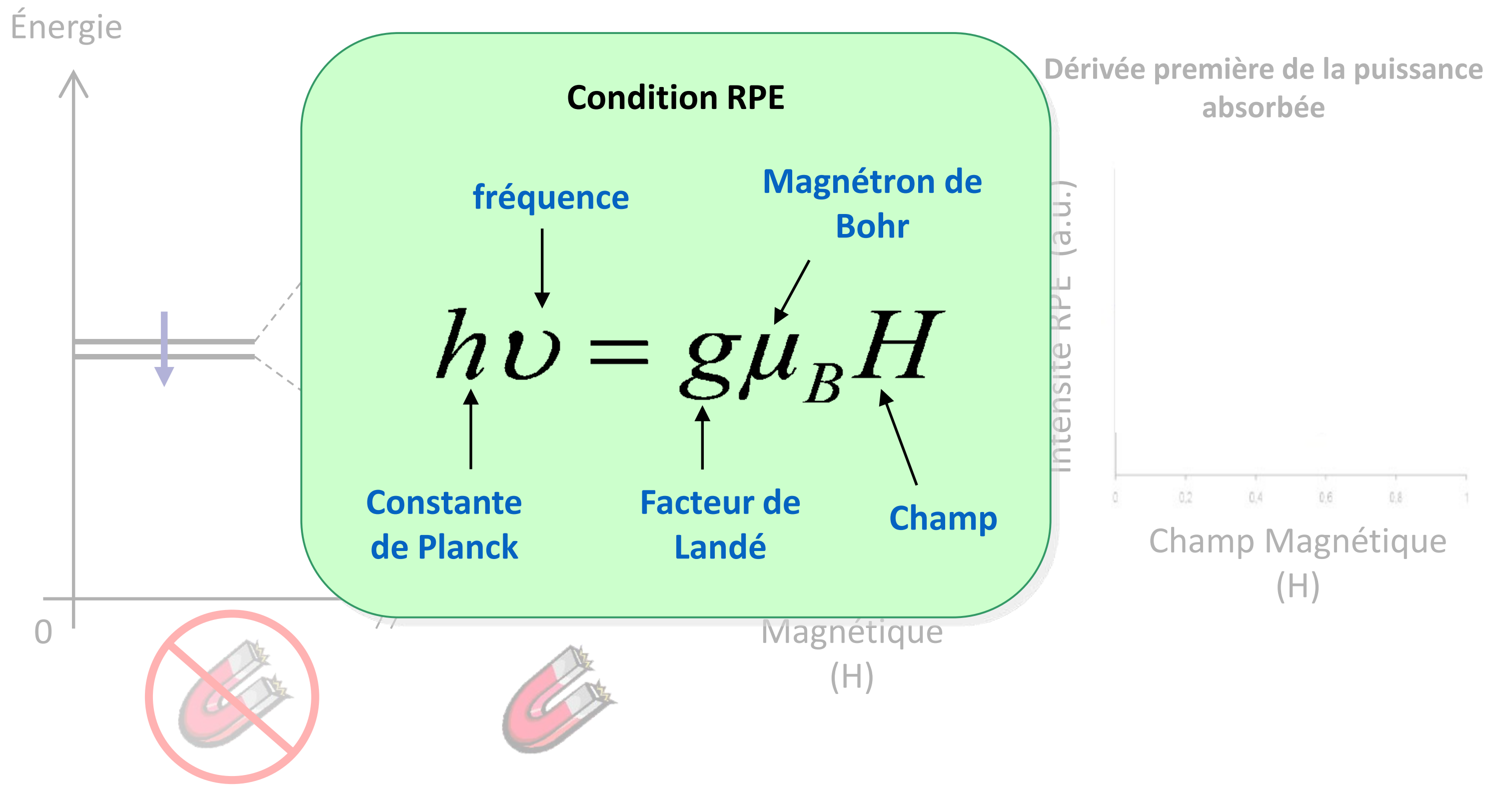

Weil *et al.* Electron Paramagnetic Resonance, (1994) Wiley Interscience.
A. Abragam and B. Bleaney, Electron Paramagnetic Resonance, Clarendon Press (1970)

Bande X: B varie; ν= 9.5 GHz

$h\nu = g\,\beta H$

Valeur du facteur g

- Espèce paramagnétique donnée
- Symétrie du site de l'ion paramagnétique

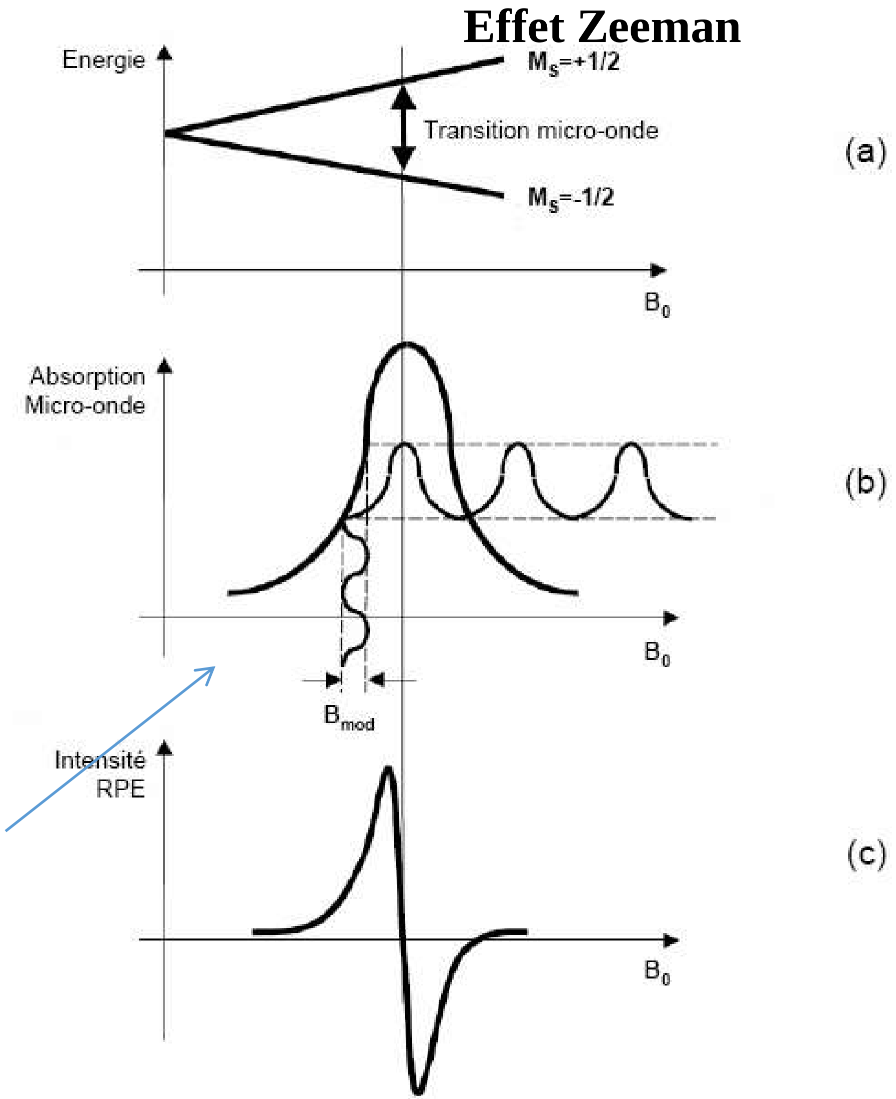

FIG. 2.7 – Principe d'une expérience de RPE.

D'après Lefèvre, 2008

Oxygen Deficient Center (ODC)

ODC (I)	7.6eV (165nm)	≡Si—O—Si≡ → ≡Si—Si≡ + 1/2 O_2
ODC (II)	5.0 eV (240nm) 3.15 eV (330nm)	≡Si—O—Si≡ → =Si: + 2 ≡SiOH ≡Si—Si≡ → =Si:

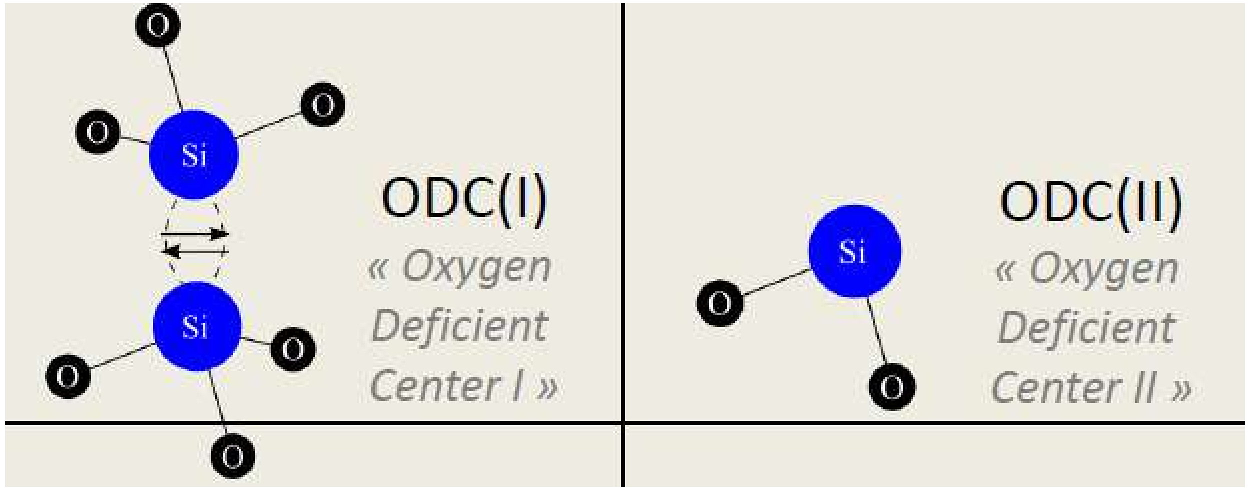

Photoluminescence

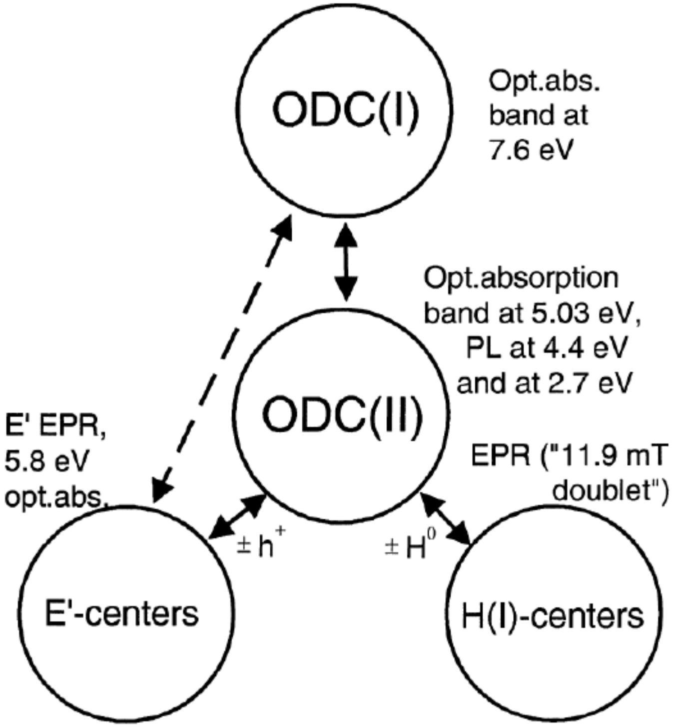

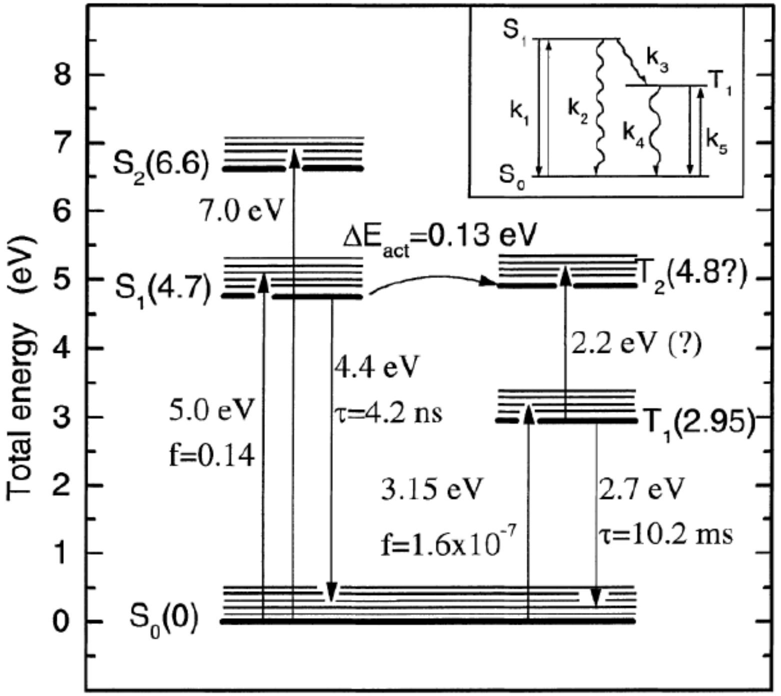

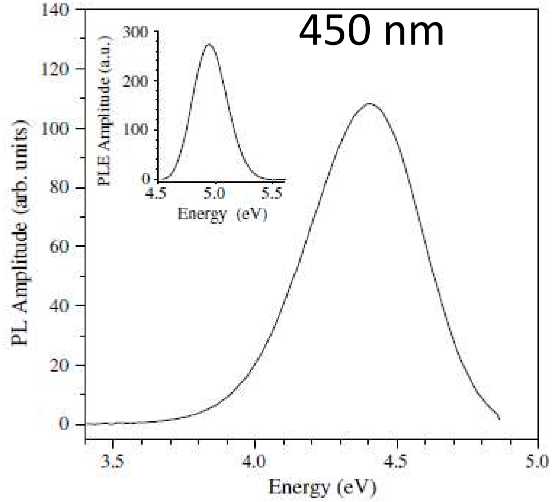

SiODC(II)

Skuja JNCS 1998

Non Bridging Oxygen Hole Center

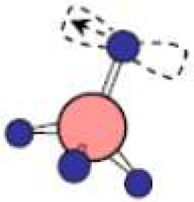	2-2.1eV, 4.8eV, 6.8eV (Nagasawa 86, Todoroki 86, Yamanaka 90, Skuja 98, Griscom 00 PL à 1.9 ou 2eV	**≡Si—O—Si≡ → ≡Si—O• + •Si≡** (e.g. Aux fortes doses) **≡Si—O—H → ≡Si—O• + •H** (e.g. Wet silica <10^7Gγ, , dry silica <10^4 Gγ) **≡Si—O—O• → ≡Si— O• + O⁻** (e.g. Irradiation UV 5eV

Photoluminescence

Non Bridging Oxygen Hole Center (NBOHC)

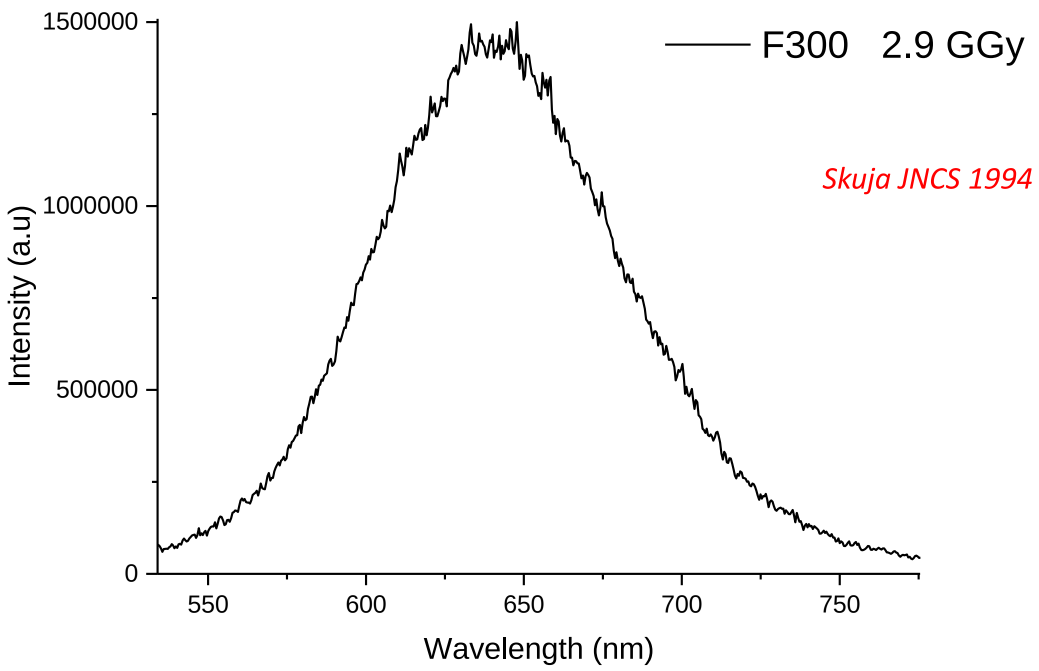

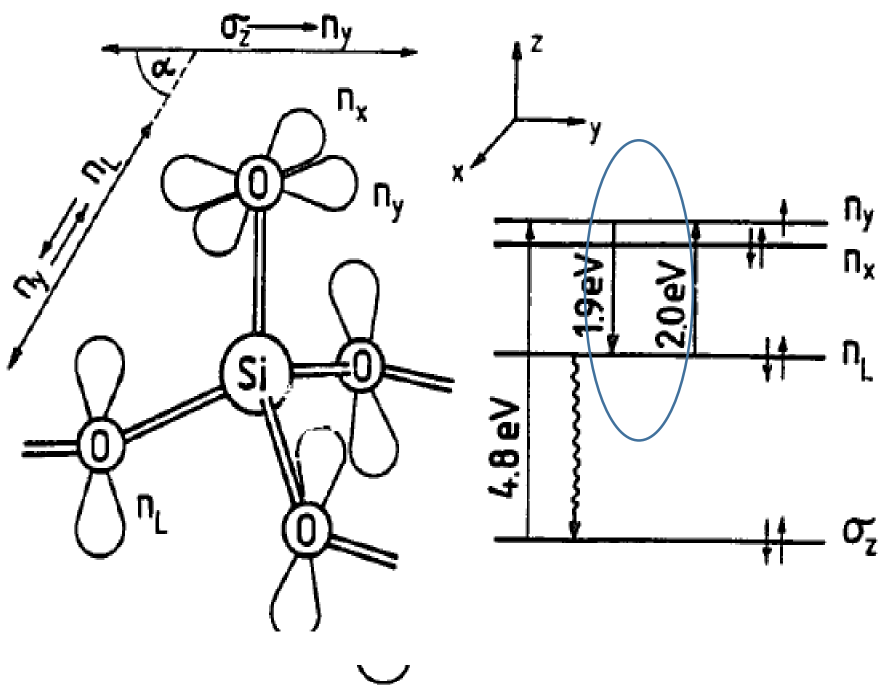

Fig. 16. An energy level scheme, suggested to explain the optical properties of the non-bridging oxygen hole center [23]. The σ-bonding in SiO_4 is depicted by straight lines; the non-bonding oxygen π orbitals are shown. n_L is the lone pair orbital one of the three ligand oxygen atoms. The 1.9 eV emission/2 eV absorption transition is $n_L \leftrightarrow n_y$ charge transfer transition polarized approximately along the line connecting both oxygen atoms. α is the angle between the transition dipole momenta of 4.8 eV absorption and 1.9 eV emission.

Peroxide Radical (POR)

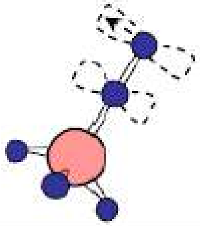	165 nm (Shelby 80, Garapon 01) 260nm (Hosono 81) ? 630 nm (Griscom 98)	$\equiv Si—Si\equiv + O_2 \rightarrow \equiv Si—O—O—Si\equiv$ $\equiv Si—O—O—Si\equiv \rightarrow \equiv Si—O—O\bullet + Si\bullet$ $SiE' + O_2 \rightarrow \equiv Si—O—O\bullet$

EPR

TABLE 2. Spin-Hamiltonian parameters for stable oxygen-hole centers in a-SiO_2.

Defect	g_1	g_2	g_3	$A_1(^{29}Si)$ (mT)	$A_2(^{29}Si)$ (mT)	$A_1(^{17}O)$ (mT)	$A_{1,2}(^{17}O)$ (mT)
POR[a]	2.0018	2.0078	2.067	0.36	0.42	4.3[c]	1.0[c]
						10.2[c]	0.9[c]
POR[b]	2.0020	2.0085	2.0027				
NBOHC	1.9999	2.0095	2.078	1.44	1.44	11.0	1.6

[a]Stoichiometric or O-rich a-SiO_2 γ irradiated at room temperature.
[b]O-rich a-SiO_2 X irradiated at 77 K; this variant has been proposed to be the SPOR.
[c]Hyperfine interactions with two inequivalent oxygens.

Really difficult to distinguish both defects by EPR !

NBOHC

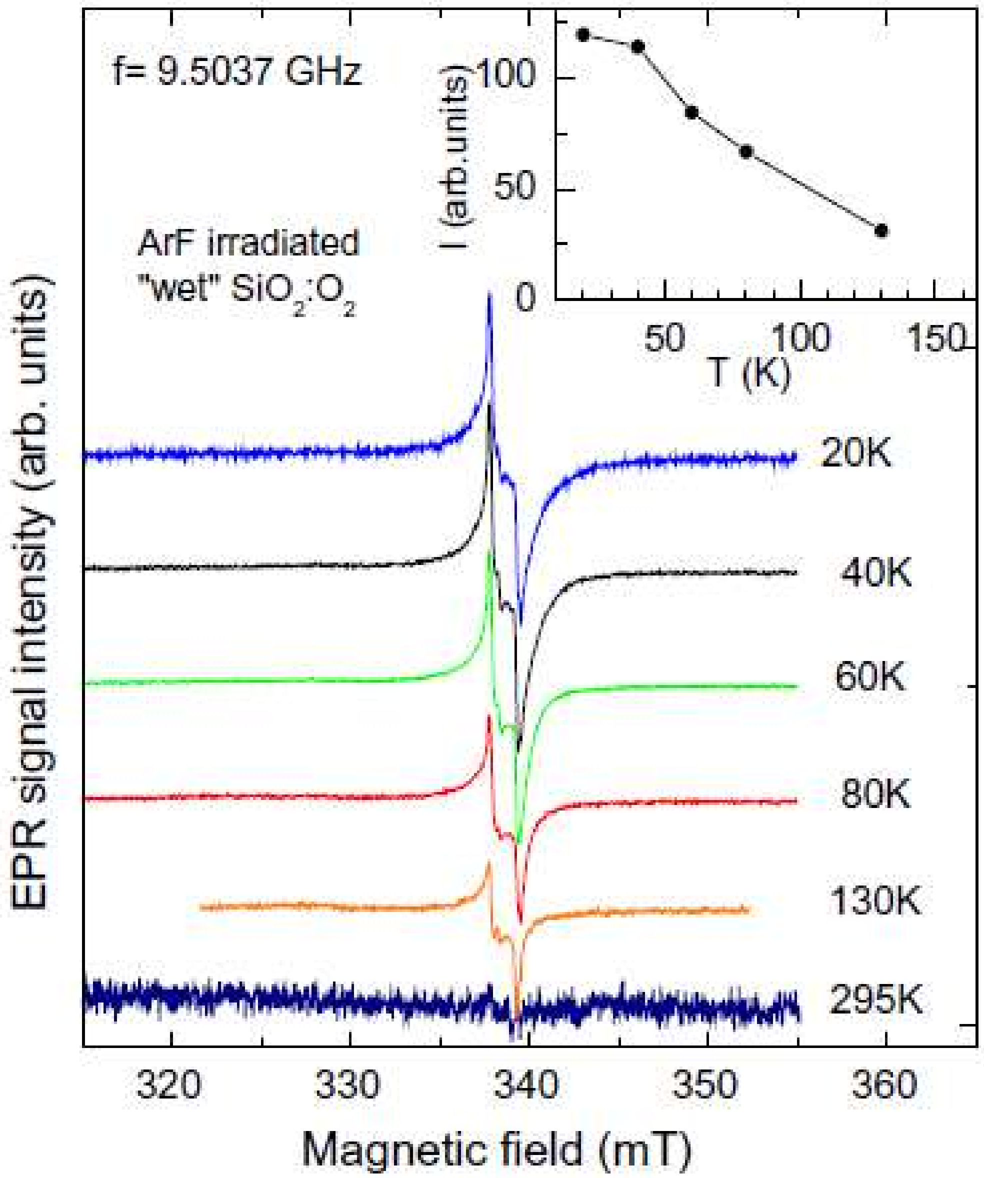

F

Nuclear Instruments and Methods in Physics Research B 286 (2012) 159–168

E’ center

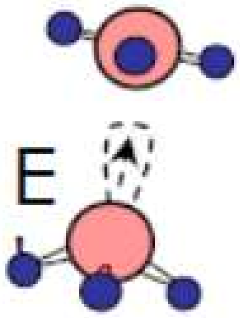	5.8eV (206 nm) No PL !!!	≡Si—Si≡ → ≡Si• + $^{+}$Si≡ (hole trapping) (faibles doses) Feigl 74 ≡Si—O—Si≡ → ≡Si—O• + •Si≡ (fortes doses, $>10^4$ Gγ in dry silica) **Sous irradiation laser (homolytic bond breaking):** **≡Si—Si≡ → ≡Si• + •Si≡** **≡Si—O—Si≡ → ≡Si• + •Si≡ + O^{2-} (NB: O^{2-} interstitiel « ESR silent »)**

EPR E’

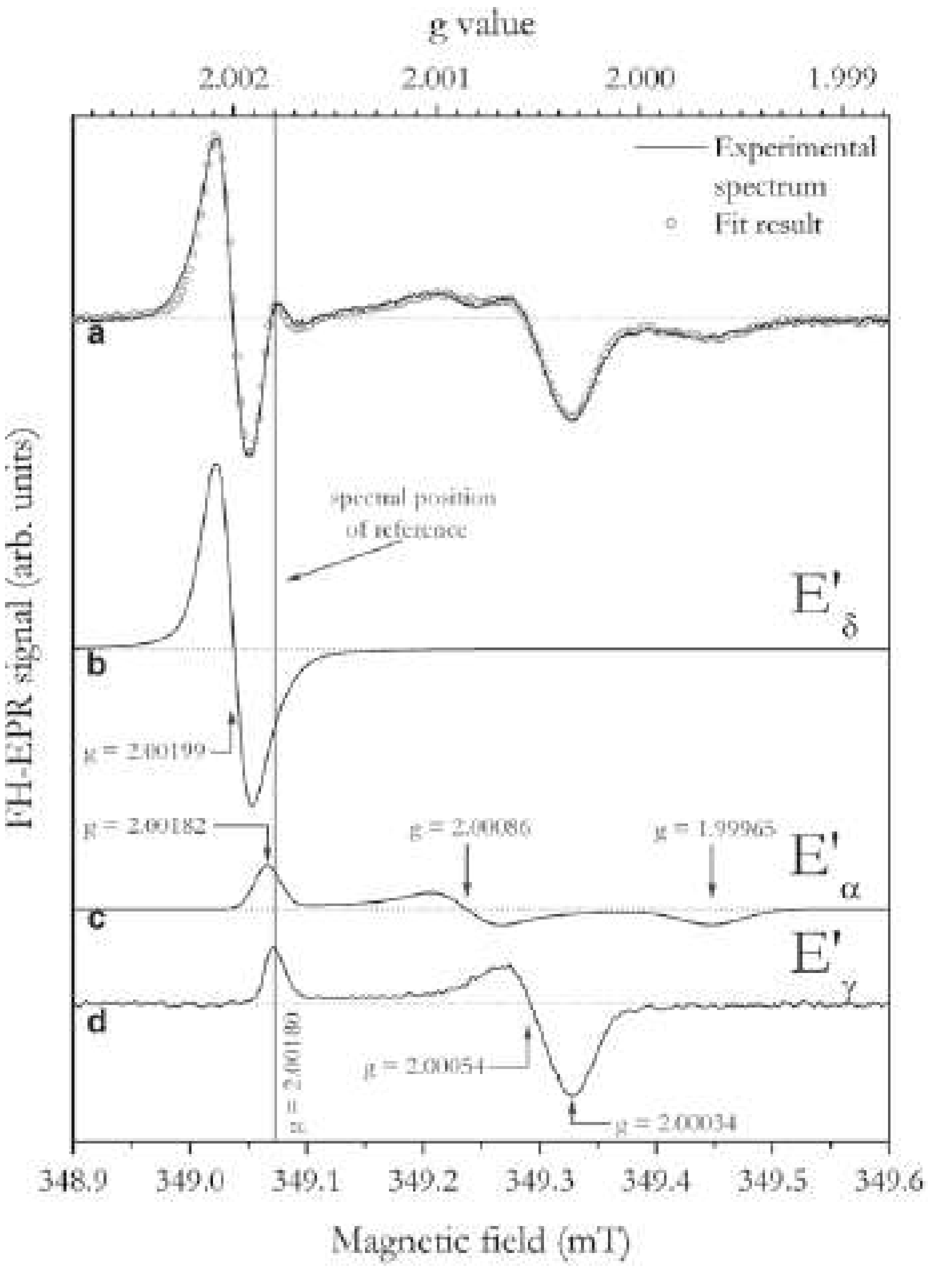

P= 80 μW
0.01 mT modulation

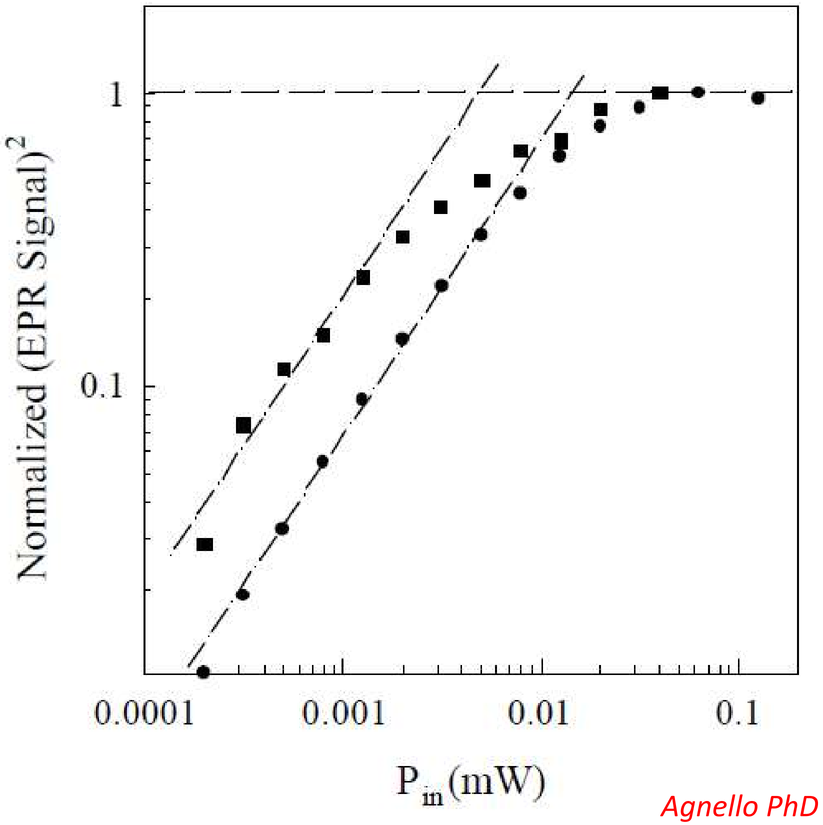

Agnello PhD 2000

Fibres optiques et défauts

- Influence impuretés: OH, Cl, F (quantités de défauts, espèces produites…)
- Défauts spécifiques associés aux dopants: Ge, P, Al,…..
- Influence dose, histoire thermique, propriétés de fibrage….

Other species of paramagnetic point defects

- Al: AlOHC, AlE’ (aluminosilicate, Al doped silica)
- B: BOHC, BE’ (borate, borosilicate)
- Ge: Ge1, Ge2, GeE’, GeLPC (Germanate, Ge doped silica)
- P: P1, P2, P3, P4, POHC, POR (phosphate, P doped silica)
- Na, K: HC1, HC2 (alkali silicate)

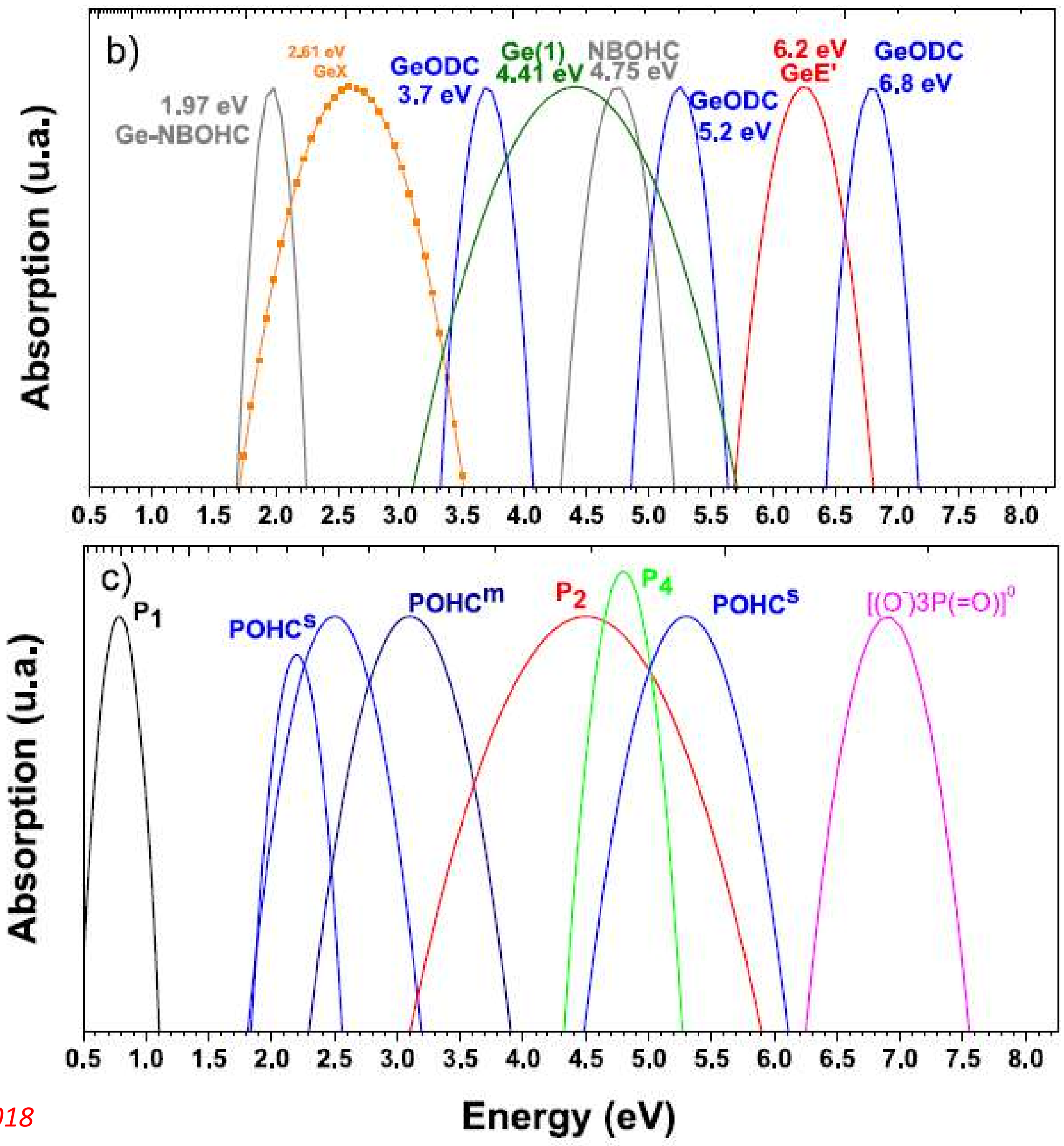

Ge

P

Girard J. Opt 2018

7 types of paramagnetic P point defects

TABLE IV. Phosphorus-related radiation-induced defects and the inferred precursor structures in a P_2O_5–SiO_2 glass.

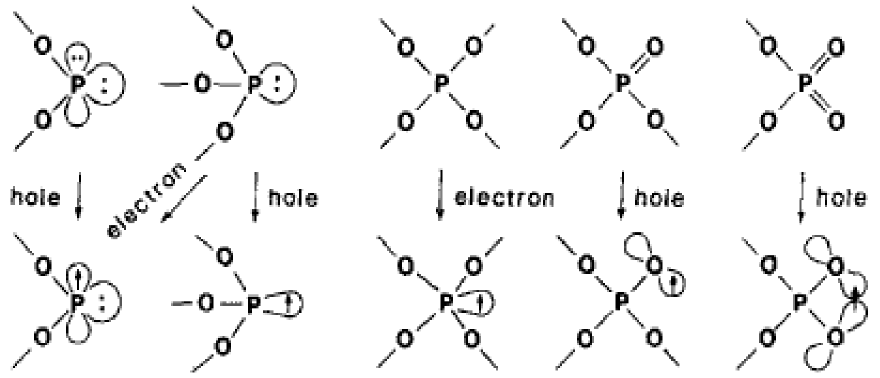

Chemical Formula	PO	P_2O_3	PO_2	P_2O_5 [a]	PO_3
Diamagnetic Precursor					
Carrier Trapping	hole	electron / hole	electron	hole	hole
Paramagnetic Defect					
Defect Nomenclature	P_4	P_1	P_2	POHC [b]	POHC

[a] Stoichiometric

[b] Metastable

D. Griscom

3754 J. Appl. Phys., Vol. 54, No. 7, July 1983

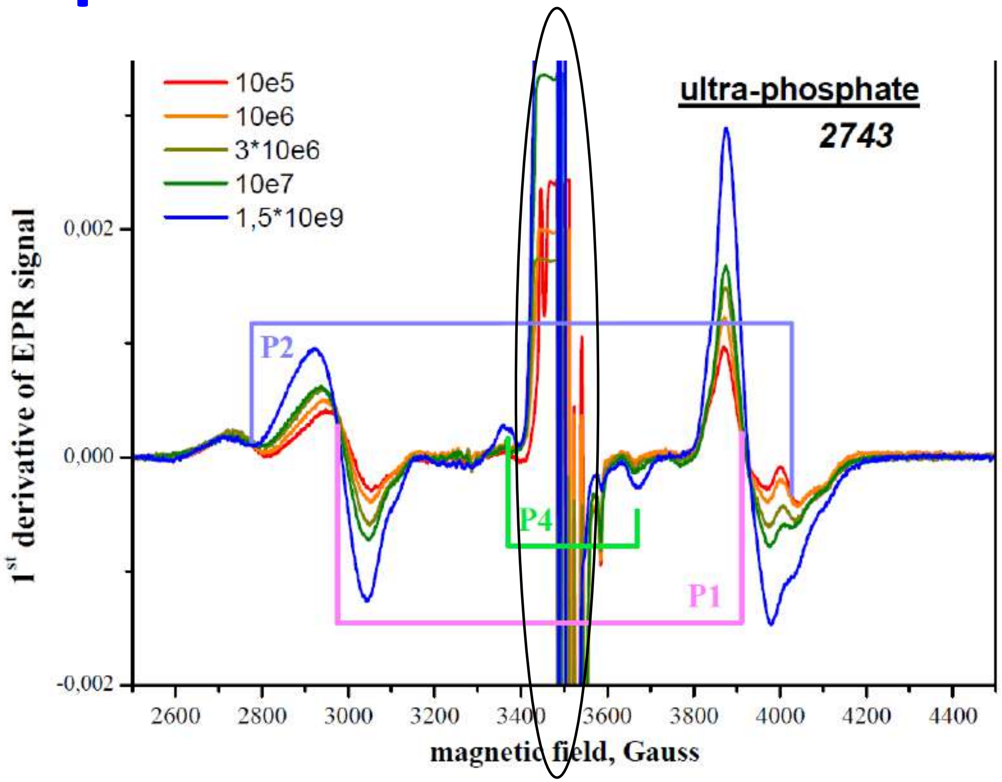

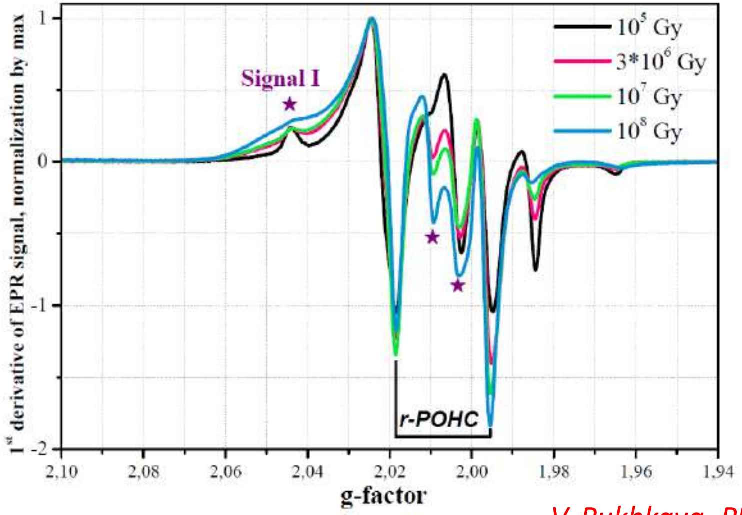

P_1, P_2, P_3, P_4, POHC (2 species), peroxide radicals

V. Pukhkaya, PhD 2013

Example of borosilicate glass (Si, B, Na, O)

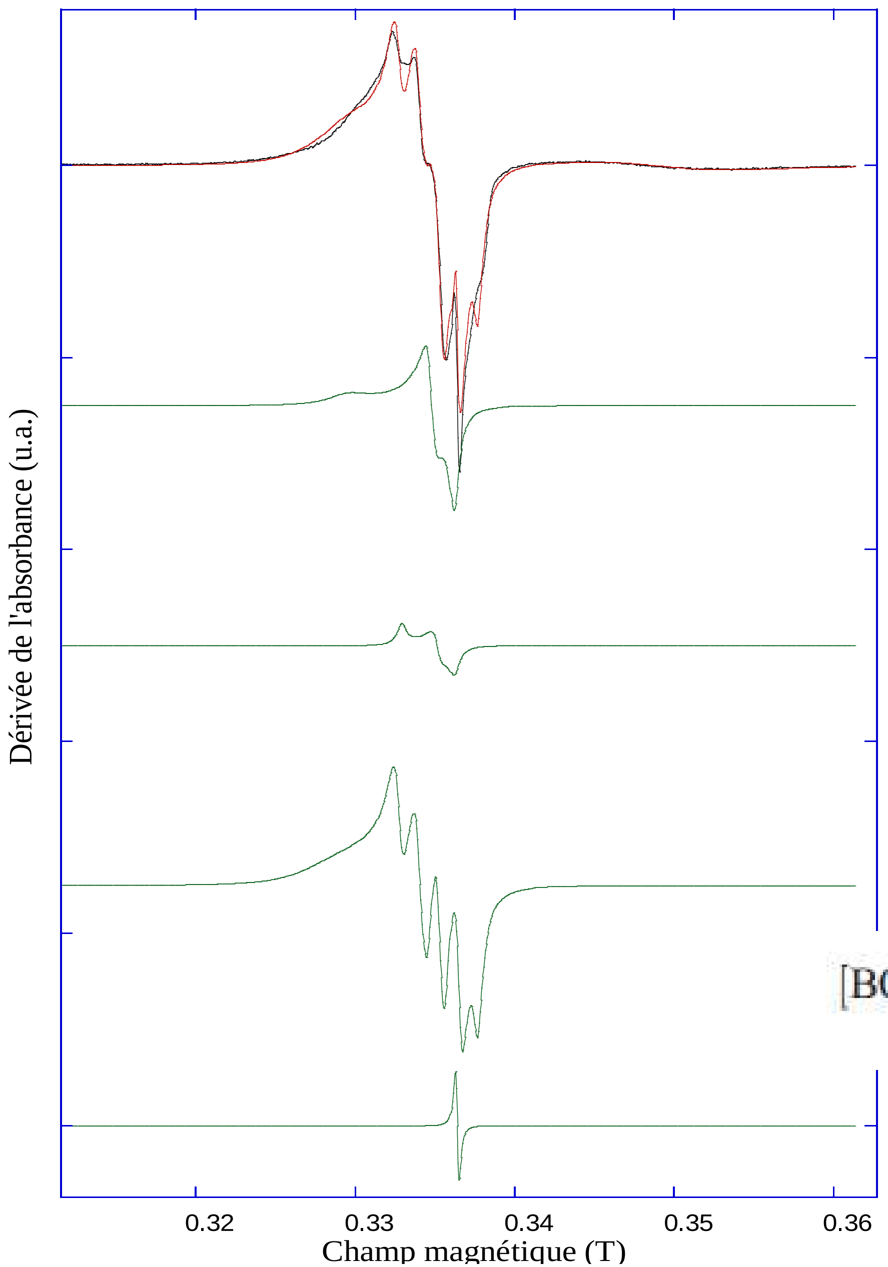

Exp. + ***Sim.***

POR (≡Si-O-O°)

HC₁ **(≡Si-O° Na⁺)**

BOHC **(≡B-O°)**

$$[BO_4]^-(= \text{precursor site}) + \text{hole}^+ \rightarrow [BO_4]^0(= B - OHC).$$

E ’ (≡Si⁻)

B. Boizot et al. Nucl. Instr. and Meth. in Phys. Res. B 141 (1998) 580.

Unknown point defects ?

The case of P_3 point defect in phosphate glasses

Expt.	P_1	P_2	P_3
P_2O_5	95	143	-
P-doped SiO_2	91	120	-
Na_2O-P_2O_5	-		**74.2**
1.3Na_2O-P_2O_5	95		**66.5**
Theory	P_1	P_2	$P_3^{a,b}$
P_2O_5	108.7(6.3)	141.2(7.2)	-
P-doped SiO_2	93.2 (6.5)		-
Na_2O-P_2O_5	-	117.0	**85(14.2)**[a]
Na_2O-P_2O_5	-	-	**68.5(9.3)**[b]

- Expt. data taken from Weeks & Bray 1968 and from Griscom *et al* J. Appl. Phys. **54**, 3743 1983.
- In RMC2-P2O5 from a Q^2 we obtained 2 P_3^a configurations with Aiso=87.4 mT and Aiso=82.1 mT.

ab initio calculation: P_3 point defect identification

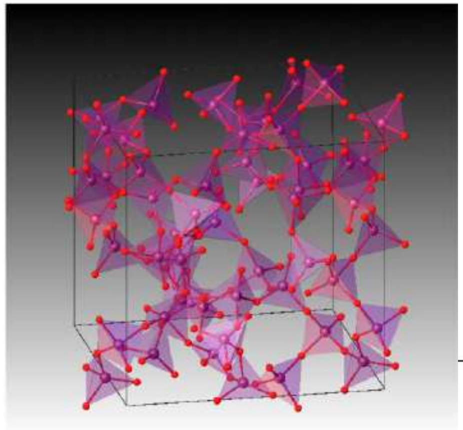

P_2O_5 glass

Shchlebanov et al. PHYSICAL REVIEW B 100, 134309 (2019)

P3a P3b

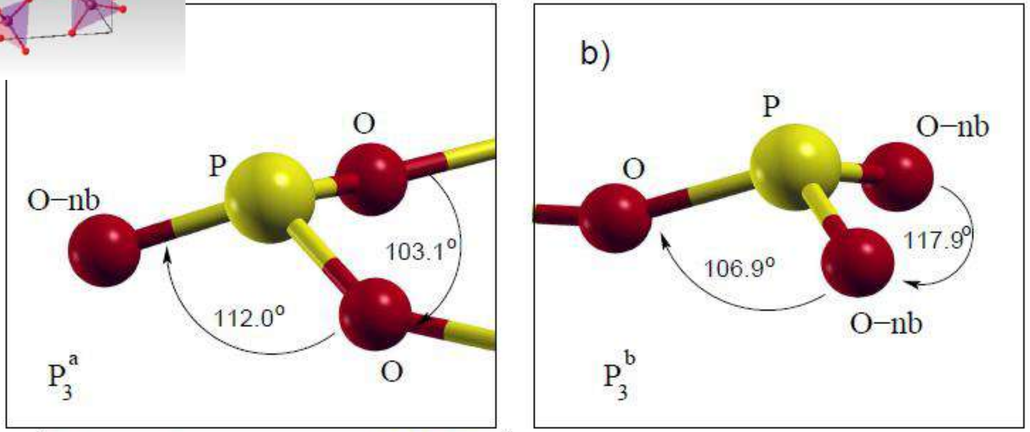

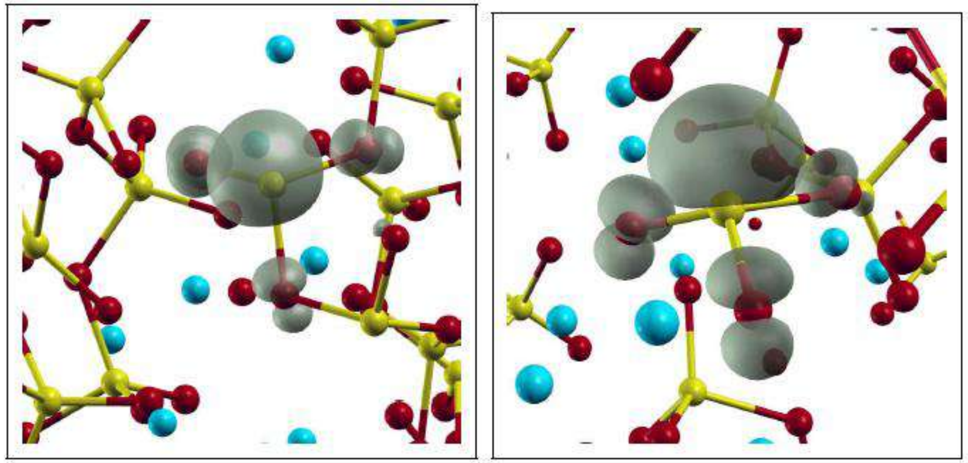

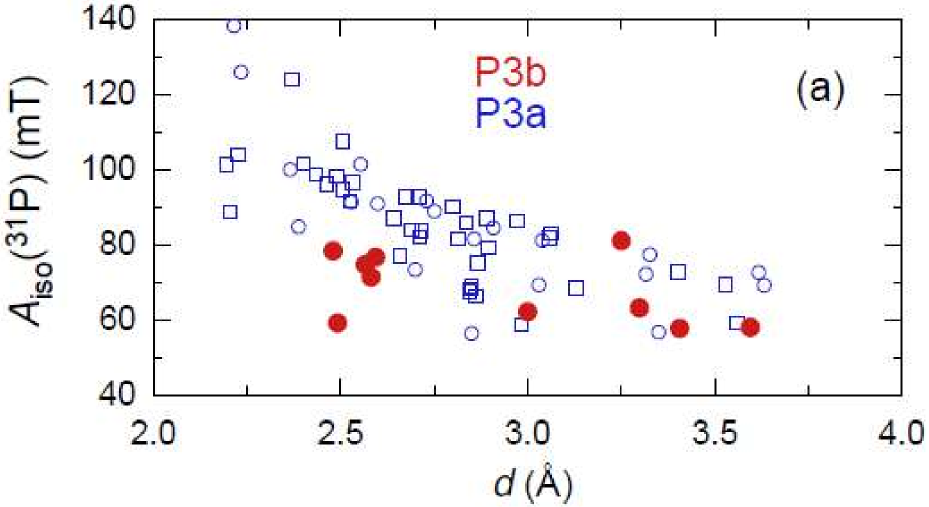

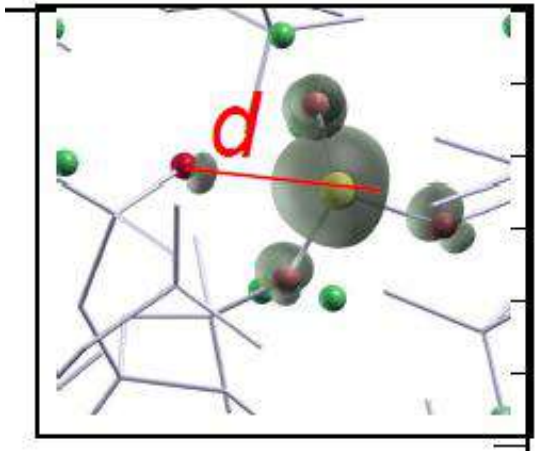

Giacomazzi et al. J. Phys. Chem. C 2021, 125, 8741–8751

Green emission in silica glass : 540 nm / 2.27 eV

Silica (optical fibers), neutrons 10^{17} n/cm^2

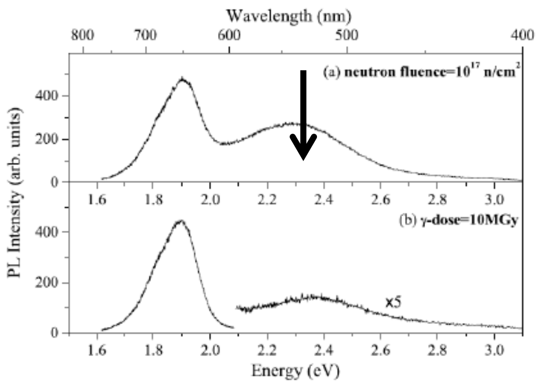

Morana et al Opt. Mat. Exp 5, 911 (2015)
Martin et al. phys. stat. Sol (2005)

Etched indented Corning 7980 fused silica samples

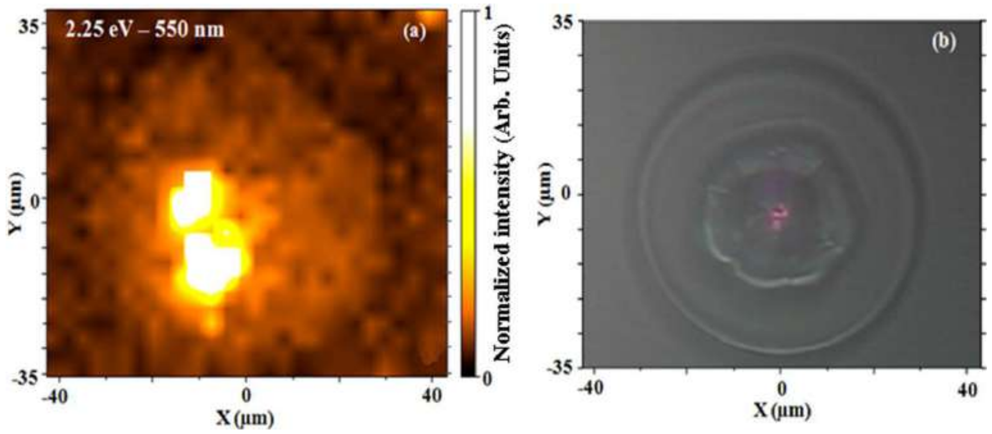

Fournier et al. Appl. Phys. Lett. 100, 114103 (2012)

488 nm exc.

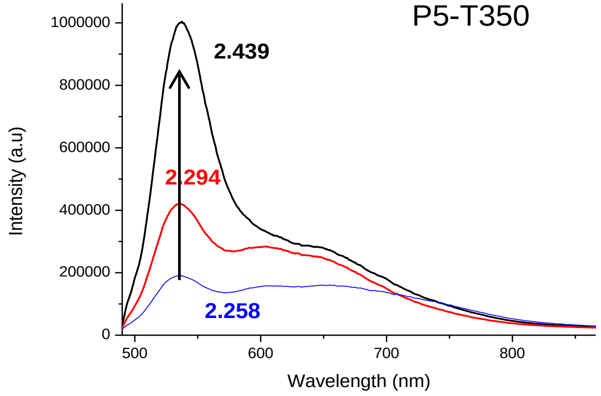

Ollier et al. JNCS 2017

fs laser damaged silica

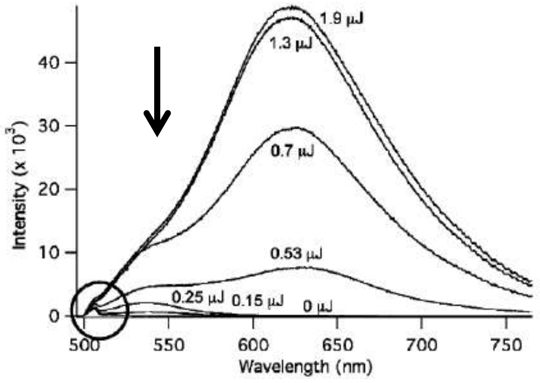

Chan et al. Appl. Phys A 2003

Indentation
fs-laser, electrons
Neutrons

→ Compaction of the silica glass network

Dose effect in silica glass

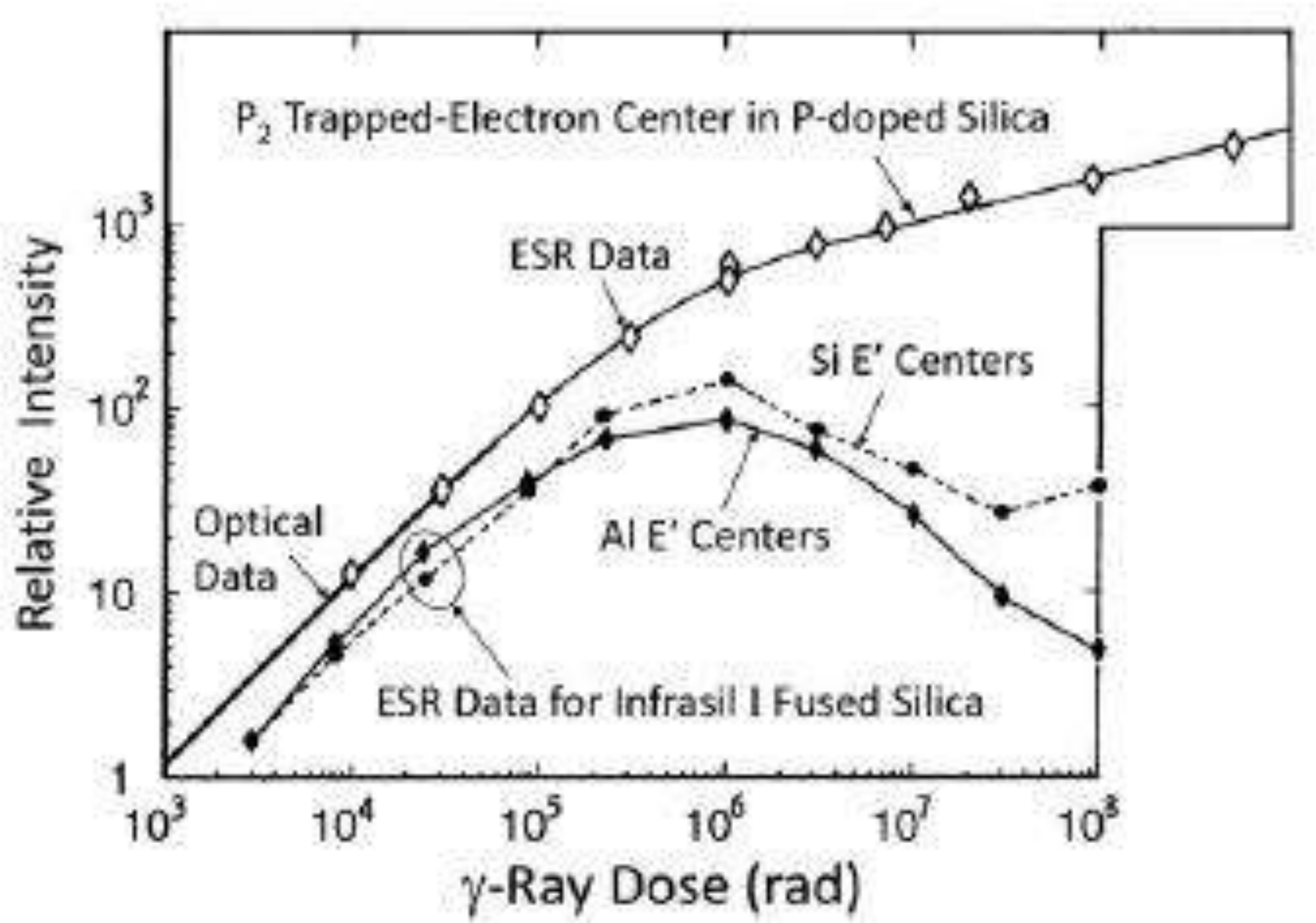

D. Griscom Journal of Non-Crystalline Solids 2011

D^n : n<1 doses >10^4 Gy

Thermal stability

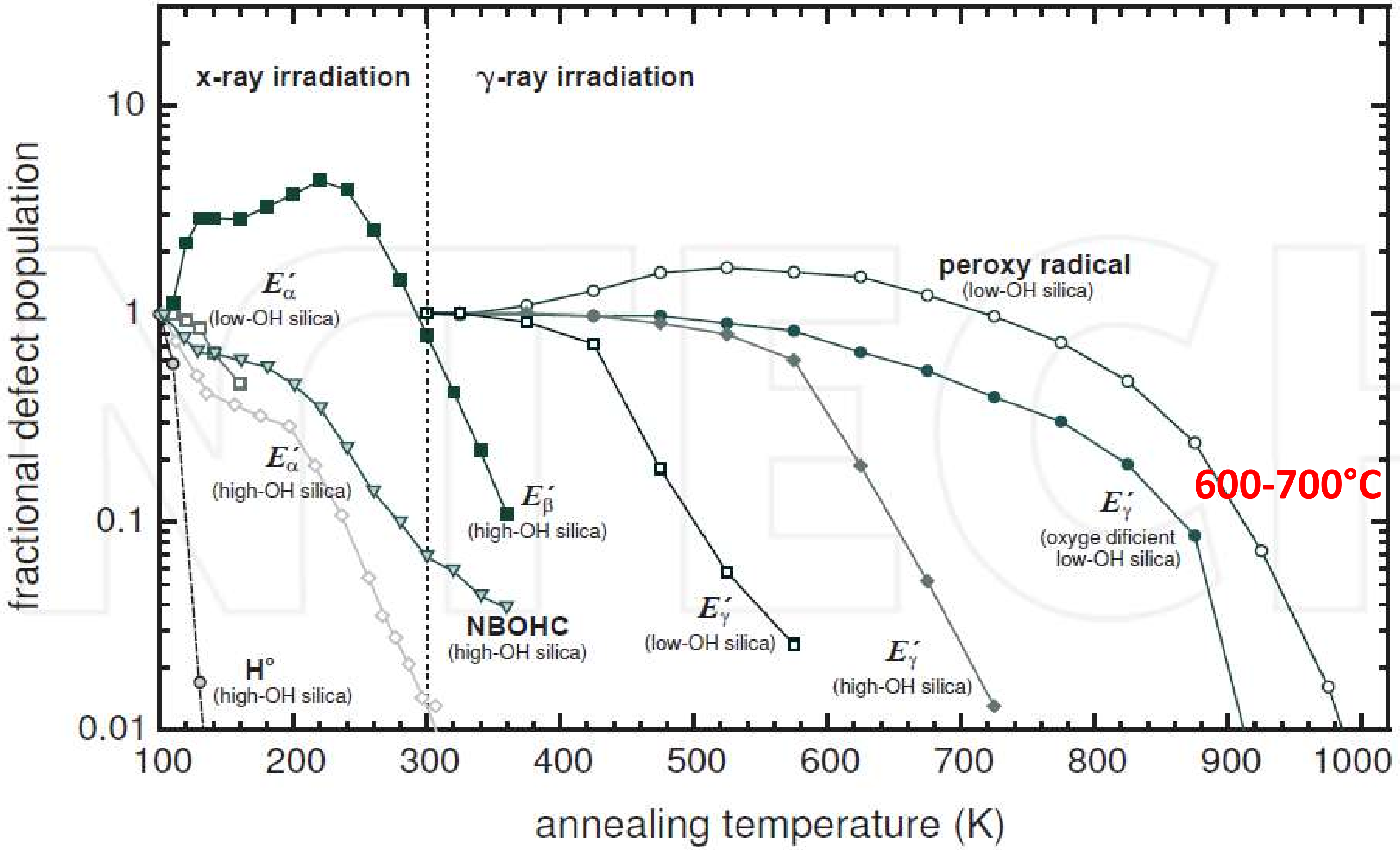

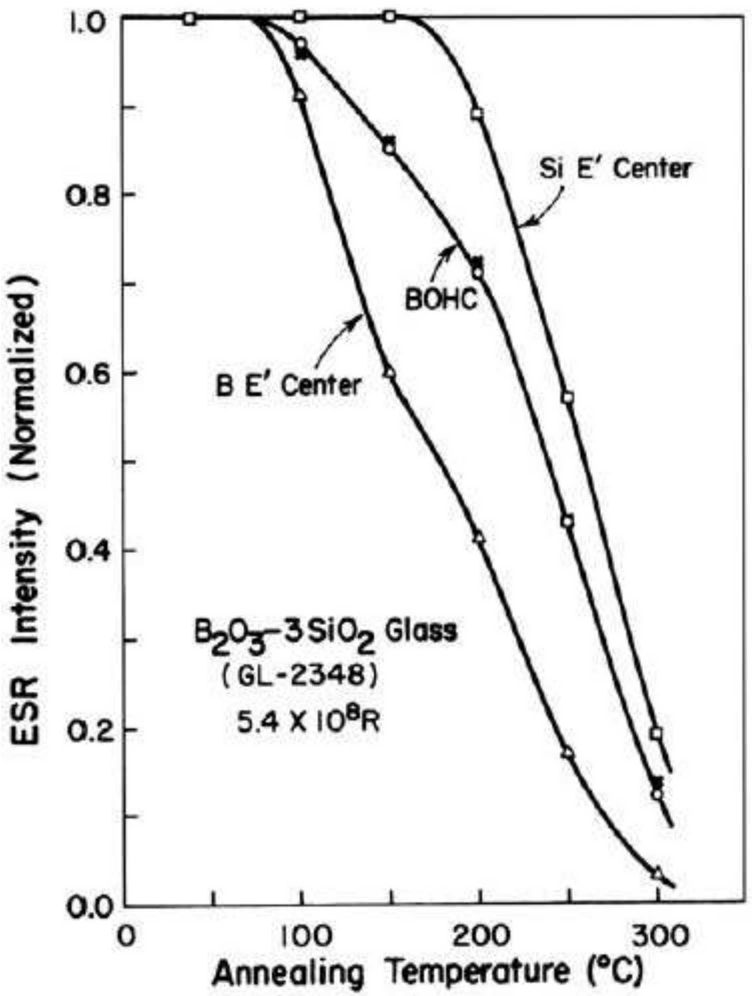

Silica glass

Verres phosphates

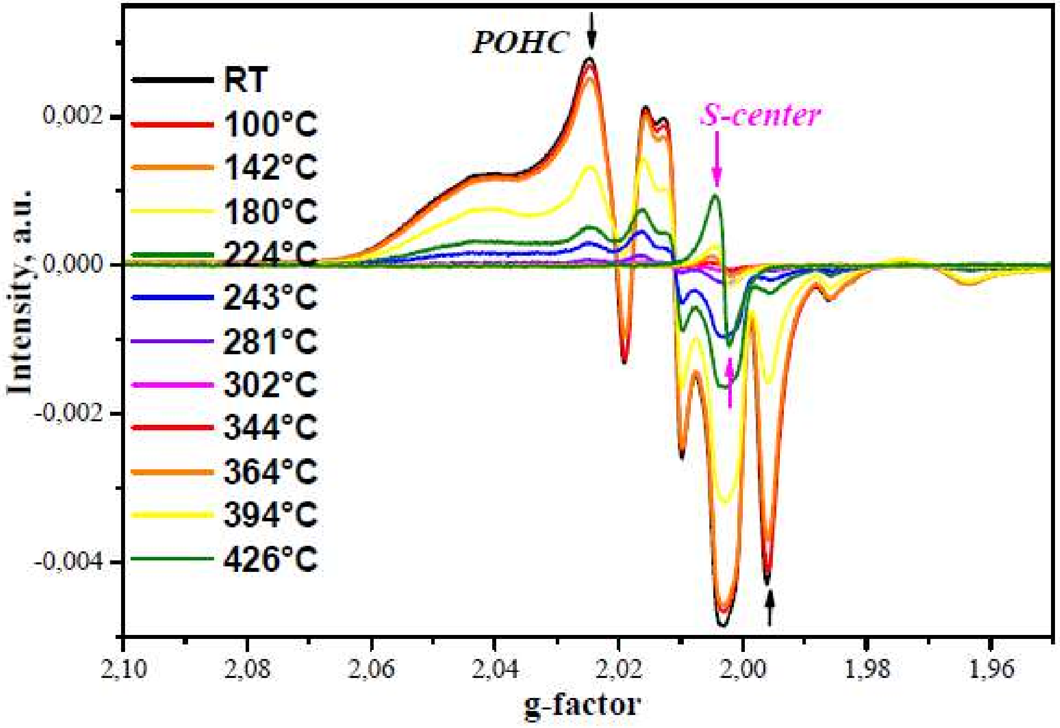

Pukhkaya PhD 2013

Verres aluminosilicates

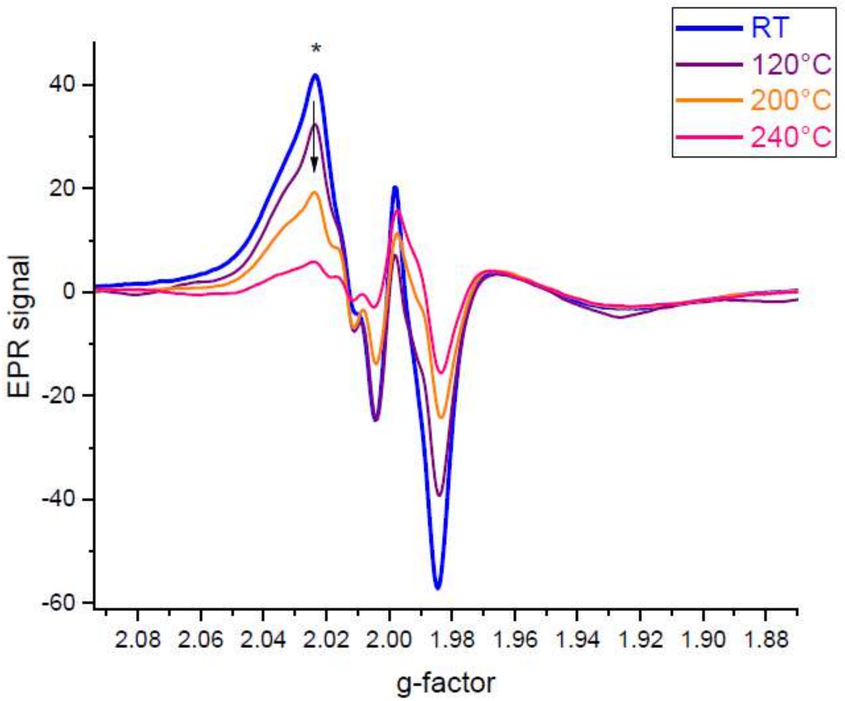

Mobasher PhD 2024

Impact des défauts sur les propriétés du verre

- Couleur
- RIA
- Propriétés optiques des verres dopés TR

Changement de couleur lié aux défauts ponctuels

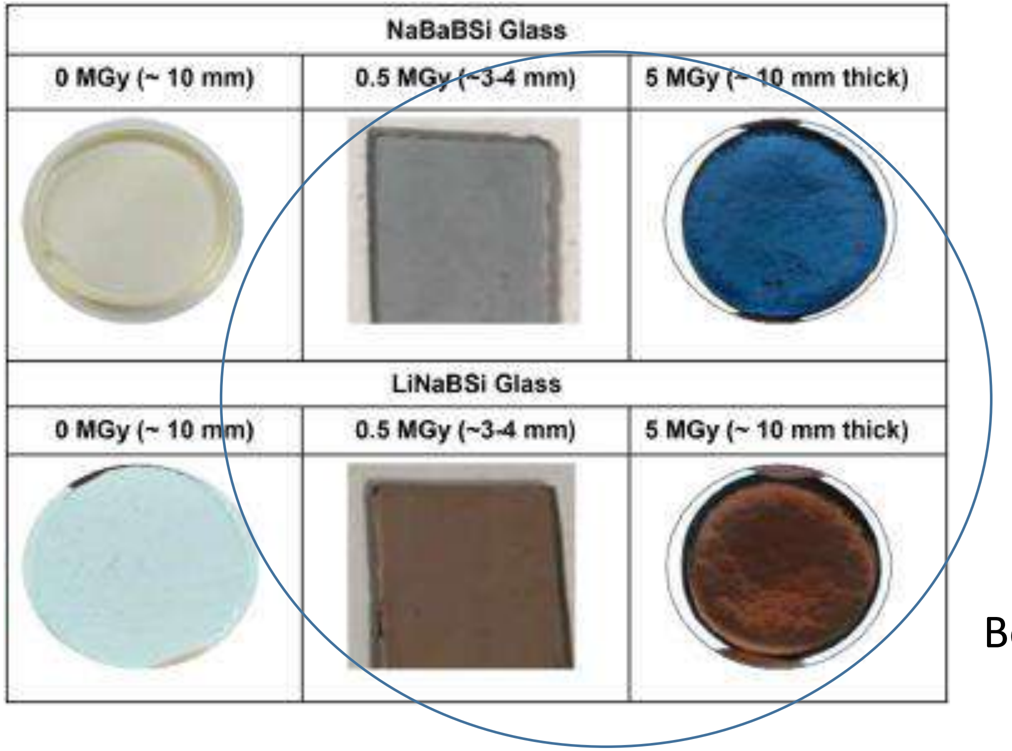

Borosilicate

P. Rautiyal, G. Gupta, R. Edge, L. Leay, A. Daubney, M.K. Patel, A.H. Jones, P.A. Bingham, Journal of Nuclear Materials, Volume 544 2021

Verres phosphates

M. Mahfoudhi Thèse EP 2019

Verres dopés (ions de transition ou ions TR)

Irradiation: modification des degrés d’oxydation (réduction ou oxydation)

4+/3+ Ce, Tb

3+/2+ **Sm, Eu**, Tm, Yb…

$Sm^{3+} + e \rightarrow Sm^{2+}$

Fe^{3+} / Fe^{2+}

Verre lunaire

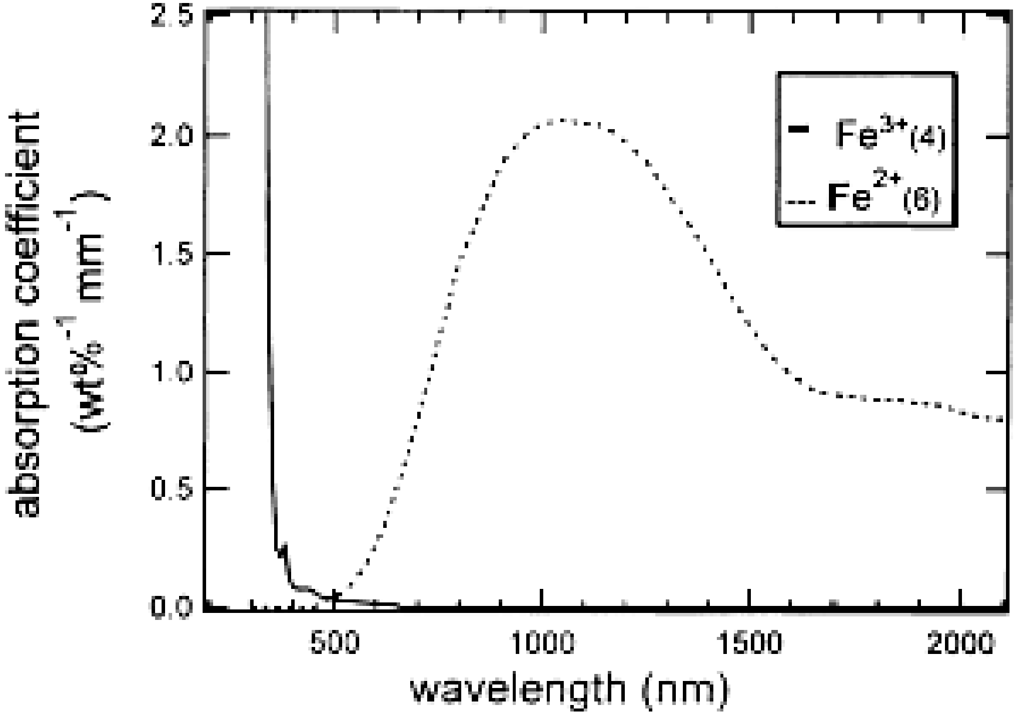

@ G. Calas

Verre au Pb irradié (MGy)

Verres photosensibles ou photorésistants solarization (UV)

- Phosphates (D. Ehrt/ D. Moncke)
- 3D/4D/5D

Zr, Nb, Mo, As, Sb, Sn, Pb, Ag, Fe, Mn, Ti, Cr ....

RPE/absorption optique

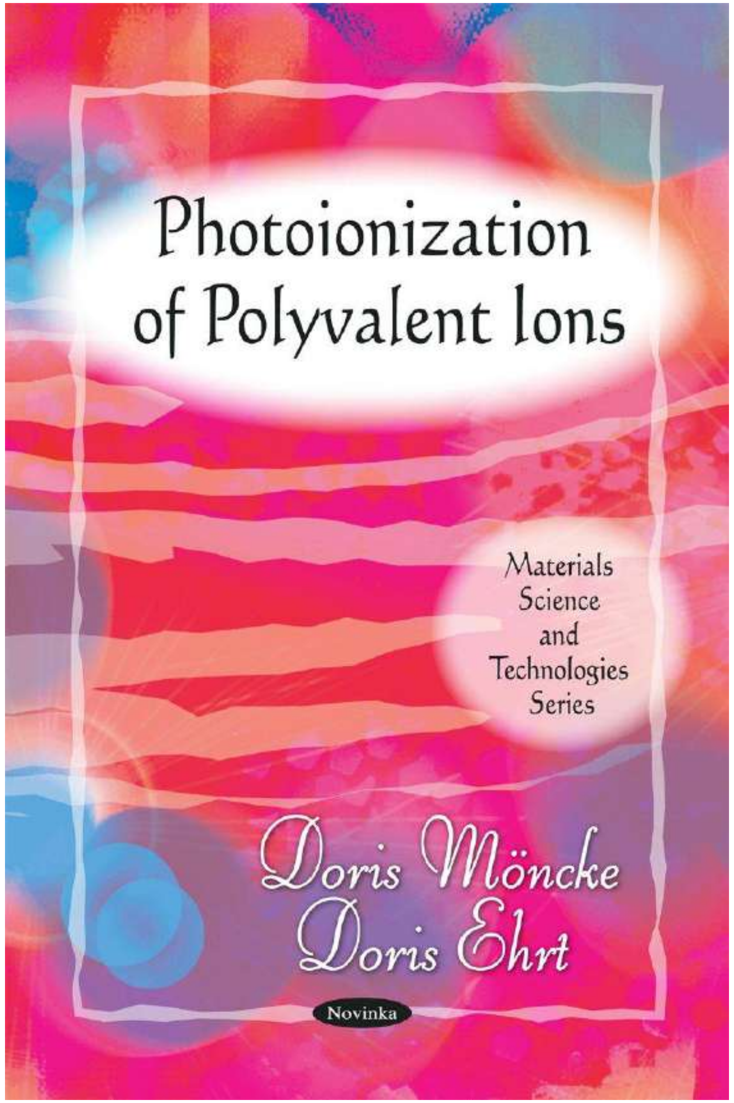

Solarisation des verres au Mn (verres du patrimoine)

Le verre peut se solariser et virer au violet, sous l'effet des photons UV
Réduction de Fe^{3+} en Fe^{2+} et oxydation de Mn^{2+} en Mn^{3+}
$Fe^{3+} + Mn^{2+} \rightarrow Fe^{2+} + Mn^{3+}$

Verre Lalique (1931)
chapelle de Douvre-la-Délivrande

Couleur violette
Ions Mn^{3+}

Restauration du verre avec un recuit
le manganèse revient alors à son état d'oxydation stable Mn^{2+} (incolore)
Et pour protéger ces verres d'une nouvelle solarisation: nouveau vitrage classique qui absorbe les UV.

Le verre de la pyramide du Louvre

Transparent, incolore, pas de solarisation

Mn pour décolorer
Se (Se^{6+}, Se^{4+}, Se°, Se^{2-})

une teneur en sélénium de l'ordre de 1 ppm a été suffisante pour décolorer le verre de la pyramide qui contenait 150 ppm de fer

Le verre de la pyramide du Louvre
P. Lehuédé Techné 49 2020

Contrôle l'environnement des ions Ti^{3+} :

3 sites d'ions Ti^{3+}

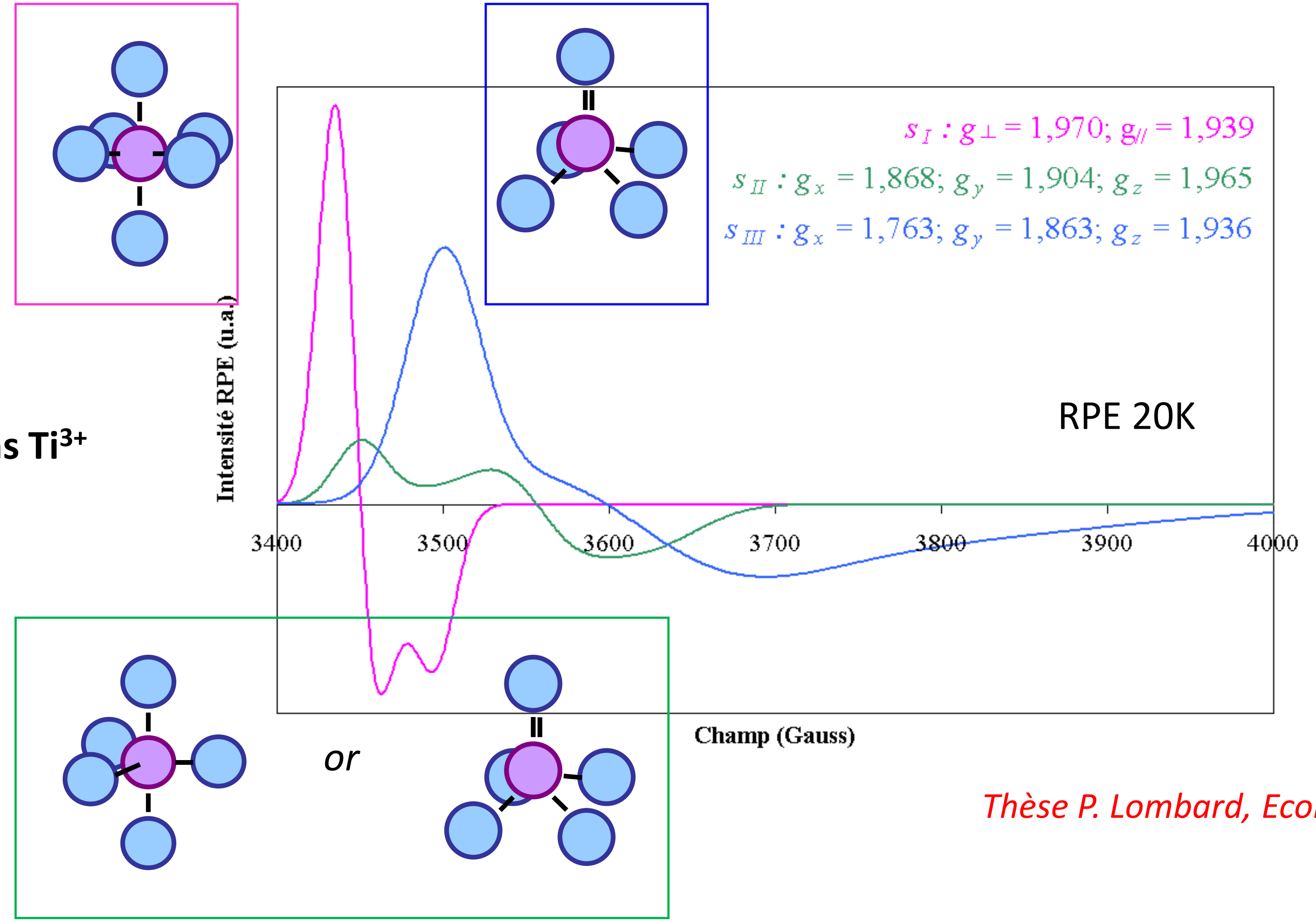

Verres BS et Silicates

Thèse P. Lombard, Ecole polytechnique 2009

Réduction des ions Ti^{4+} en Ti^{3+} et stabilisation sous irradiation (dose d'irradiation /composition du verre)

Contrôle l'environnement des ions Ti^{3+} :

Composition du verre Silicaté

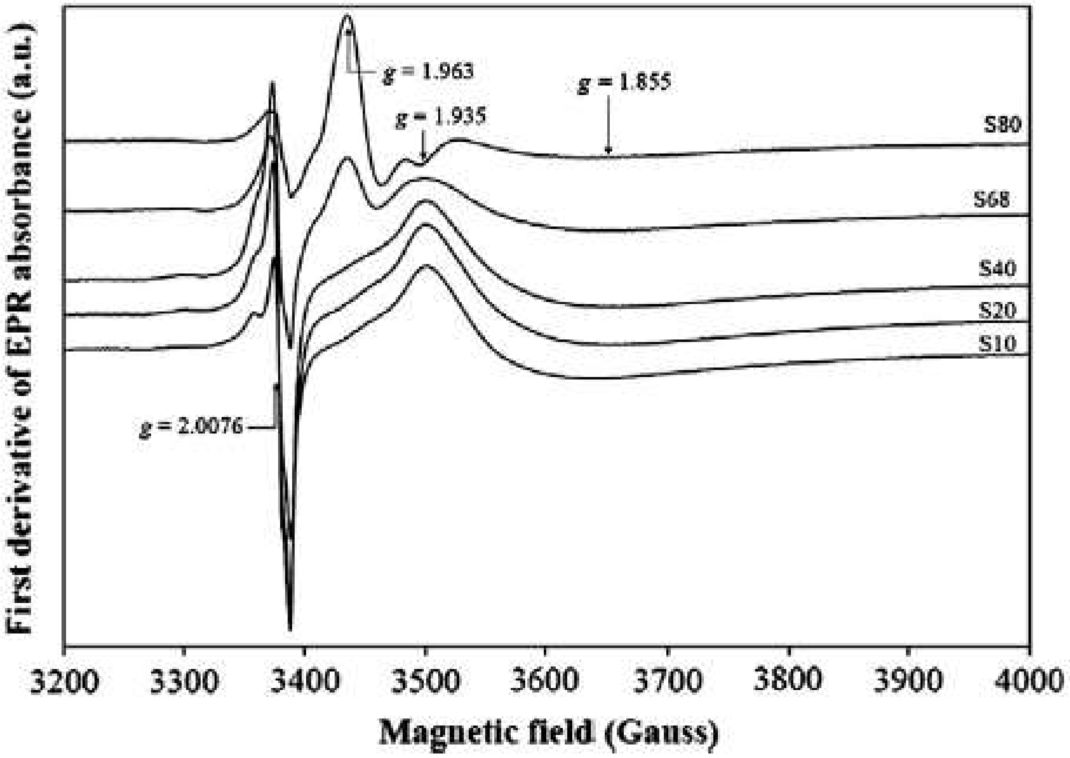

Dose

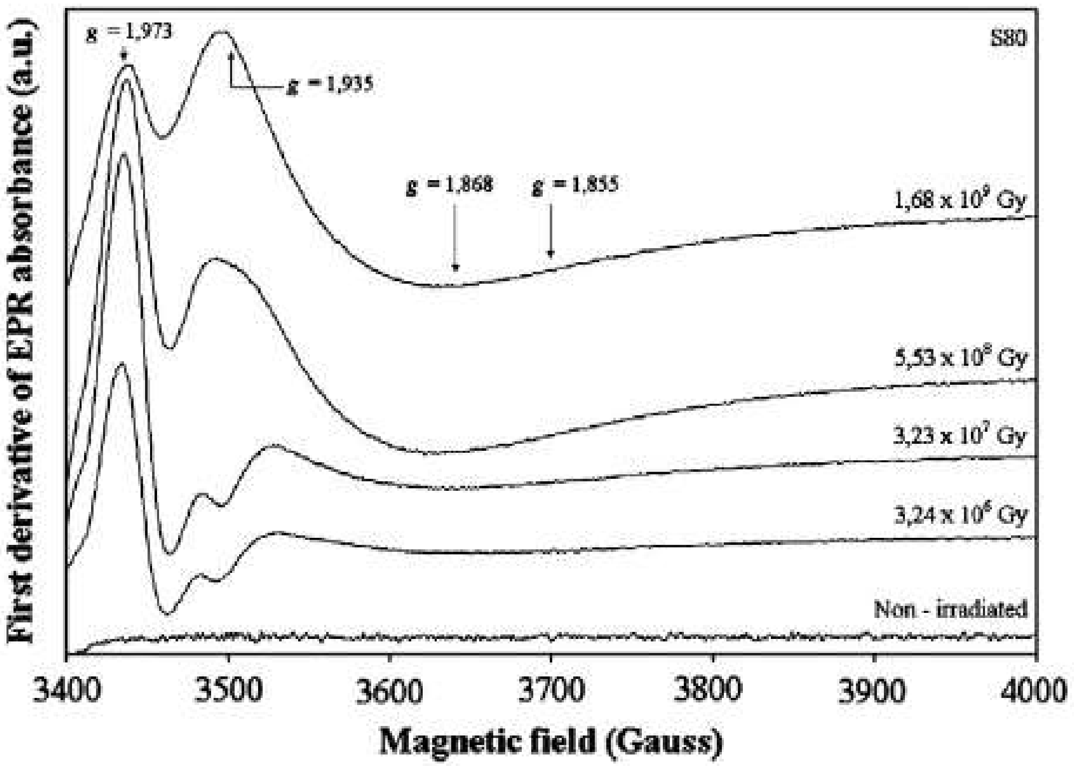

P. Lombard et al. / Journal of Non-Crystalline Solids 357 (2011) 1685–1689

Verres phosphates dopés Ag/Bi

T. Cardinal Bordeaux

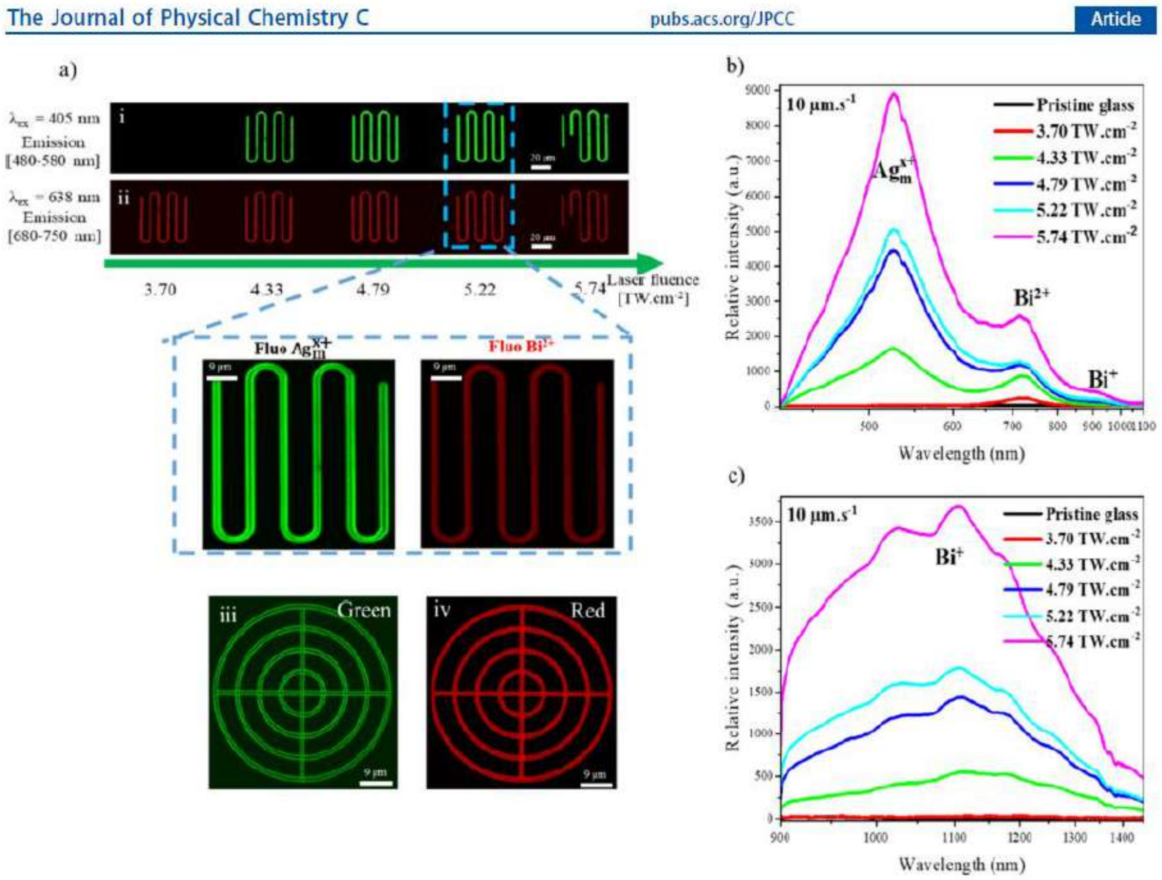

Alassani et al J Phys Chem C 2024

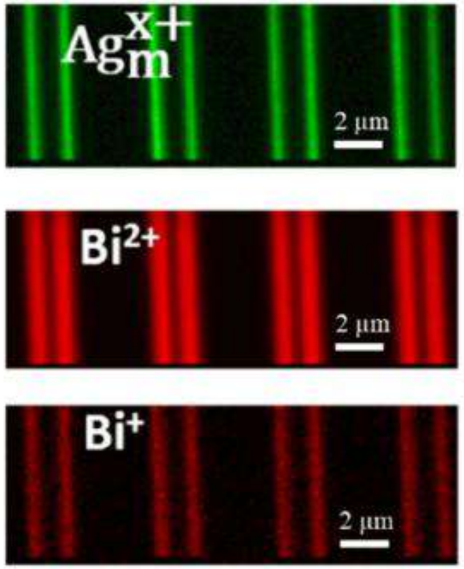

Radiation-Induced Attenuation (RIA)

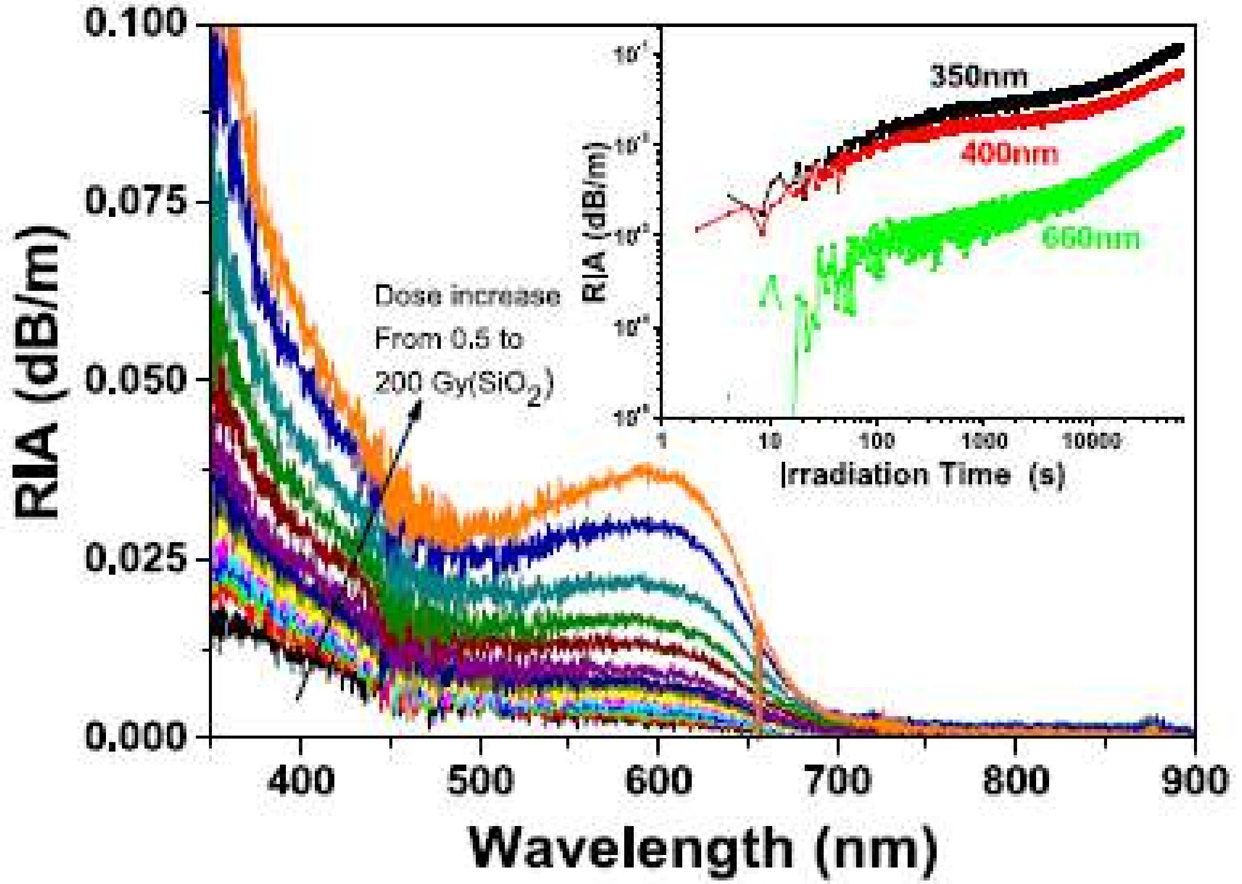

S. Girard et al. J. Opt 2018

Radiation effects

Mainly RIA

But RIE (Cerenkov effect…)

And silica glass compaction so refractive index is modified !

IEEE TRANS. NUCL. SCI.

Overview of Radiation Effects on Silica-Based Optical Fibers and Fiber Sensors

S. Girard, *IEEE Senior Member*, J. Kuhnhenn, A. Gusarov, A. Morana, *Member, IEEE*, P. Paillet, *IEEE Fellow*, T. Robin, L. Weninger, *IEEE Student Member*, F. Fricano, *IEEE Student Member*, M. Roche, *IEEE Student Member*, C. Campanella, G. Mélin, D. Lambert, *IEEE Senior Member*, E. Marin, A. Boukenter, and Y. Ouerdane

S. Girard et al. 2024

RIA depends on ionizing dose, dose rate, temperature, wavelength, and nature of **dopants in the fiber**

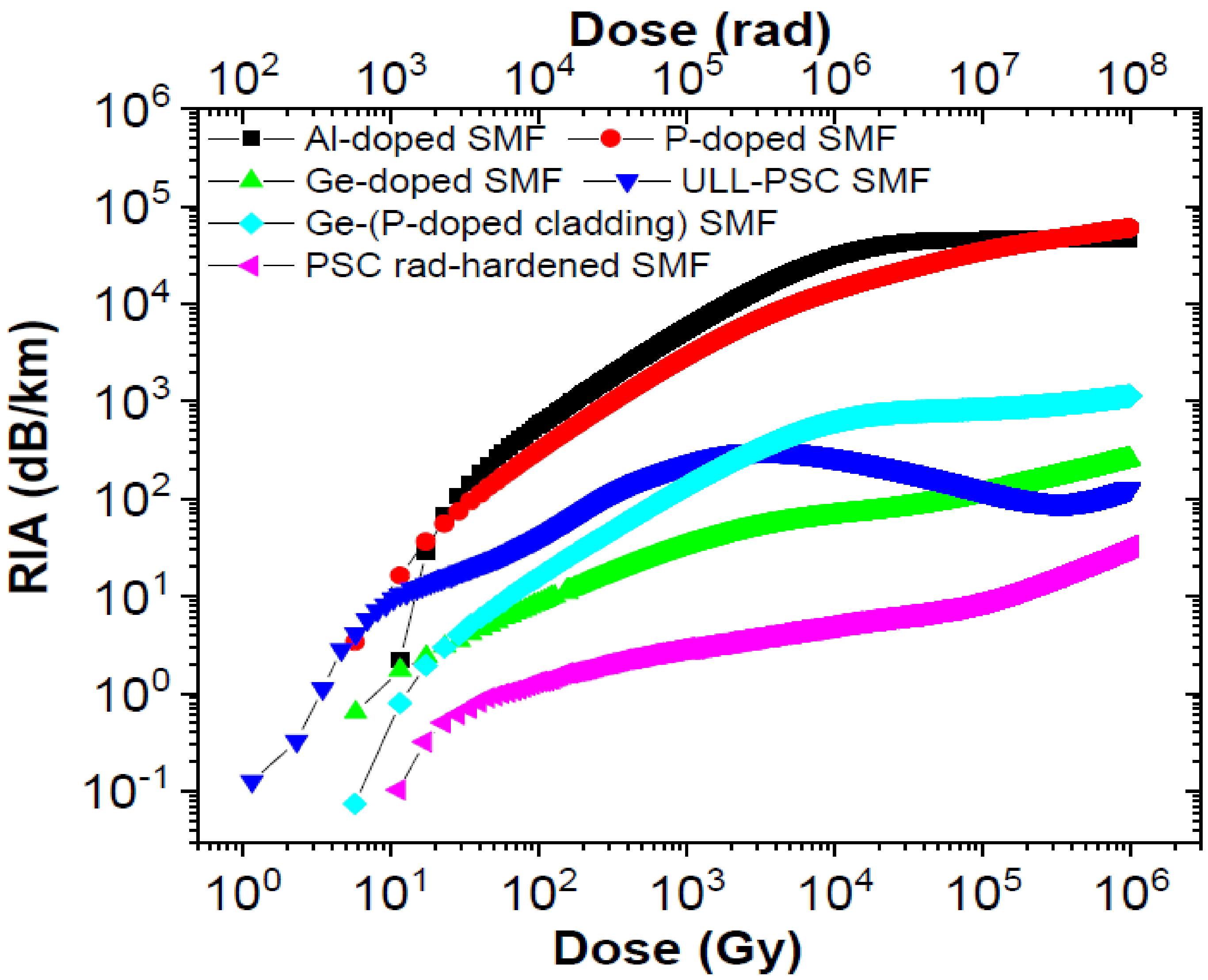

Petrie et al JNCS 2019

P, Al, Ge give rises to specific point defects

Verres dopés TR (laser, amplificateur)

Photodarkening/Radiodarkening: Yb doped optical fibers

- High power laser fiber (1 µm)
- **Photodarkening**

  Formation of color centers
  under the IR laser pump:
  decrease of laser efficiency

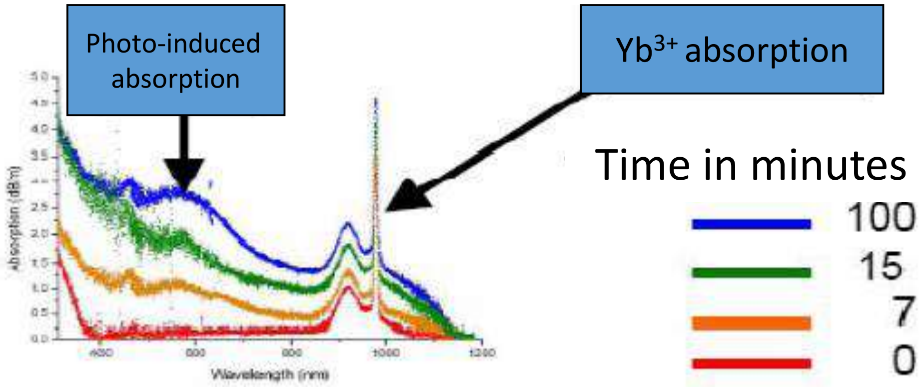

I. Mannek-Hönninger *et al*, OE **15**, 1606 (2007)

- **Radiodarkening:** spatial or nuclear applications

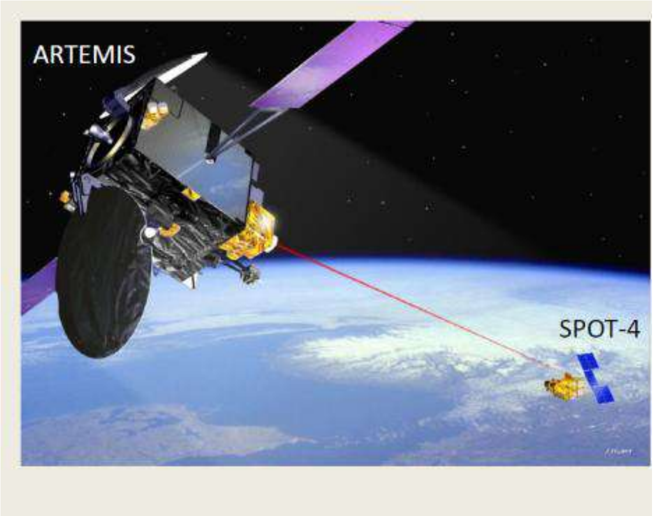

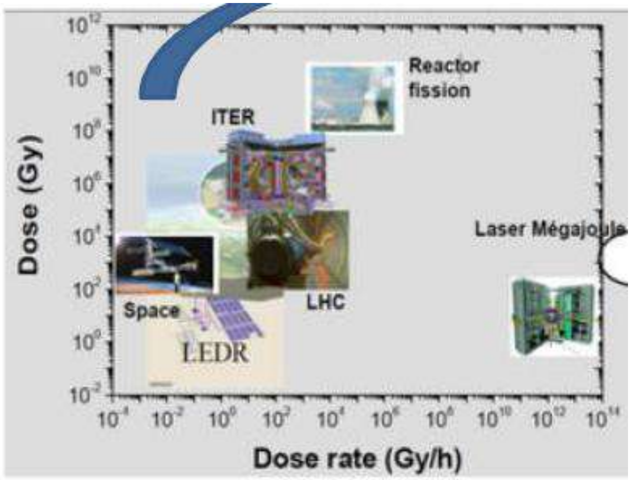

P/Al doped silica preform

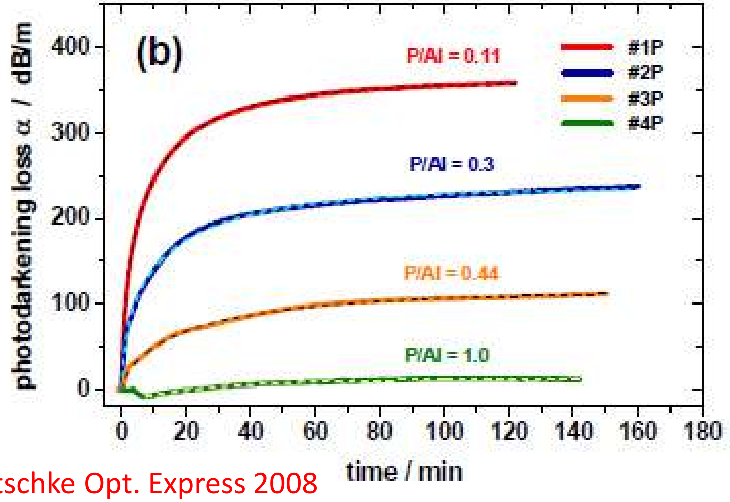

Jetschke Opt. Express 2008

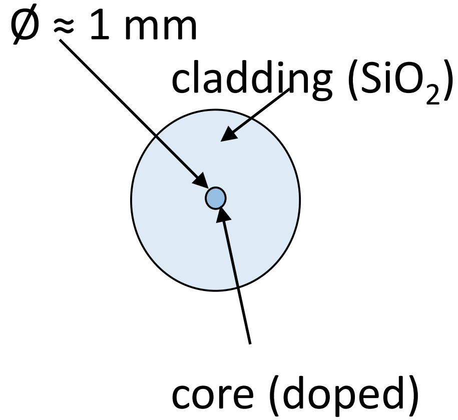

Al/P decrease

P 0.3 ← 1 → 2.8 Al

before gamma irradiation

After gamma irradiation

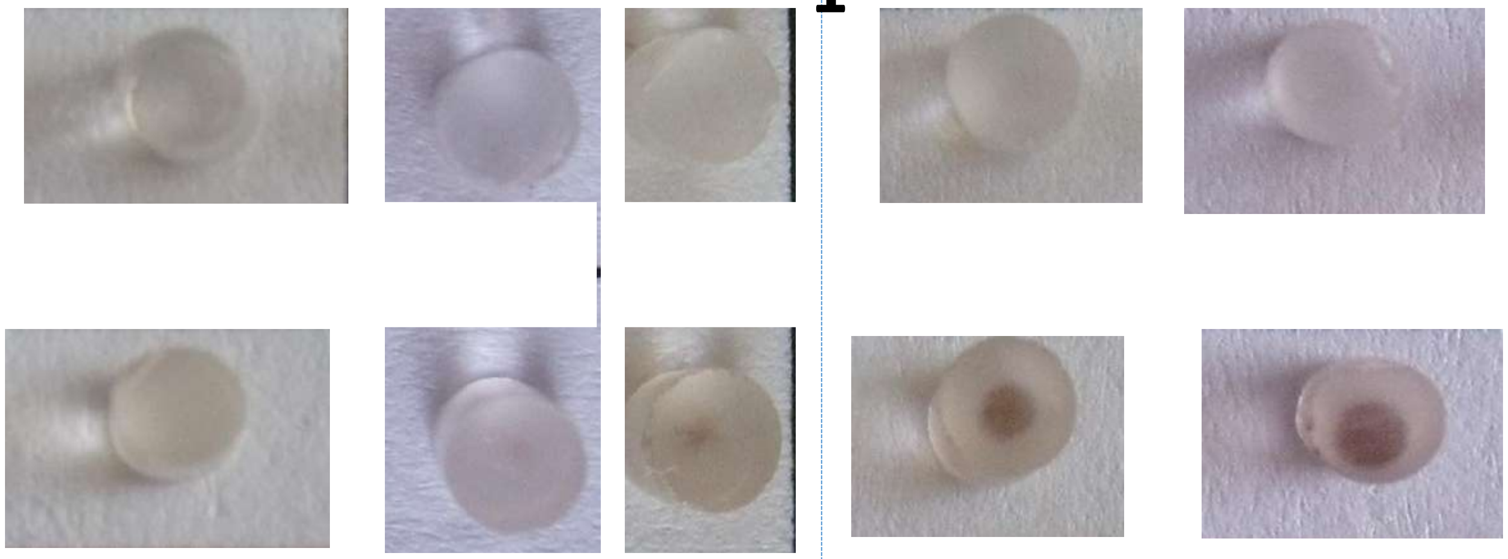

Al/P <1 low coloration of the core under gamma radiation at 1800 Gy

Analysis of point defects in Al/P preforms

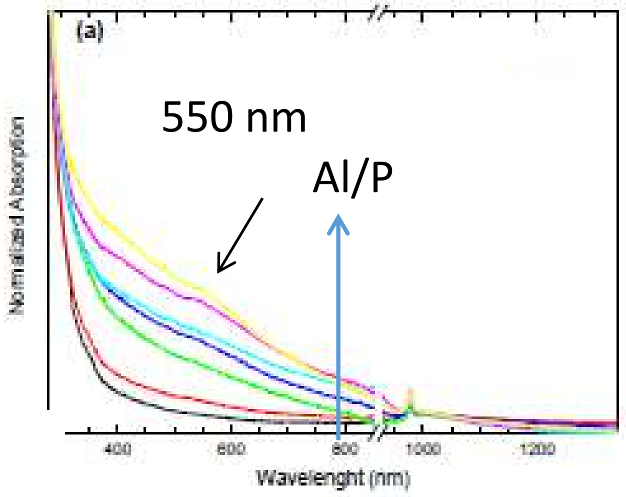

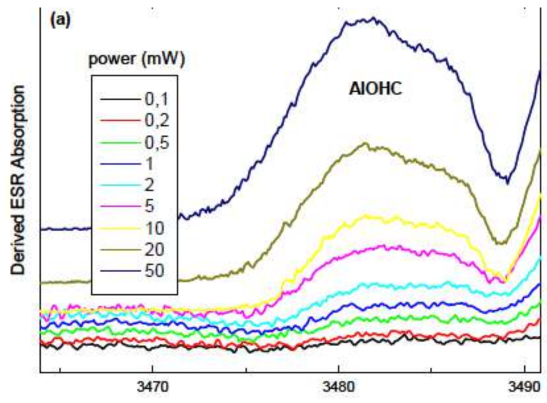

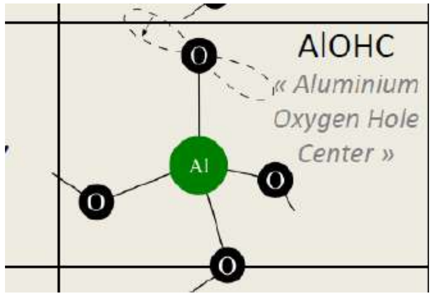

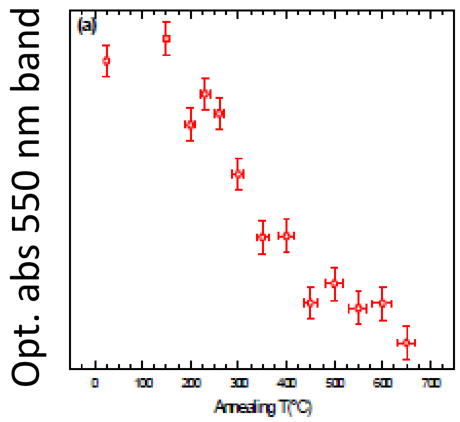

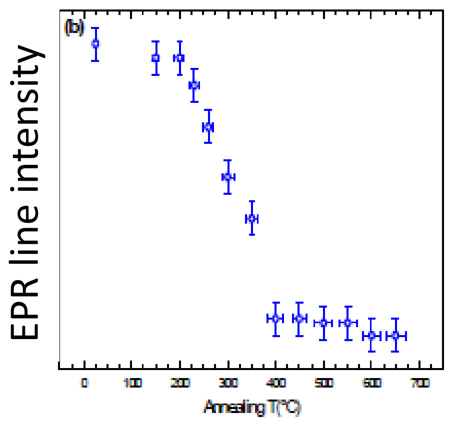

Annealing thermal treatment: attribution of the 550 nm band to AlOHC (Al Oxygen Hole Center)

Identification of defects responsible for preform coloration under gamma irradiation: AlOHC
Al/P<1 no AlOHC

T. Deschamps, H. Vezin, C. Gonnet, N. Ollier (2013) Optics Express 21 8382.

Structural explanation

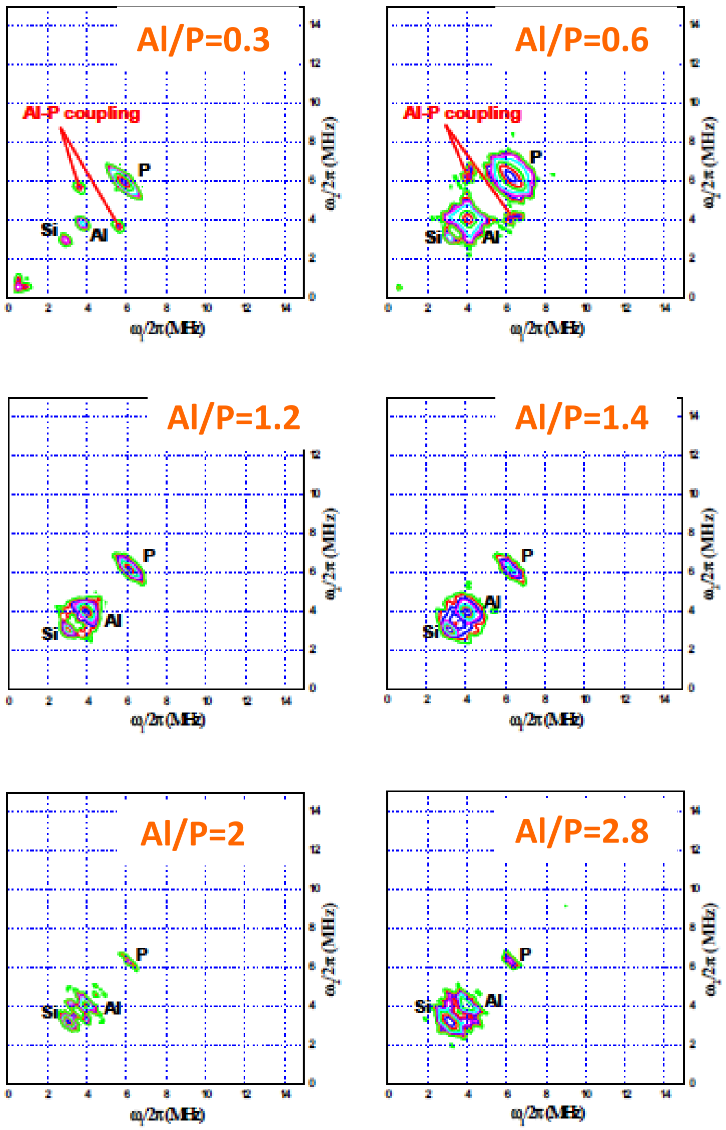

Fig. 7. 2D-HYSCORE pulse ESR spectra of the pristine samples A, B, D, E, F, and G recorded at liquid He temperature and at a magnetic field of 350 mT. A and B samples reveal off-diagonal peaks showing the proximity of Al and P nuclei around Yb^{3+} when phosphorous is introduced in excess compared to aluminium.

Al/P<1

Al-P coupling close to Yb^{3+} ions
$AlPO_{4\ units}$, P-O-P and P=O linkages (Raman)
Inhibition of AlOHC formation thanks to phosphorus presence with P>Al

Al/P>1

no Al-P coupling, isolated Al atoms around Yb^{3+} and formation of AlOHC defect and preform darkening

Phosphorus doping (P>Al) thanks to Al-P coupling inhibits the AlOHC point defect formation

T. Deschamps, H. Vezin, C. Gonnet, N. Ollier (2013) Optics Express 21 8382.

Formation d'ions Yb^{2+}

In situ PL measurements (SIRIUS accelerator)

After the electron beam cut off
Exc: UV pulse laser 355 nm

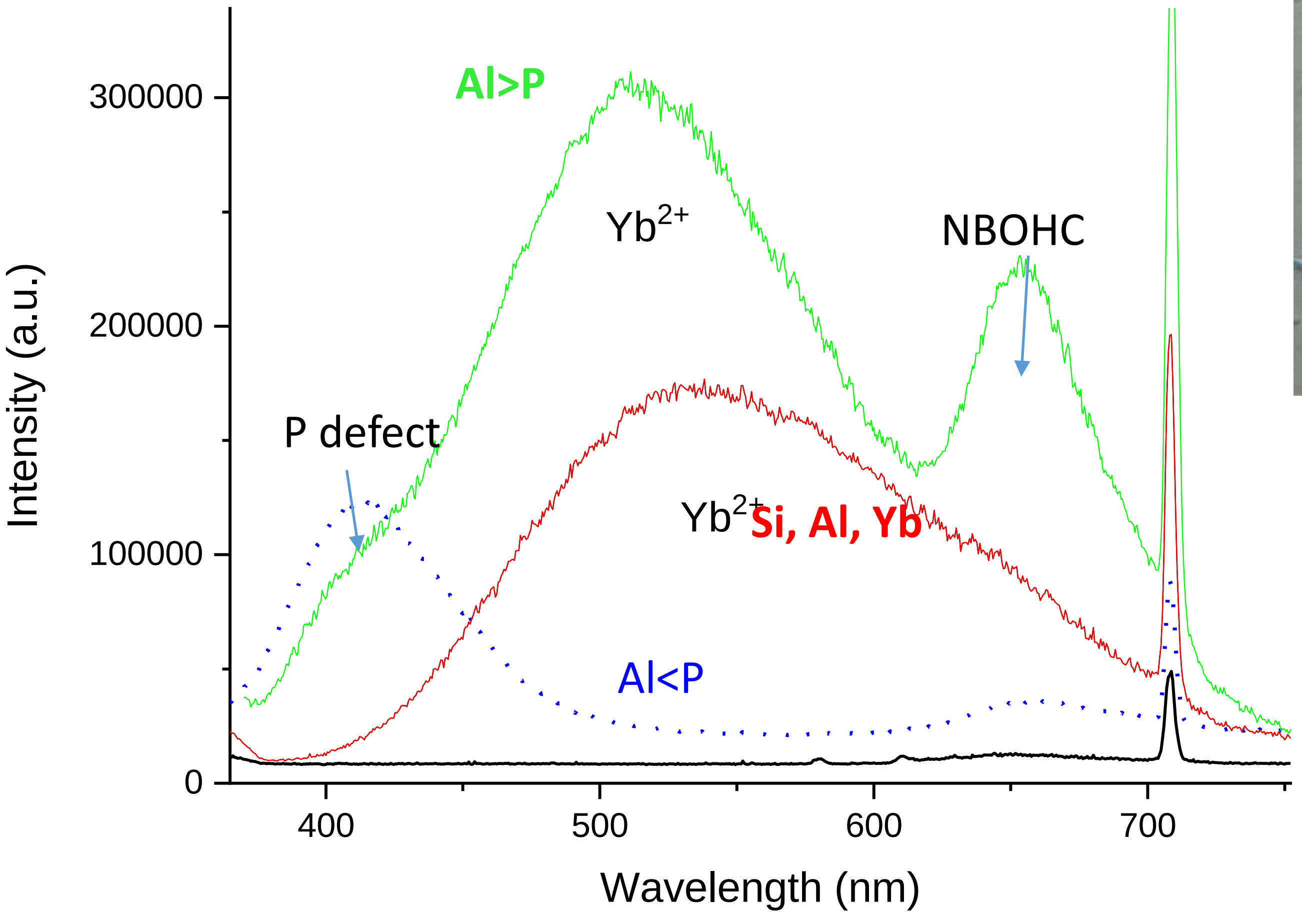

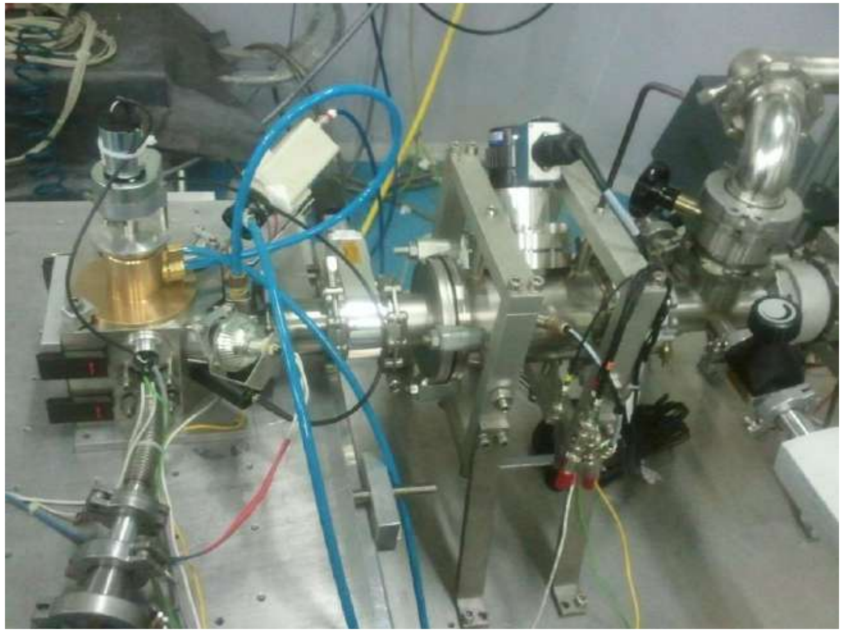

Ollier et al. Opt Letters 2016

Mechanisms for radiodarkening in Yb doped optical fibers

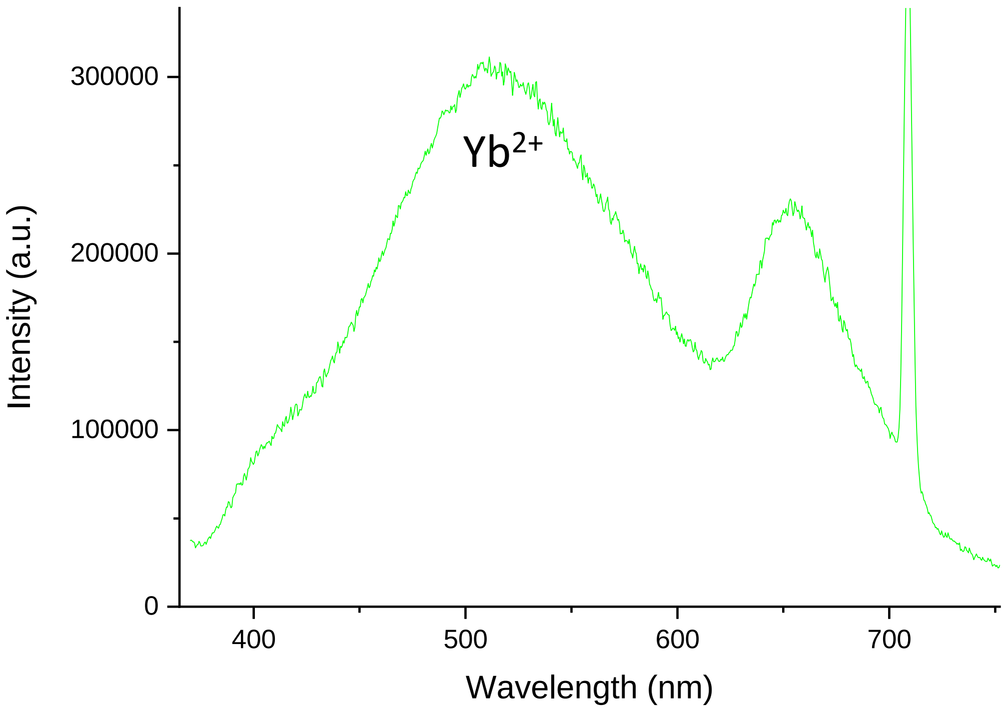

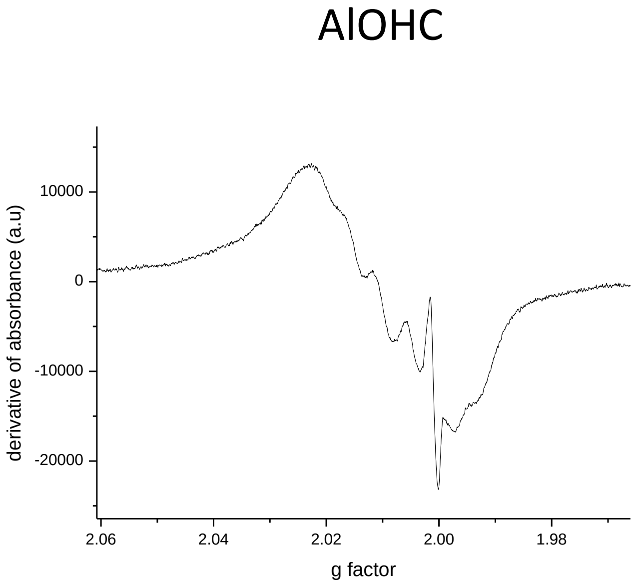

Association of AlOHC-Yb^{2+}

T. Deschamps, H. Vezin, C. Gonnet, N. Ollier (2013) Optics Express 21 8382.

Environnement des ions Yb3+
Présence de clusters

e^--irradiation
γ-irradiation

Défauts ponctuels

Nature

Stabilité

Propriétés de luminescence des ions Yb3+

Thèse de V. Pukhkaya (IP 2013)

Verres aluminosilicates dopés avec 5wt. % Yb_2O_3

Sample name	SiO_2, % mol.	Al_2O_3, % mol.	Na_2O, % mol.	ASI Al/Na	
AS22	74	6	20	0.3	+ 5% mass. Yb_2O_3
AS23	68	12	20	0.6	
AS24	62	18	20	0.9	
AS26	58	22	20	1.1	

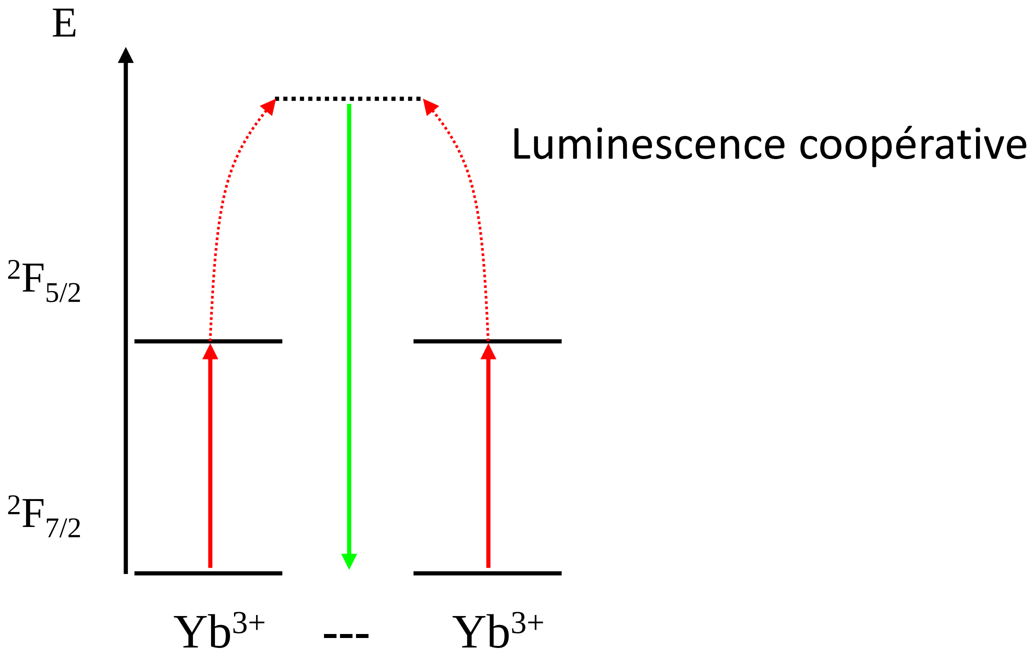

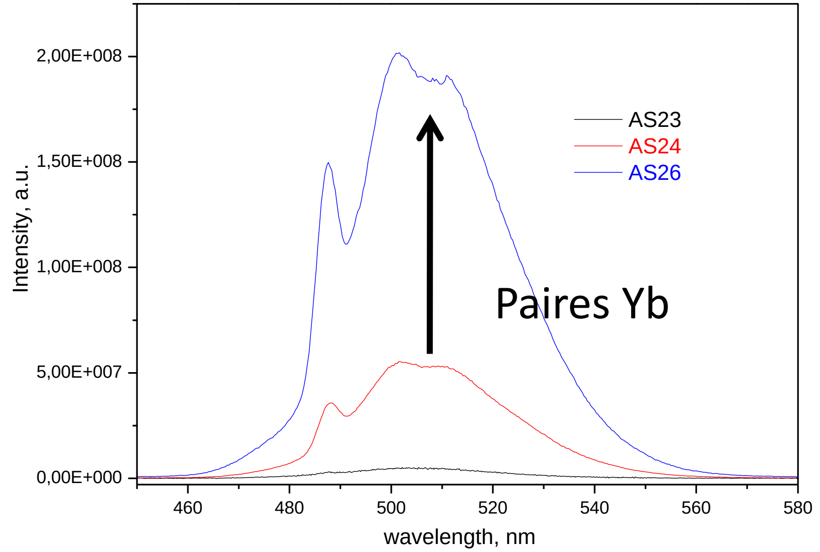

Nombre d'agrégats augmente avec la diminution du nombre d'oxygènes non pontants

Teneur en Yb: défauts

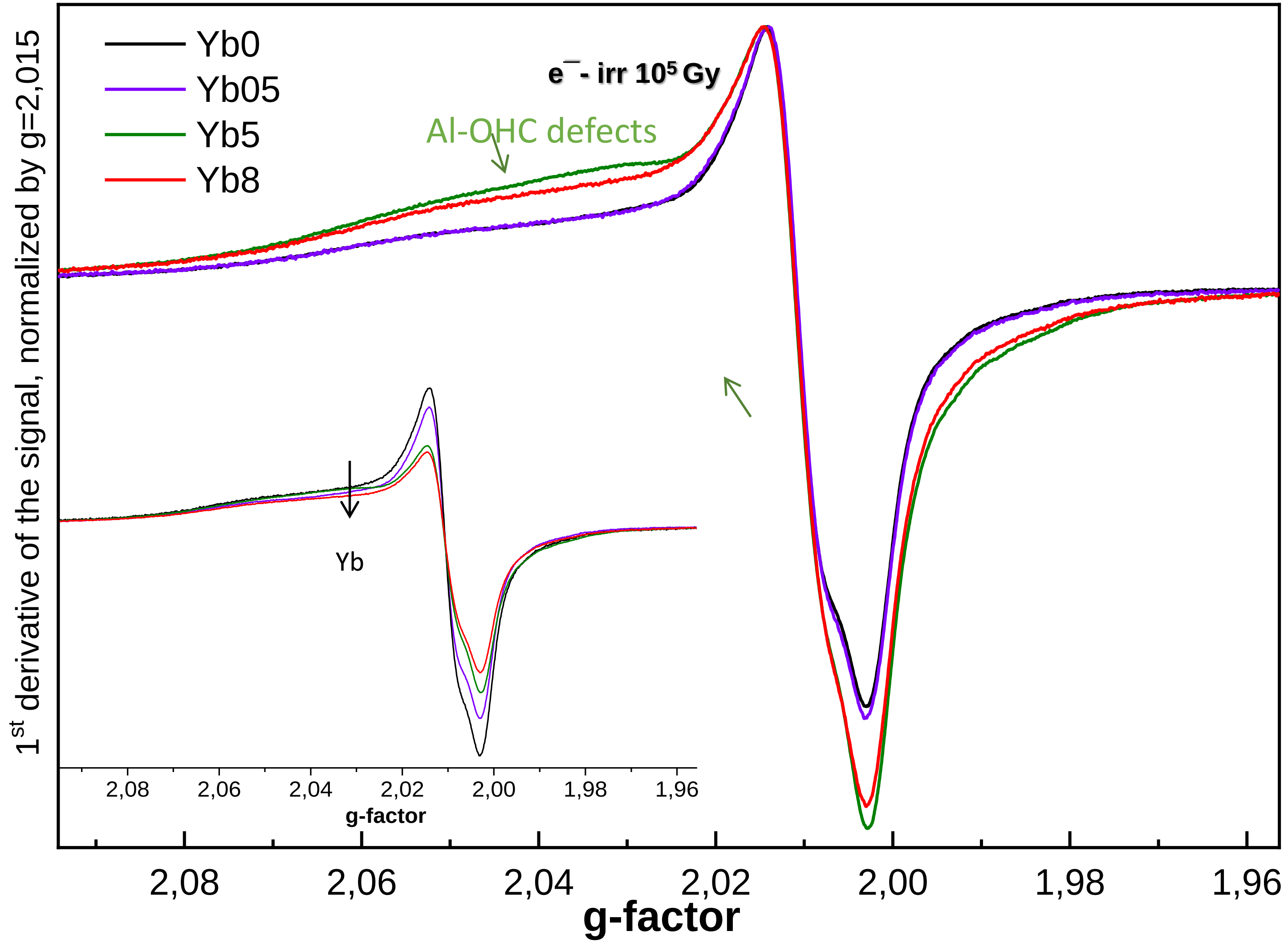

- **In Yb-doped glasses less hole centers are created. Yb-doping leads to relatively higher amount of Al-OHC defects up to 5% mass. of Yb_2O_3**

Limitation of point defects by glass doping

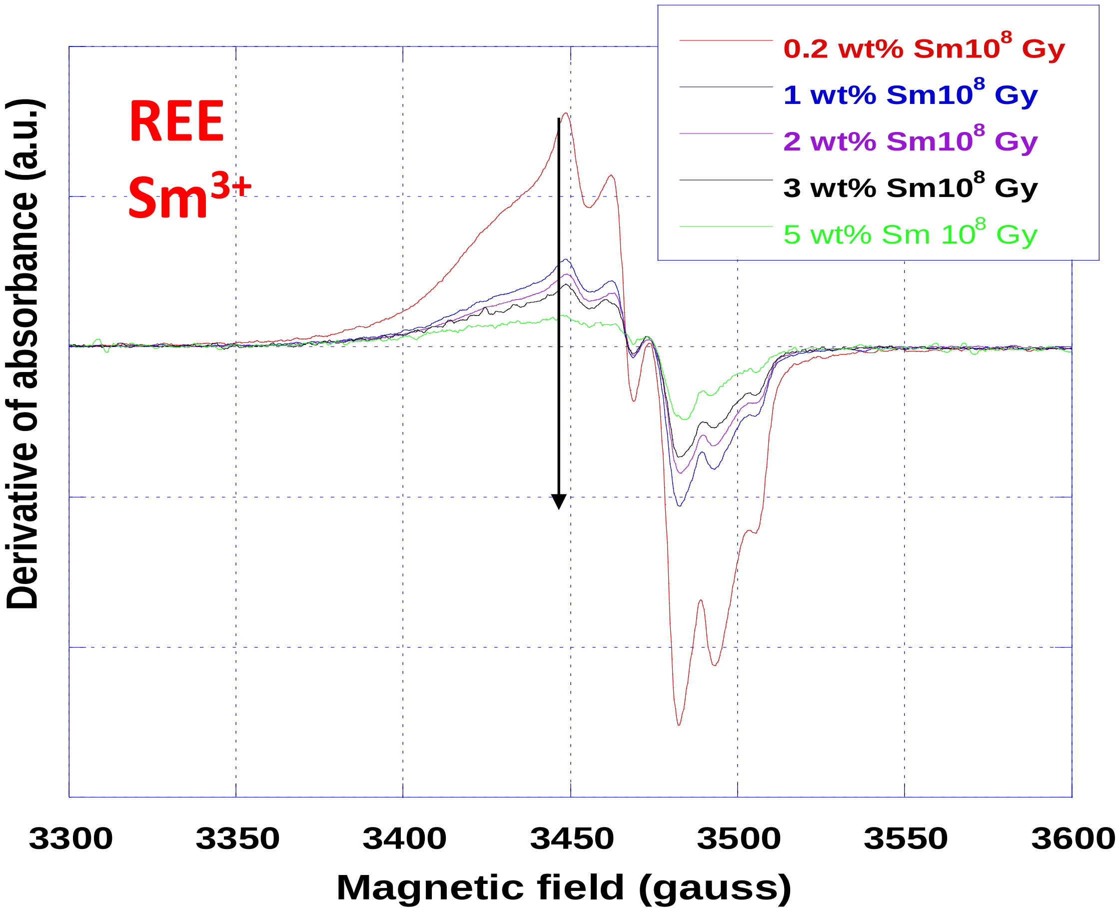

Malchukova, et al., Nucl. Instr. and Meth. in Phys. Res. A 537 (1-2) (2005) 411.

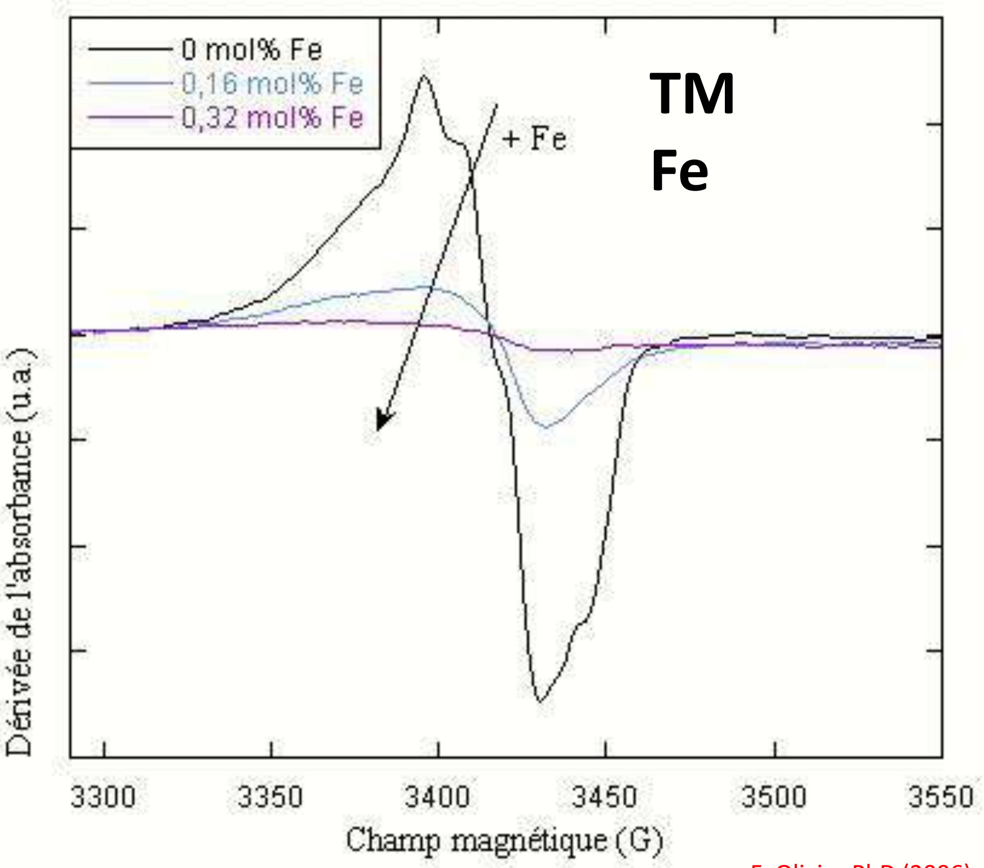

F. Olivier PhD (2006)

$Fe^{3+} + e^{-} \Rightarrow Fe^{2+} + h^{\circ} \Rightarrow Fe^{3+}$

$Fe^{2+} + h^{\circ} \Rightarrow Fe^{3+} + e^{-} \Rightarrow Fe^{2+}$

Same effect with Gd^{3+}, Eu^{3+}, Mn^{2+}, Cr^{3+}...

Stabilité des défauts paramagnétiques après irradiation: impact des clusters

Défauts paramagnétiques (g=2)

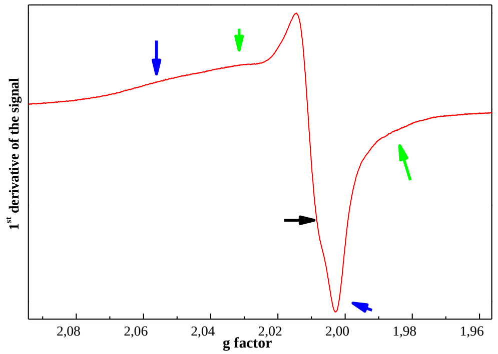

Pukhkaya et al. Opt Exp 2013

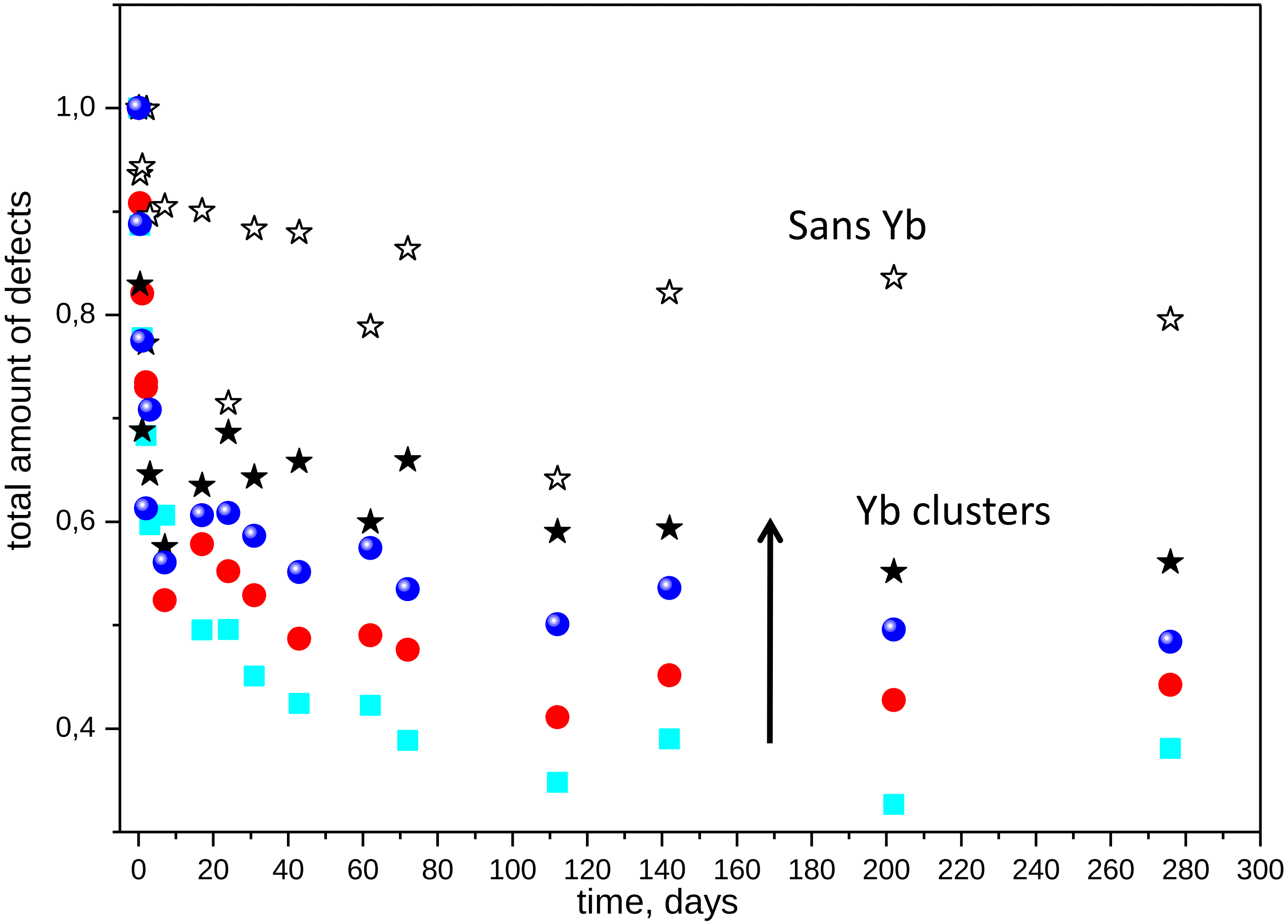

Dopage en Yb accélère la recombinaison des défauts paramagnétiques en accord avec les verres ABS

Présence de clusters d'Yb ralentit la recombinaison des défauts (piégeage stable de charges au sein des clusters)

Evolution de la durée de vie du niveau $^2F_{5/2}$ avec la dose intégrée

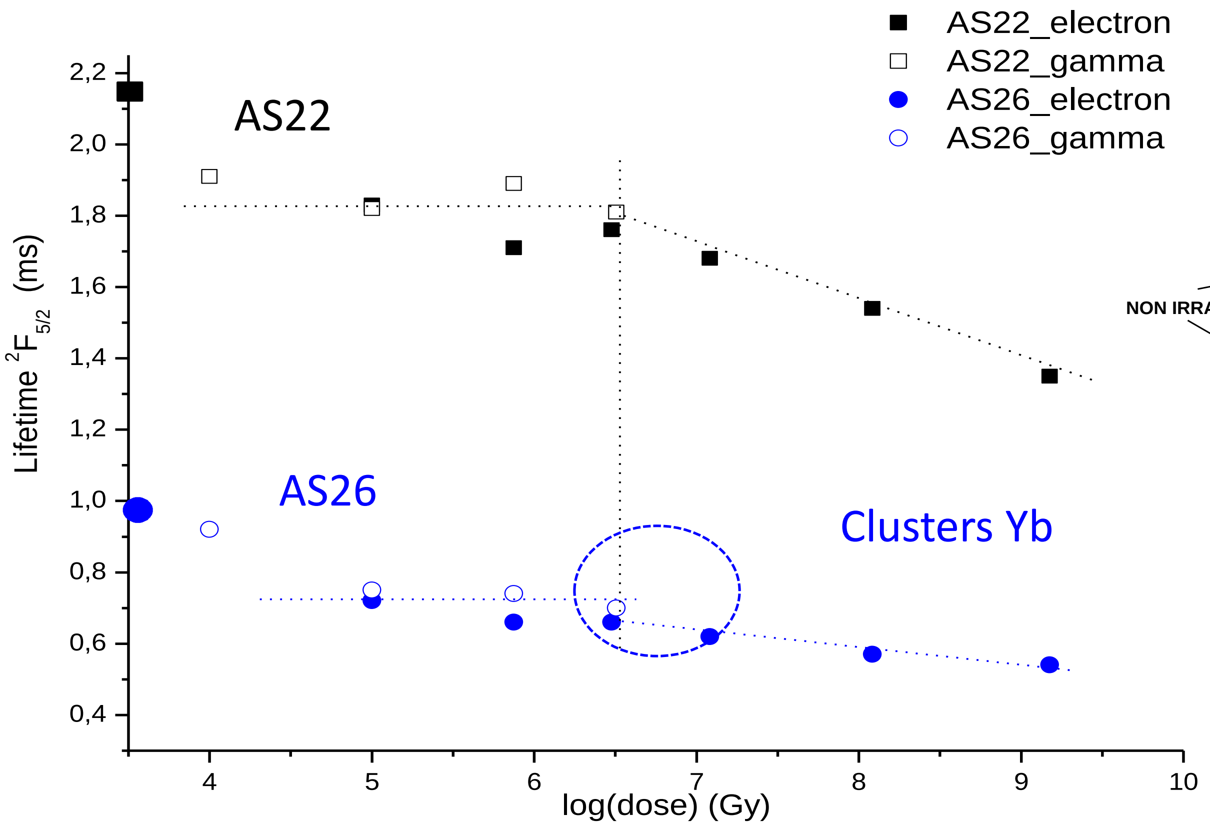

Pukhkaya et al. Opt Exp 2013

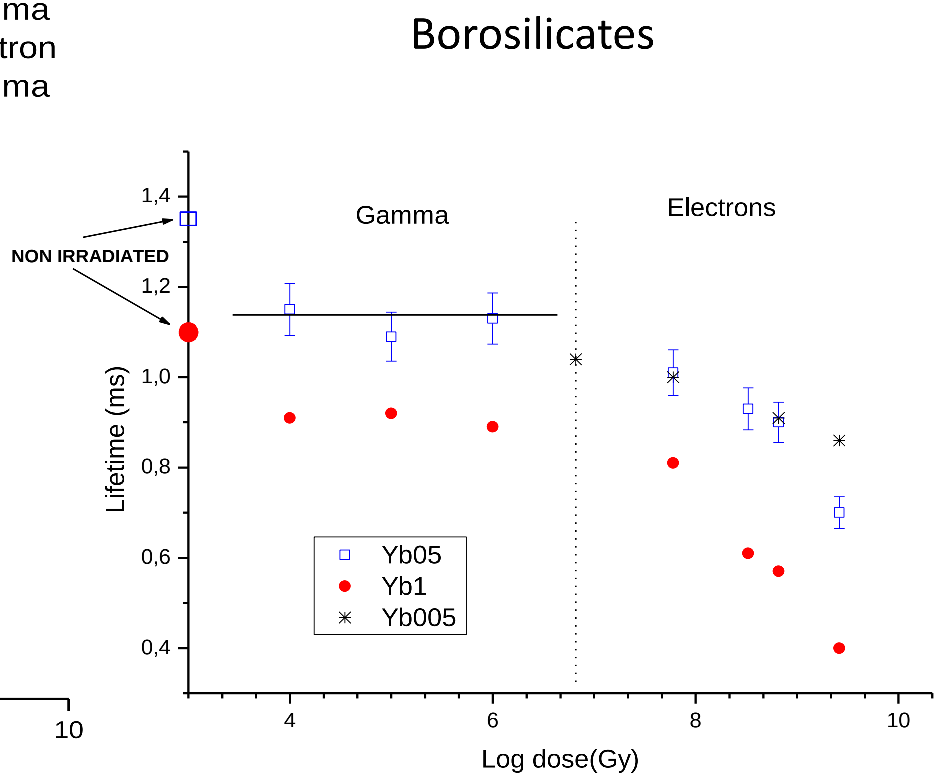

Ollier et al. JNCS 2011

2 régimes: plateau et diminution linéaire avec le log de la dose

Effet atténué par la présence de clusters

Changement de densité sous irradiation
La silice

Densification of silica (and relaxation) under radiation

Gamma, X-rays,
neutrons, electrons,
and ions irradiation

Densification limited to 3%

But also relaxation of densification

Defects formation

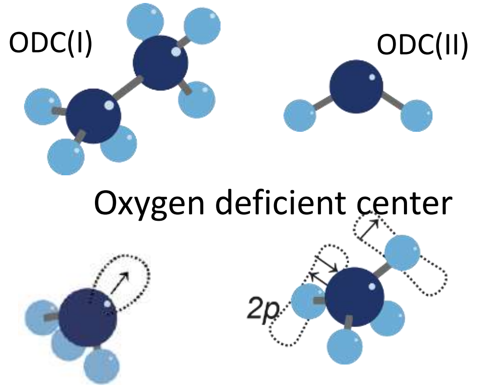

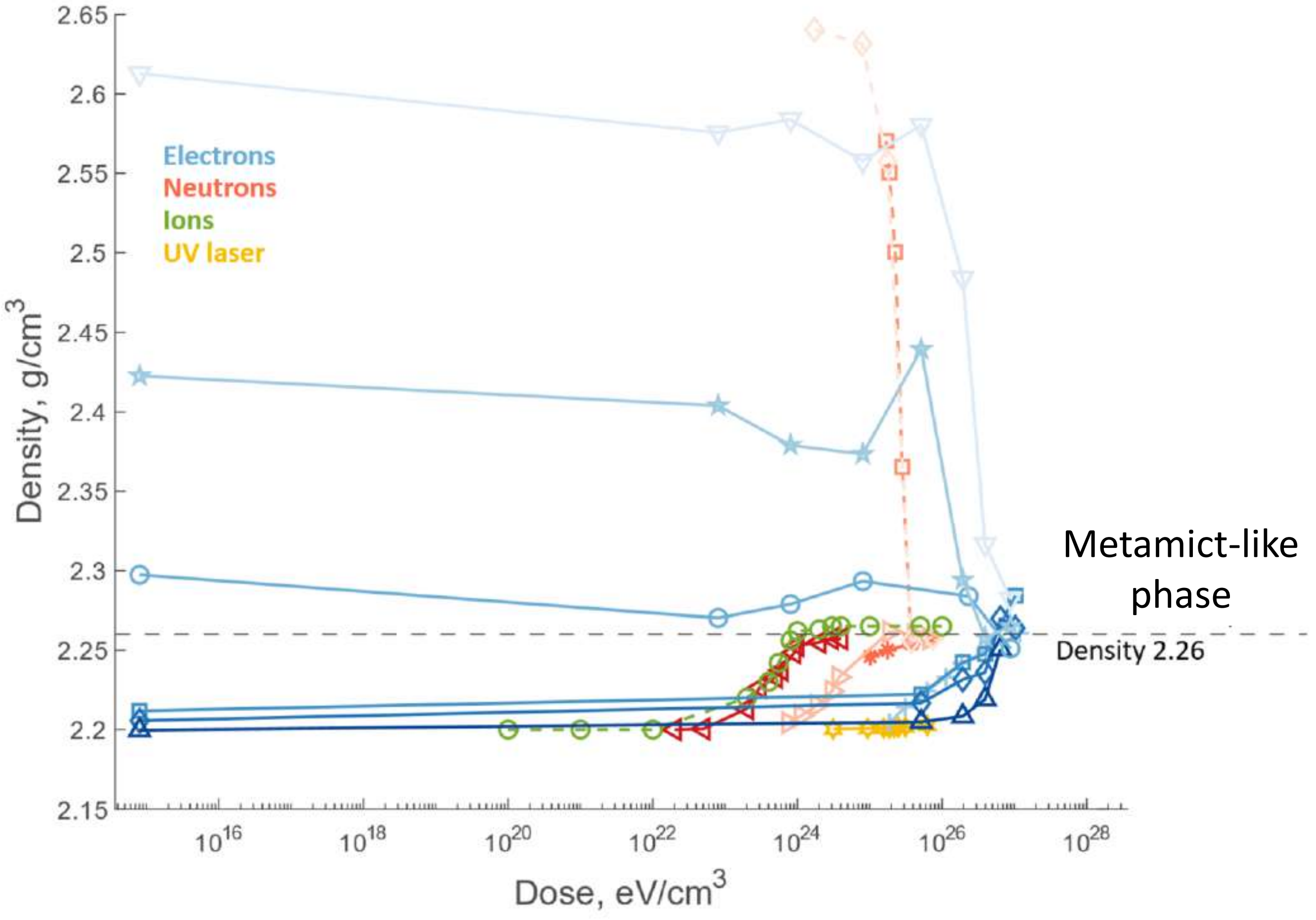

Dependence of silica density on the irradiated dose

Mobasher M.et al. JNCS, 597 (2022)

Evolution de la bande D2 avec la dose

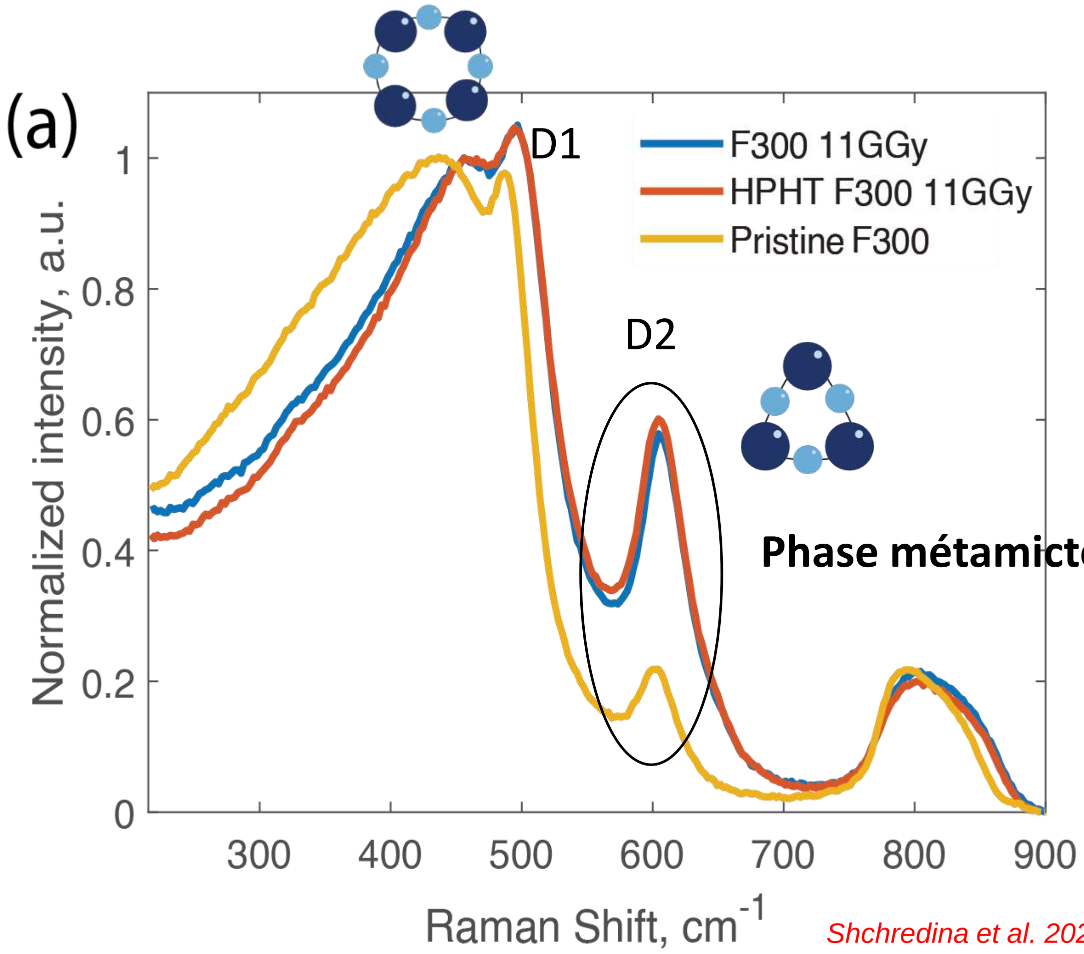

Shchredina et al. 2025 JNCS

Augmentation de l'intensité de la bande D2 avec la dose

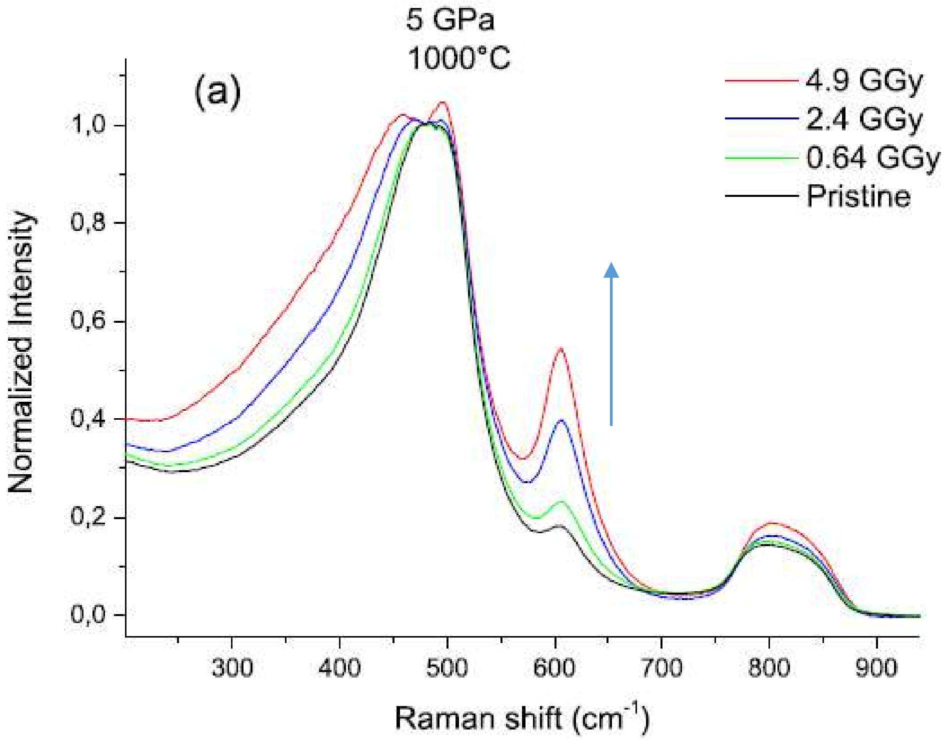

Ollier et al. Sc. Rep 2019

D1 and D2 band intensity: high number of 4 and 3 membered rings
Shift of 17cm^{-1} of main band (- 3° of Si-O-Si angle decrease)

Fiber Bragg Grating sensors in nuclear environment

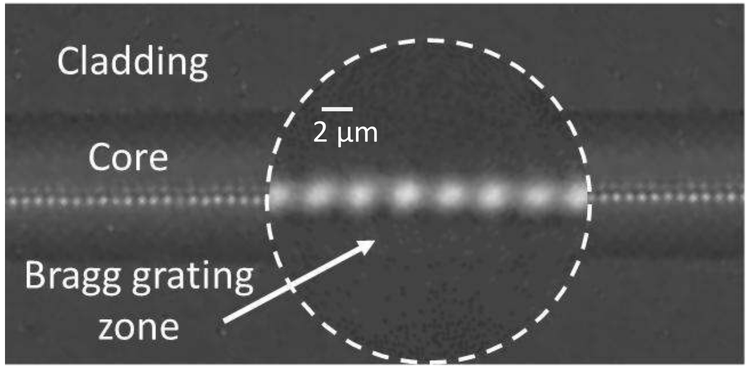

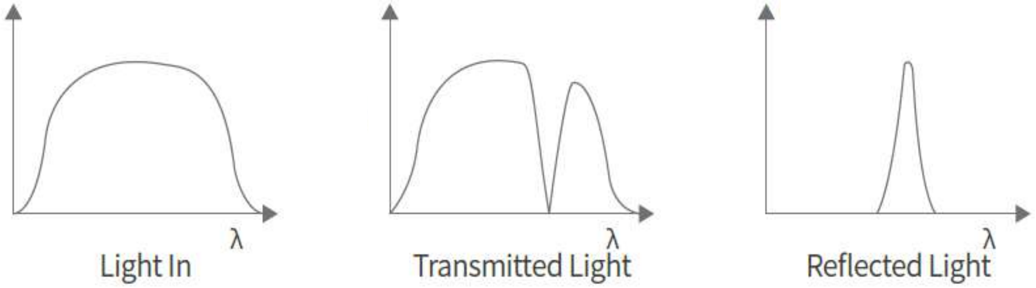

Bragg wavelength

Fs-laser FBG sensors for monitoring

pressure temperature stain/stress

Environment		Radiation Nature	Dose	Dose-Rate	Temperature	References
Nuclear Reactor Core		γ-rays neutrons	GGy 10^{20} n·cm^{-2}	<10^{15} n·cm^{-2}·s^{-1}	RT → 800 °C	[18–31]
Fusion-devoted facilities	Tokamak (e.g., ITER)	γ-rays 14 MeV neutrons	<10 MGy <10^{18} n·cm^{-2}	1 kGy/h <10^{14} n·cm^{-2}·s^{-1}	RT → 400 °C	[32]
	LMJ, NIF	X-rays γ-rays 14 MeV neutrons	<1 kGy	>MGy/s	RT	
High-energy physics facilities	LHC	photons electrons other particles	<100 kGy	<0.1 Gy/h	RT	[33–36]
Nuclear Waste Storage		γ-rays	<10 MGy	<10 Gy/h	RT → 90 °C	[37,38]
Medicine		X-rays protons	10^{-2} Gy → 50 Gy	<1 Gy/s	RT	[39]
Space		X-rays γ-rays protons electrons	<10 kGy	10^{-5} → 10^{-3} Gy/h	−200 °C → 300 °C	[40]

Morana et al. Sensors 2022

Change in silica refractive index/ density ?

Effets d’irradiation sur les fibres à réseaux de Bragg

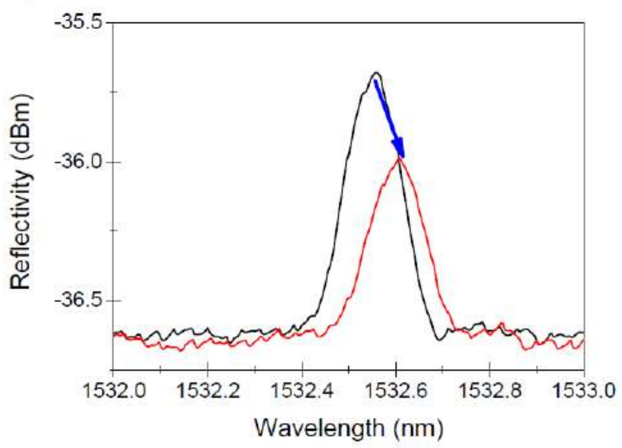

Figure 2. An example of the radiation-induced effects on a Bragg peak reflection spectrum, before (black line) and after (red line) X-ray irradiation at 1.5 MGy TID at RT. Data extracted from [73].

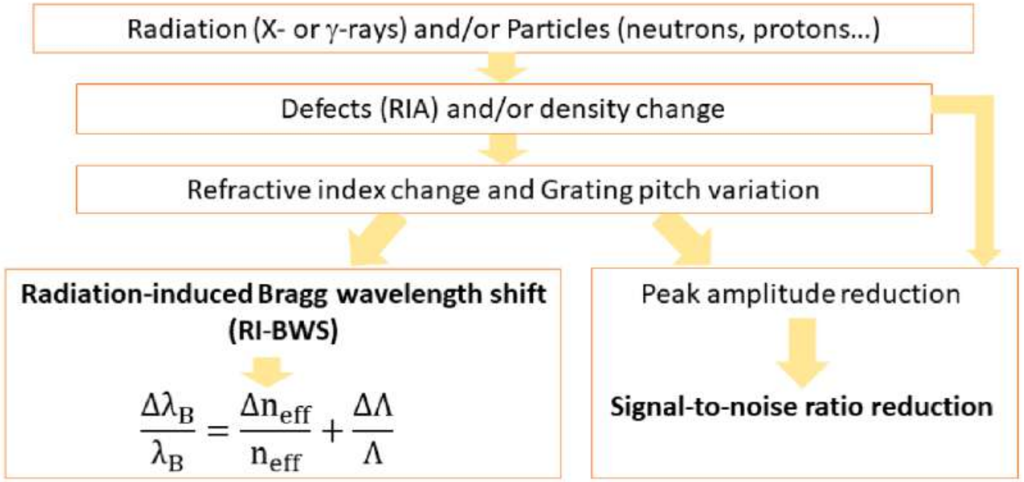

Review

Radiation Effects on Fiber Bragg Gratings: Vulnerability and Hardening Studies

Adriana Morana [1], Emmanuel Marin [1], Laurent Lablonde [2], Thomas Blanchet [3], Thierry Robin [2], Guy Cheymol [4], Guillaume Laffont [3], Aziz Boukenter [1], Youcef Ouerdane [1] and Sylvain Girard [1,*]

C.Petrie Oakridge USA
G. Laffont CEA
S. Girard LHC St Etienne

Shift sensible à la dose, température, type d’inscription…

Morana et al. Sensors 2022

Threefold rings: D2 band vs dose and temperature

SiO_2

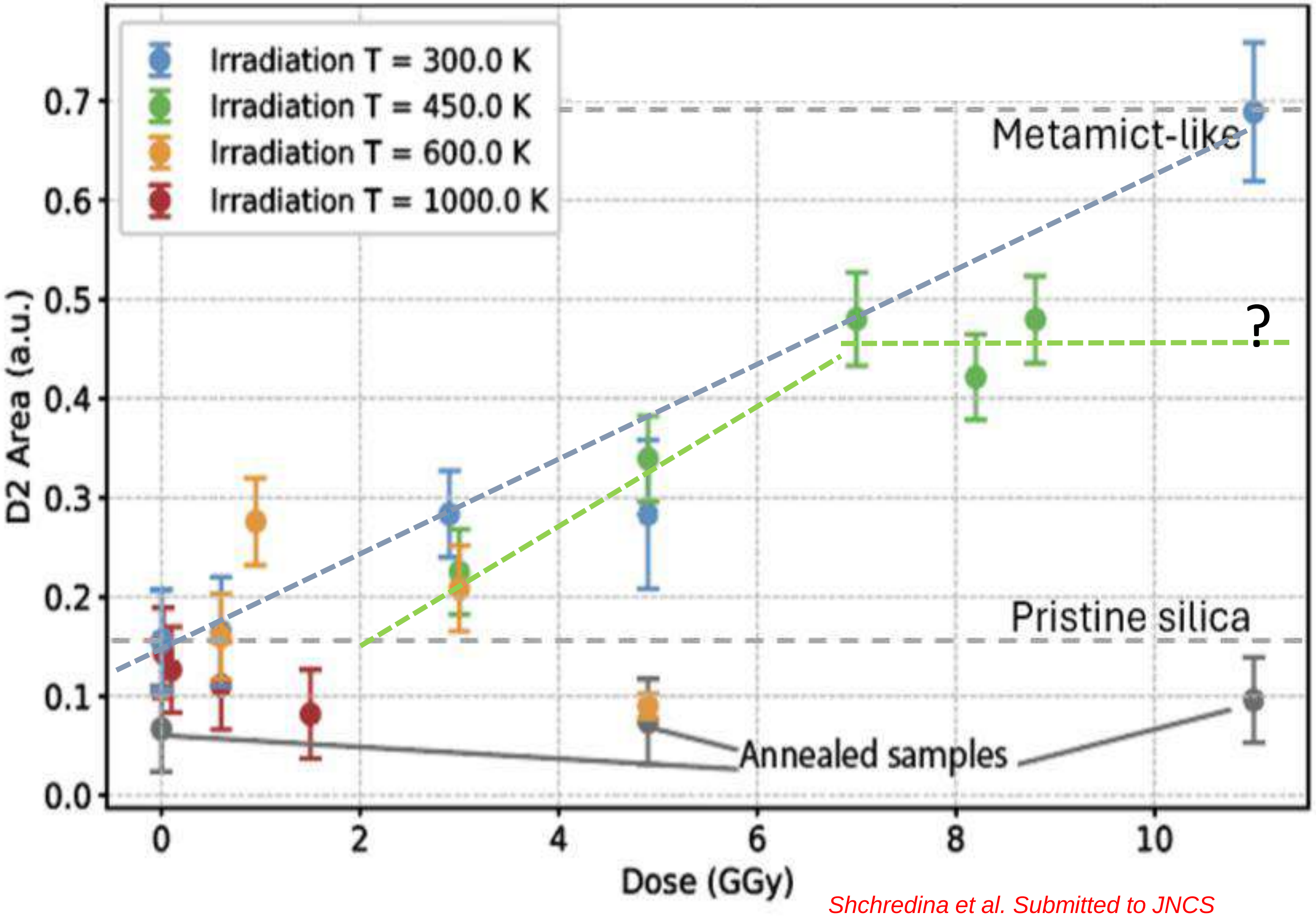

Shchredina et al. Submitted to JNCS

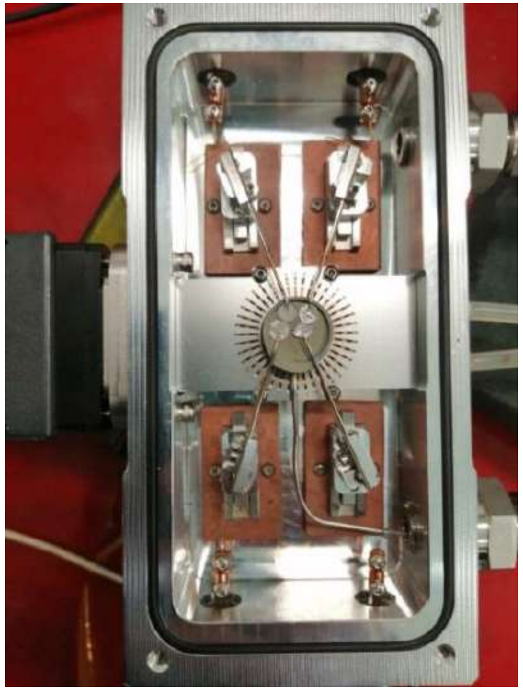

- forward reaction of **electron-driven defect production** (and associated densification), whose rate constant k_1(dose,T)
- **backward-erasure reaction** i.e. a thermally activated defects annihilation with a rate constant k_{-1}(T).

SiO_2

Défauts: centres E’

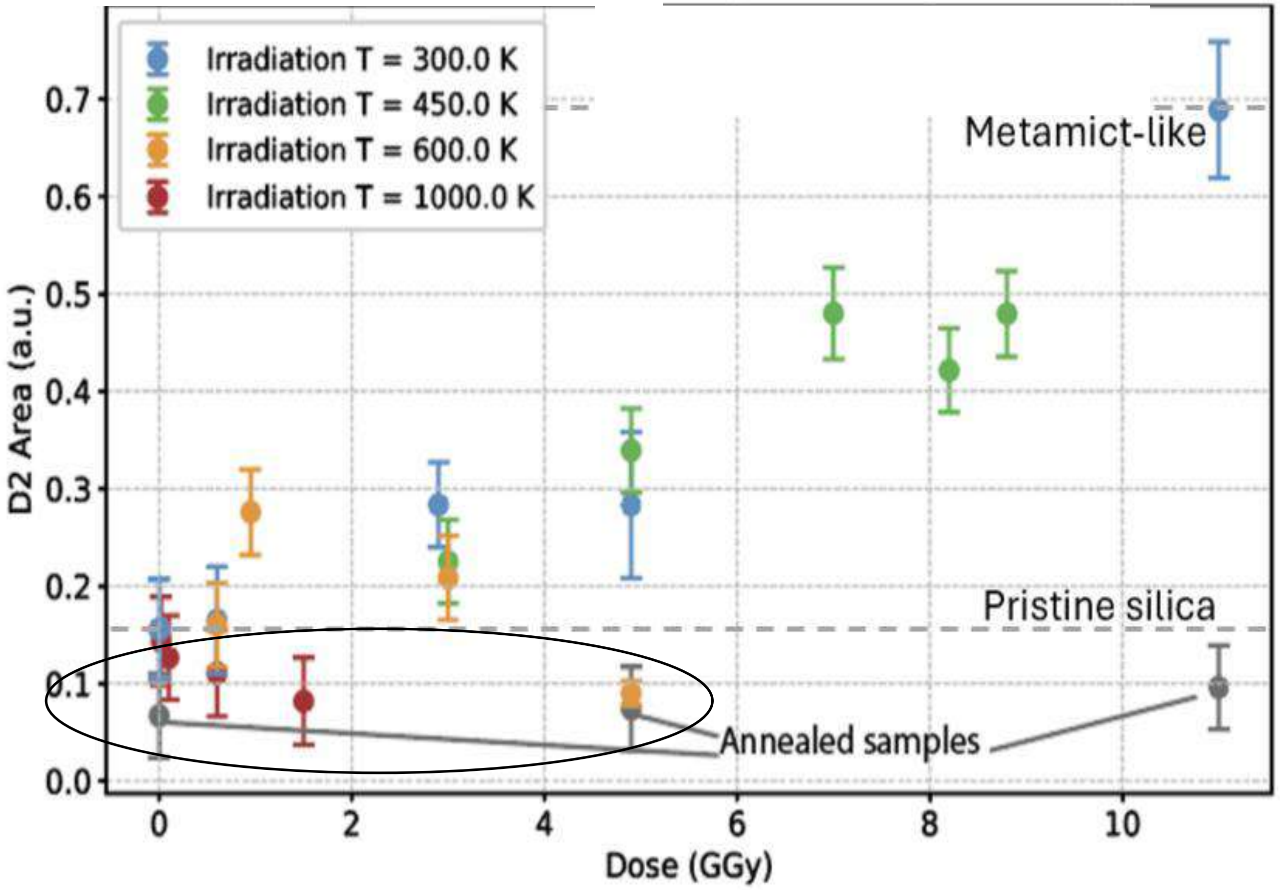

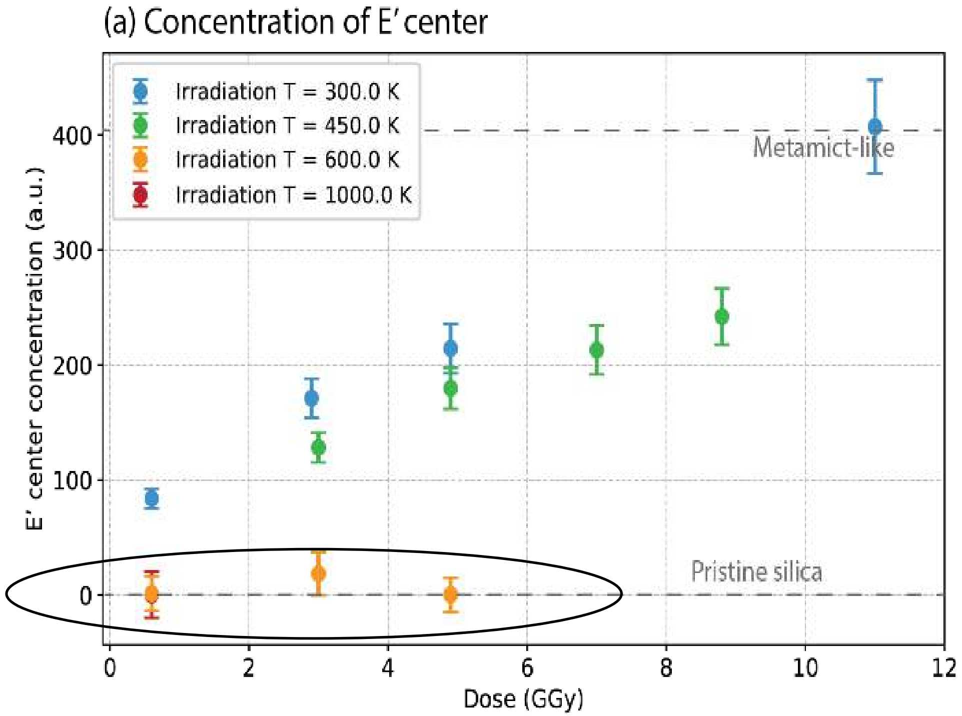

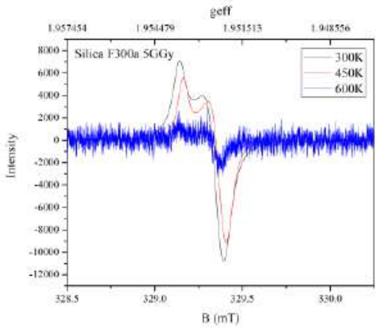

Shchredina et al. Submitted to JNCS

Verres pour l'optique en environnement radiatif

Défauts ponctuels

- Couleur
- Transmission et efficacité laser des fibres optiques
- Indice de réfraction/ densité
- Propriétés de luminescence (durées de vie)

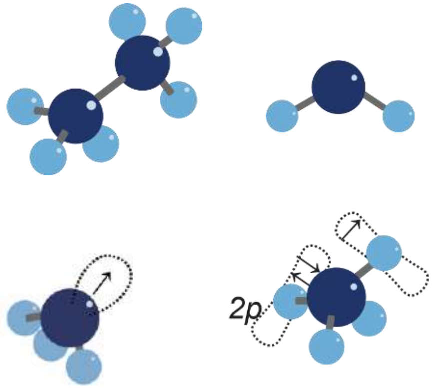

E' center

Silica density impact on the green emission band

Ollier et al. JNCS 2017

Hypotheses on the origin of the green emission from literature in silica

•Silanone surface groups in Si Nanoparticles
2.27 eV
25 ns

$(\equiv Si-\dot{O})_2Si{=}O$

Vaccaro et al J Phys Chem C 2011

• **E'$_\delta$ (point defects)**
2.20 eV

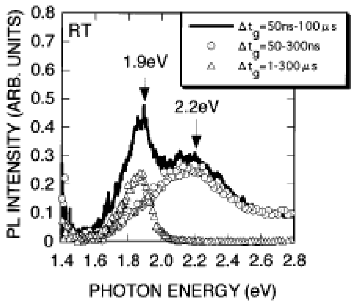

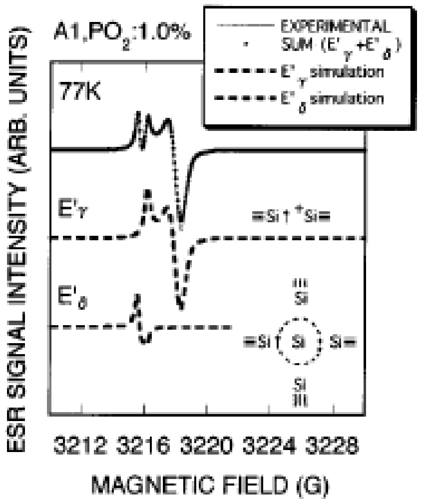

Nishikawa et al JAP 1996

the unpaired electron is delocalized over four sp^3 hybrid orbitals of nearby Si atoms

• **Defect associated with Si excess (Si+ implanted silica)**

Shimizu-Iwayama et al JAP 1994

•Self Trapped Excitons (STE)
•Small Peroxy Radicals (SPOR): Y. *Sakurai et al. JAP 2000*

Conclusions

Glass composition has an impact on defects formation under ionizing irradiation…:

❖ ASI increase→total amount of defects decreases, more Al-OHC defects are formed

❖ Incorporating of Yb→less defects formation, less E' centers and relatively more Al-OHC defects

…and its afterwards relaxation:

❖ Al content and/or Yb clusters influences on relaxation rate

Er^{3+}

Impact of defect on glass properties

- Refractive index variation (laser interaction)

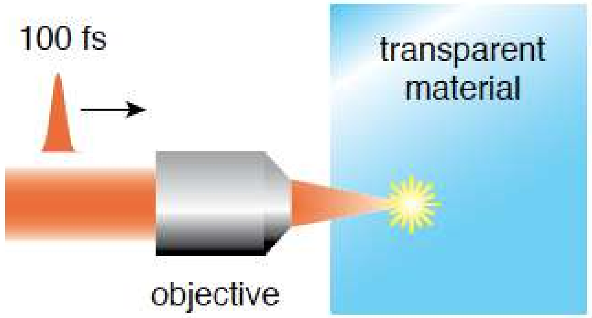

$$\Delta n(\lambda) = \frac{1}{2\pi^2}\int_0^{\infty} \frac{\Delta\alpha(\lambda')}{1-\left(\frac{\lambda'}{\lambda}\right)^2} d\lambda'$$

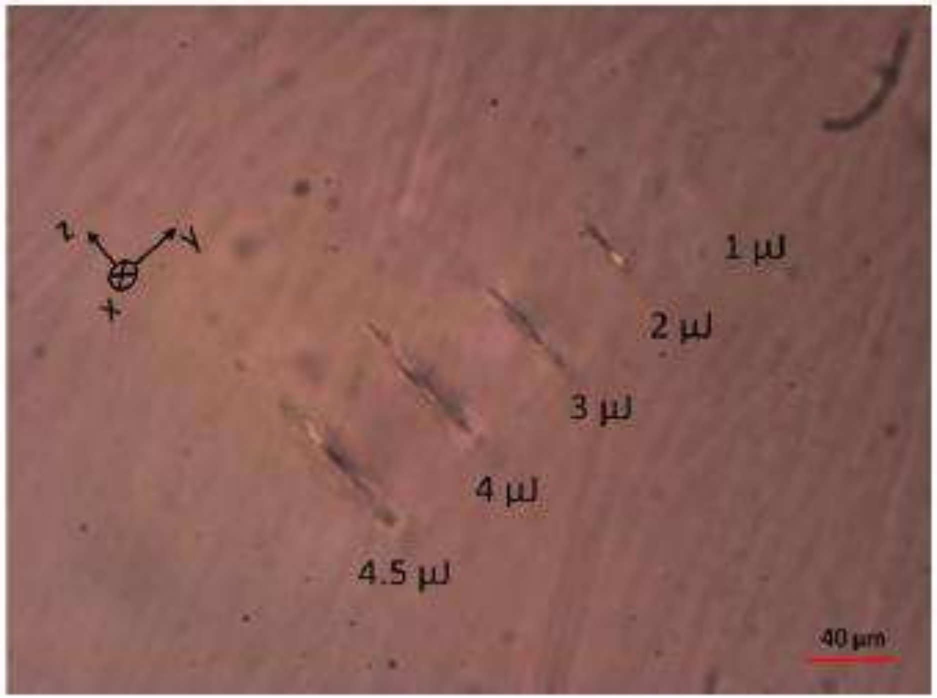

Bragg gratings in optical fibers !!

Mahfoudhi PhD (2019)

- Dosimetry: Gorilla glass, optical fibers ….

Thanks for your kind attention !

The defects related to the green luminescence ~550 nm

- The origin of defects that generate the green luminescence at ~550 nm is still unknown!

- Some investigations assigned them to the **STE** (Self Trapped Excitons) but they can be observed at RT!

- Other studies suggest to attribute this luminescence to **E'**$_{\delta}$, however, the in no clear correlation between the EPR signal and this luminescence.

- These defects that emit at ~550 nm are radiation induced defects (either observed in the samples densified by means of irradiation (neutrons, ions, UV lasers …) or in mechanically densified silica after being irradiated.

Density impact on NBOHC emission band

532 nm exc.

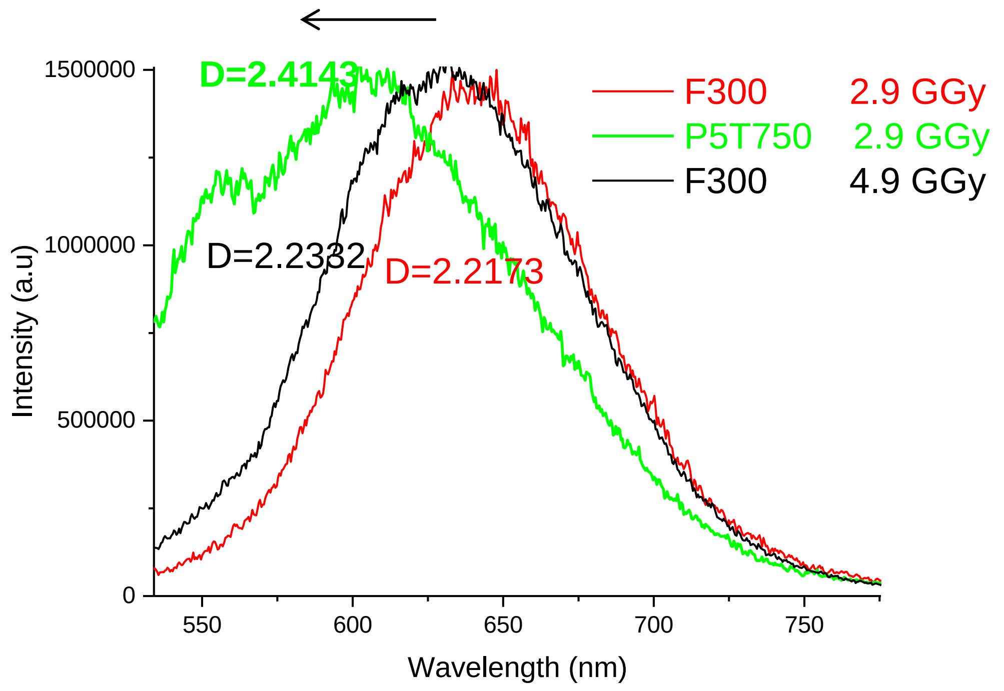

Ollier et al. JNCS 2017

In densified silica :shift and different FWHM of the band

Effect of densification on NBOHC species distribution

Impact on EPR line shape (E' center)

- Broadening : high concentration dipolar effect : or/and densification ?

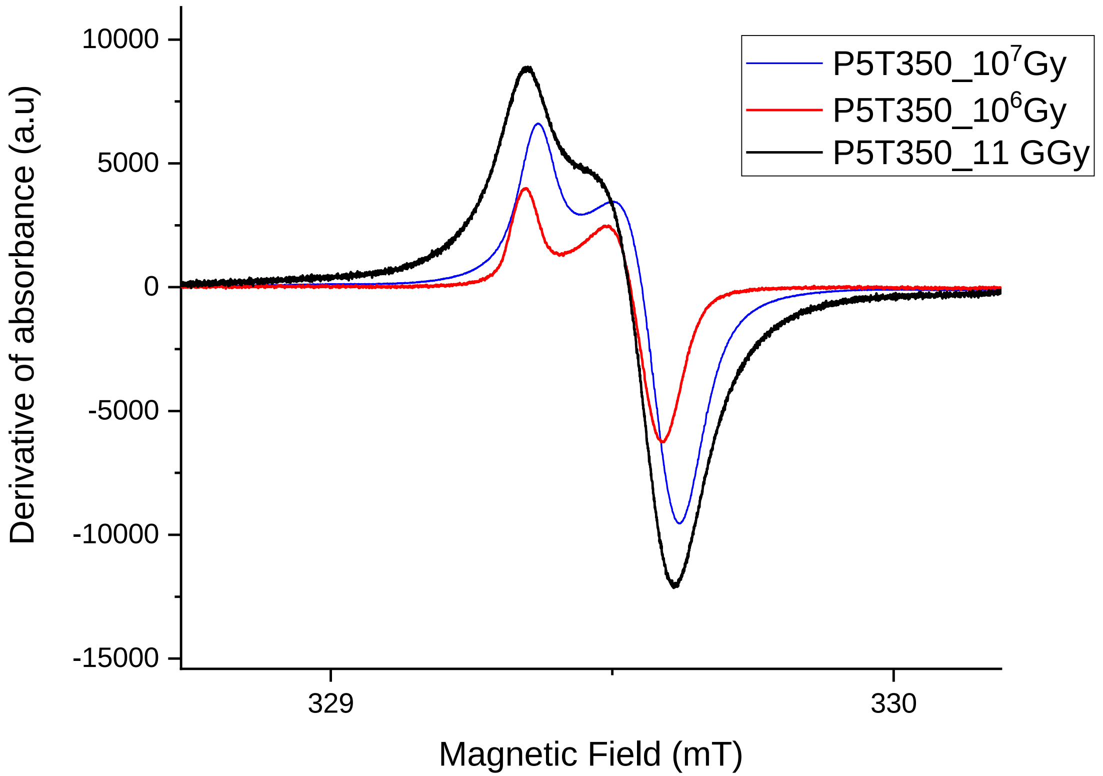

Discussion: Type I densification mechanisms

Type I

Isotropic index change

$\Delta n = 20\% \, \Delta n_D + 80\% \, \Delta n_V$

~~T_f change only?~~

~~Defects accumulation only?~~

What can cause the densification?

Densification level is ~3%

Similar to electron irradiated silica

Type I has lower thermal stability than T_f [4]

Type I has higher thermal stability then metamict-like silica [5]

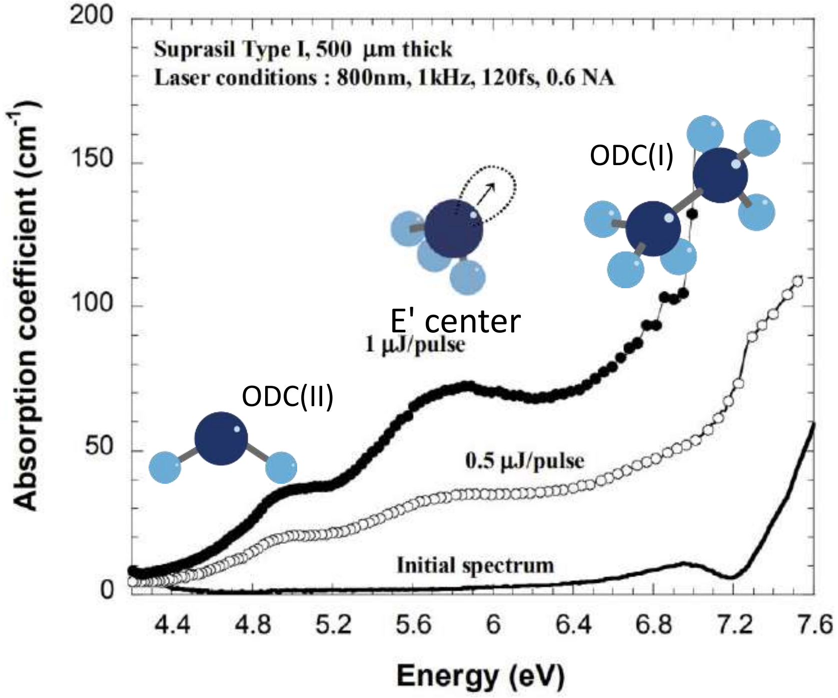

UV-VUV absorption [1]

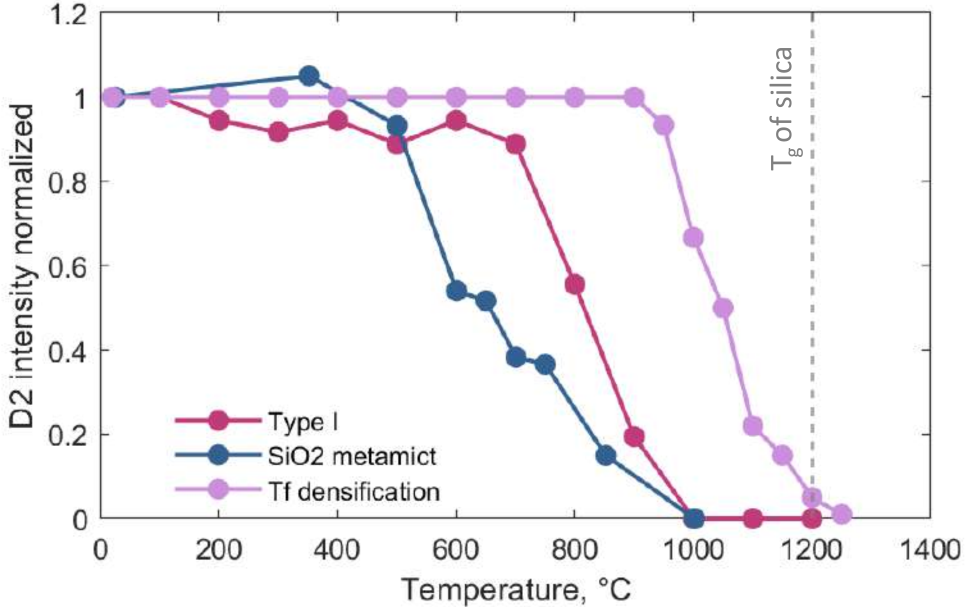

Isochronal annealing

[4] D.Grobnic et al. *Meas. Sci. Technol*. 17 (2006)
[5] M. Mobasher et al., *J. Non-Cryst. Solids* 597 (2022)

Also NBOHC, peroxy radicals [1,2,3]...

[1] M. Lancry et al. *Opt. Mater. Express* 2.12 (2012)
[2] H.-B. Sun et al., J. Phys. Chem. B 104.15 (2000)
[3] H. Hosono et al., Nucl. Instrum. Methods Phys. Res. B 191 (2002)

Defects accumulation and thermal effects ✓

Irradiation

Accélérateur d'électrons SIRIUS, LSI (réseau EMIR)

NEC, type Pelletron

Energie Electrons

150 keV – 2.5 MeV (qq mm^3)

Température

20 K – 623 K

Petit 2020

Vanadium is one of the most investigated element among the transition metals as it can be incorporated in phosphate glasses with a large percent with three possible oxidation forms (trivalent, tetravalent, and the pentavalent states). The addition of Vanadium leads to the formation of glasses with interesting semi-conducting and magnetic properties [36].
The addition of transition metals leads to the appearance of new absorption bands after irradiation, which are characteristics for each transition metals [37]. The response of the glass to radiation depends primarily on the type and concentration of these dopants (or impurities). One should also mention that some ions could be photoionized during the irradiation whereas others could change their oxidation states more indirectly. According to [21], a decrease in the electro-negativity of the ions leads to an increased tendency toward photo-oxidation. For example, Möncke reported that V4+ in fluoride phosphate glasses could be photo-oxidized to the empty valence shell d0 ion while Co2+, Mn2+, and Fe2+ were all photo-oxidized to the trivalent state when irradiating the glasses with an excimer laser in the UV range [21]. Mn2+ was reported in [21] to be more easily photo-oxidized than Fe2+, and all three, including Co2+, were found to be more easily photo-oxidized than Ni2+. Ni2+ and Ti4+ were reported to be photo-reduced. Similar results were reported in [38] that a larger amount of defects can be formed in phosphate and fluorophosphate glasses when adding Co2+ or Ni2+, the Co2+ having a stronger impact on the defects formation. The radiation photo-oxidizes Co2+ to (Co2+)+ and photo-reduces Ni2+ to (Ni2+)- in phosphate glasses. These defects replace partially the intrinsic

Yb^{2+} stability: importance of in situ measurements

Ex situ measurements

No apparent reduction of Yb^{3+} after irradiation in sample 3 by EPR

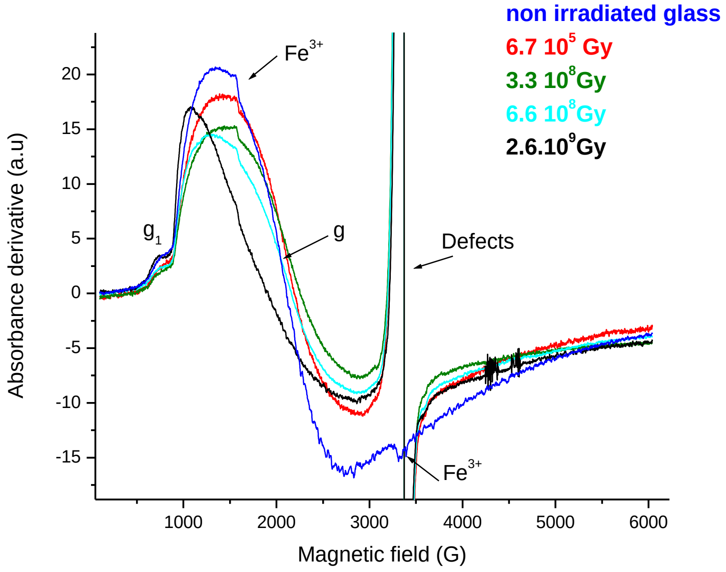

Ollier et al NIMB 2008

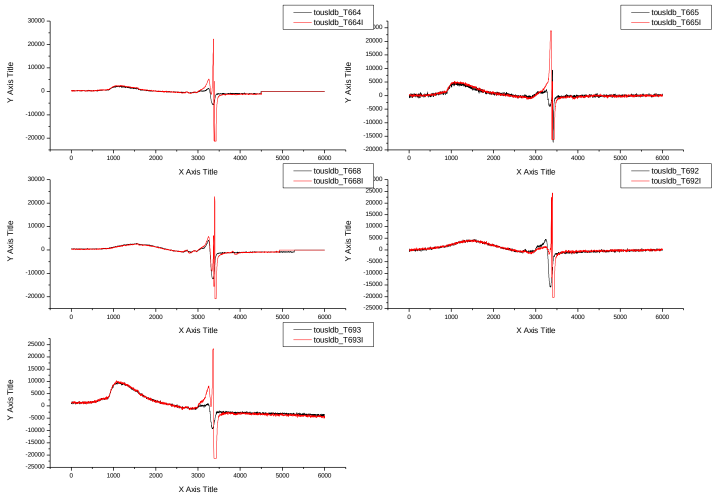

No Yb^{2+} emission was detected under 355 nm excitation in samples 2 and 3

AlOHC/Yb affinity

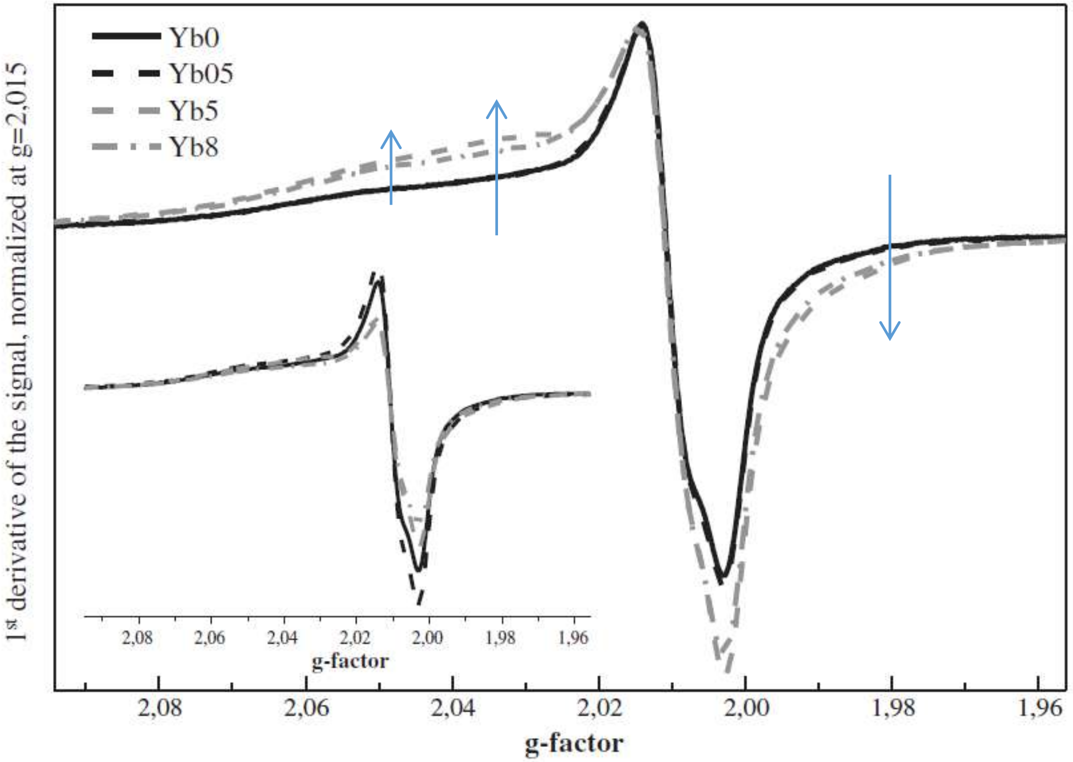

Pukhkaya et al JNCS 2013

Increase of AlOHC with Yb content in AS glasses

Environnement des ions Yb^{3+} par RPE continue

Préformes (MCVD, DRAKA) avec Al/P variable compris entre 0.3 et 2.8 et Yb: 0.1%

Yb^{3+} ion paramagnétique $4f^{13}$ (S'=1/2), RPE en Bande X , à basse température

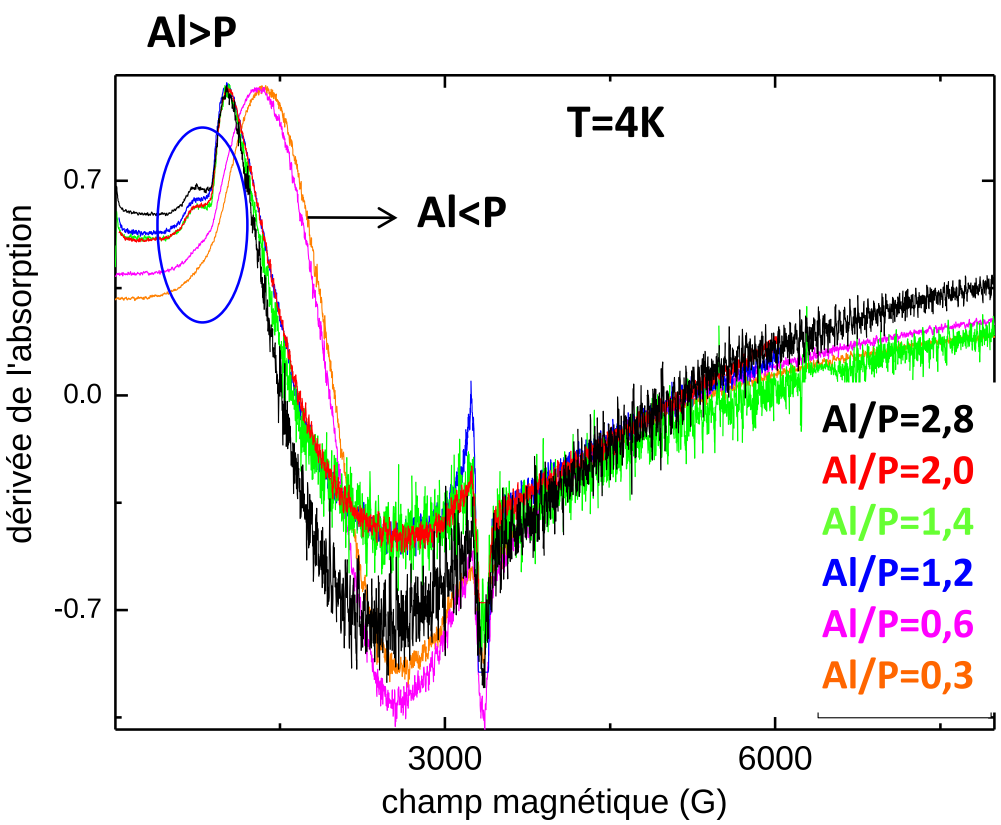

^{27}Al	I=5/2
^{31}P	I=1/2

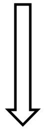

RPE pulsée: interaction hyperfine

2 environnements Yb^{3+} différents contrôlés par le rapport Al/P
symétrie du site et présence de clusters

THE JOURNAL OF CHEMICAL PHYSICS 136, 014503 (2012)

Clusters dissolution of Yb^{3+} in codoped SiO_2-Al_2O_3-P_2O_5 glass fiber and its relevance to photodarkening

T. Deschamps,[1,a)] N. Ollier,[1] H. Vezin,[2] and C. Gonnet[3]

Coll. H. Vezin (LASIR)

HYSCORE (Hyperfine Sublevel Correlation) 3500 G

Al/P=2,8

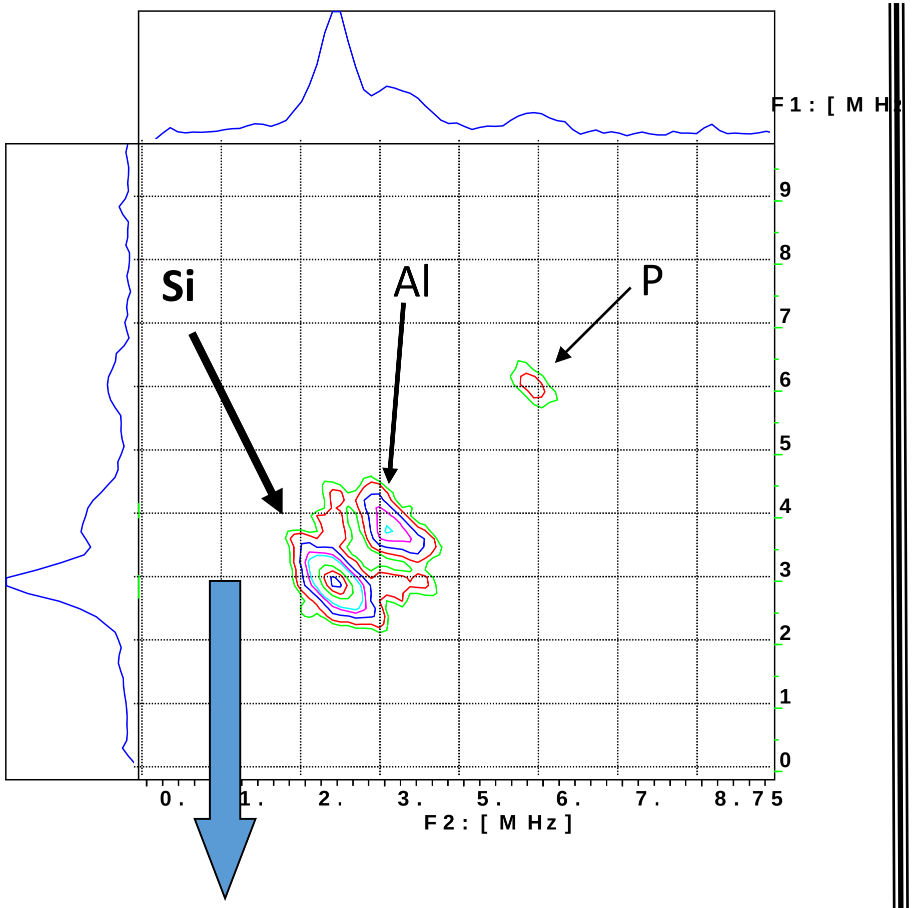

Al>P : Yb^{3+} proche de Si et Al
Tache de Si: présence de clusters ?

Al/P=0,3

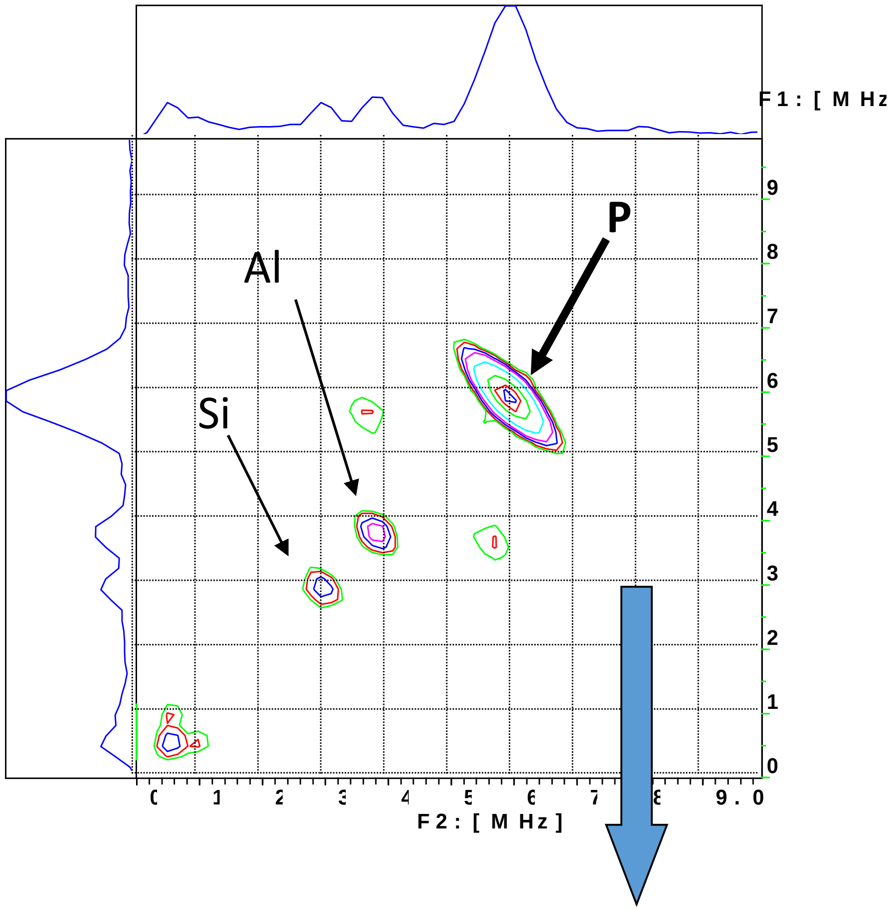

P>Al : sphère de solvatation P

Saitoh et al J. Phys Chem B 2006

Clusters d'Yb

Projections des spectres HYSCORE

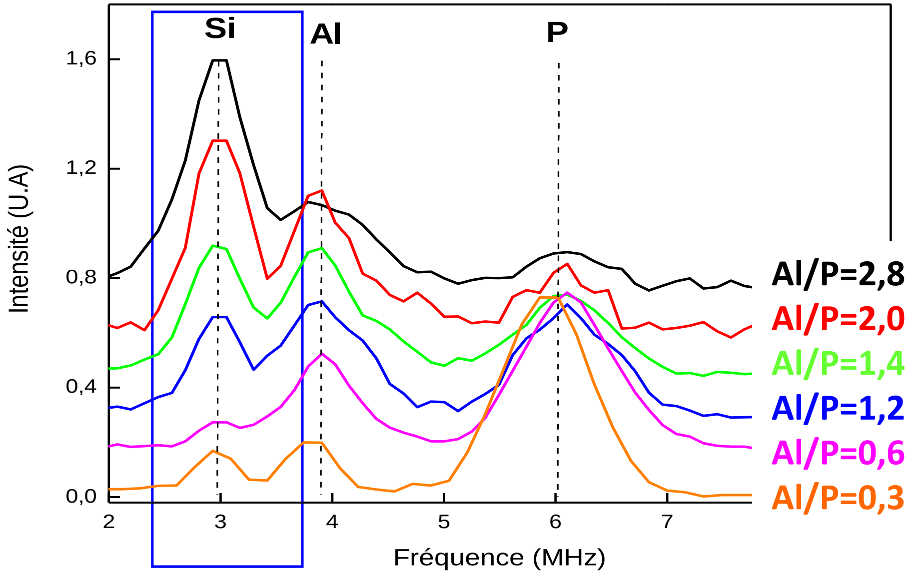

Photoluminescence (exc. à 980 nm)

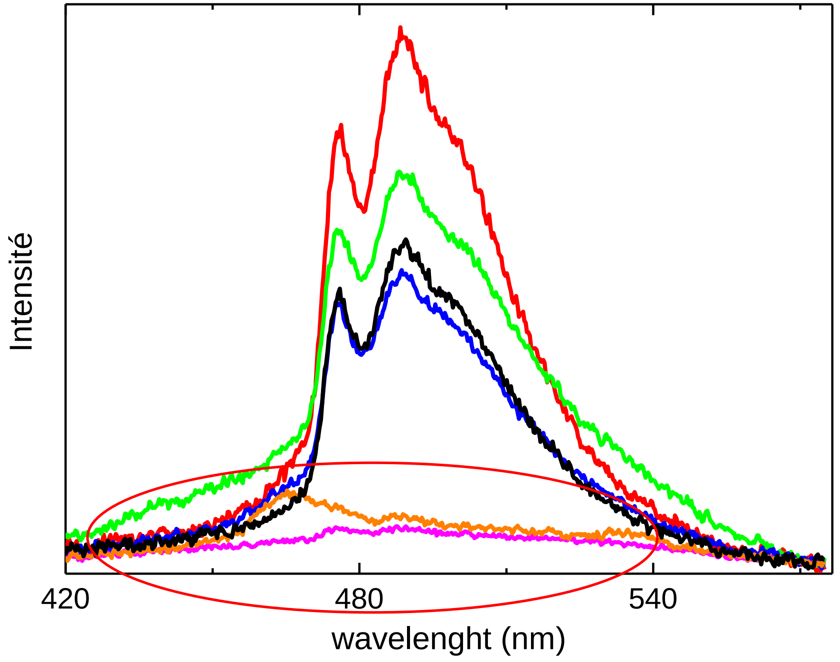

Nombre de clusters diminue lorsque Al/P<1

- Al/P conditionne l'environnement des ions Yb^{3+} et leur répartition avec dissolution efficace des clusters pour P/Al >1

- **P plus efficace que Al pour dissoudre les ions Yb^{3+}**

  Brevet FR 1100359

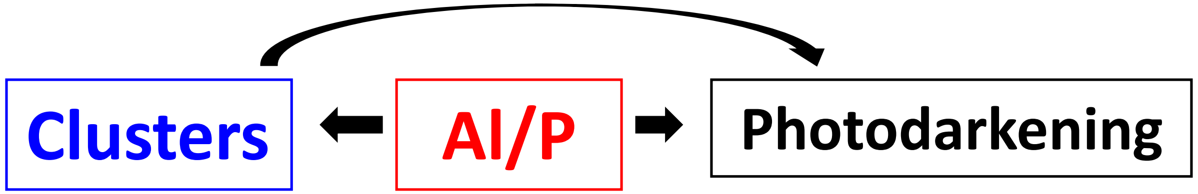

Luminescence coopérative

désexcitation simultanée de paires Yb^{3+}

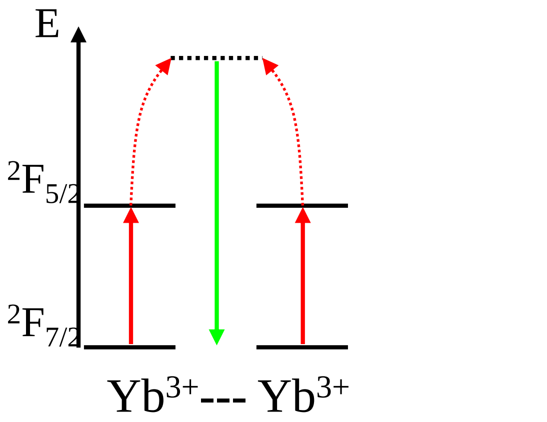

Context

Yb-doped aluminosilicate glasses

Optical applications

- Effect on Yb-clusters *N. Ollier et al. JNCS **357** (2011) 1037-1043*
- Induce of point defects
- Effect on glass structure (doses >10^9 Gy)

Yb^{3+} ions $4f^{13}$ configuration

- Absence of non-radiative quenching
- Possible to achieve high power of emission
- Emission wavelength is ~1 μm

- Phenomenon of clustering

Ionizing irradiation

Limit of applications

Limit of solubility

Limit of emission intensity

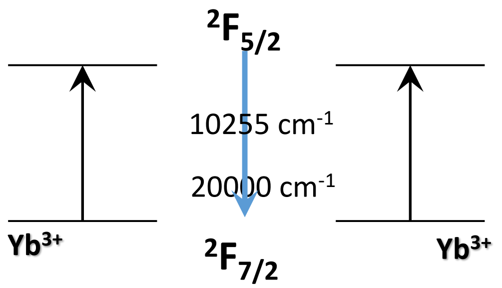

Glass structure characterization: Raman and NMR

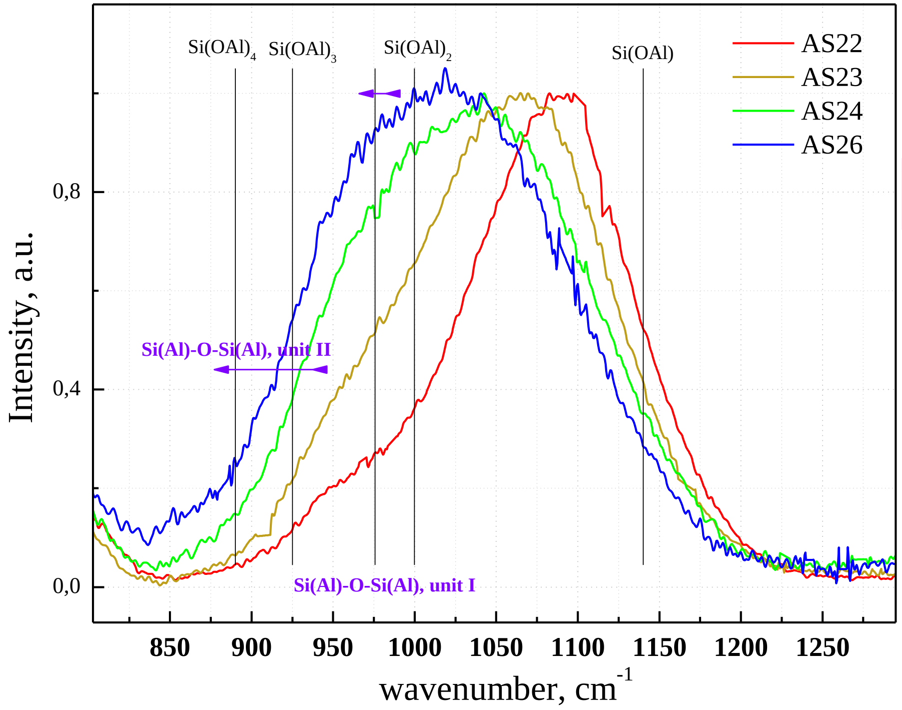

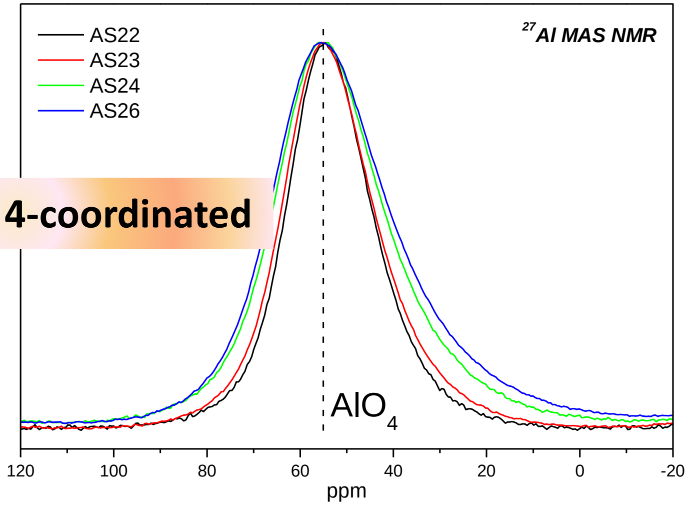

Al^{3+} ions are 4-coordinated

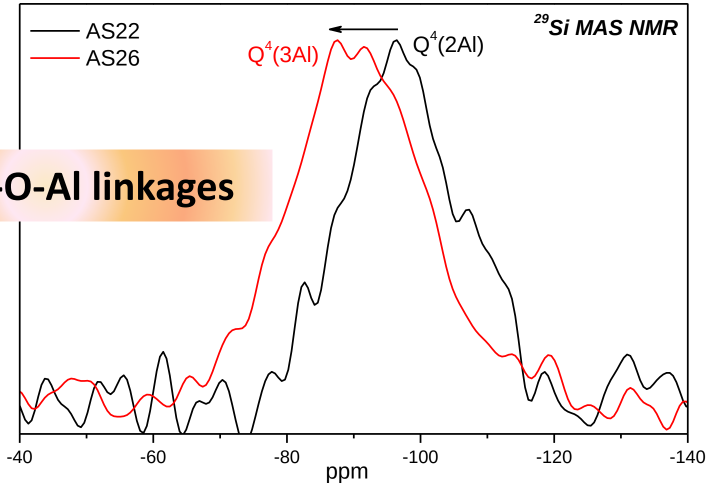

more Si-O-Al linkages

Al is a network-former ion, ASI increase tends to polymerize glass network more→less Non-Bridging Oxygens (NBO)

LADIR, Paris VI

Collaboration with Thibault Charpentier
CEA, Saclay

Samples

cooperative luminescence of Yb^{3+}

Aluminosilicate glasses from dissertation of B. Schaudel PhD (2000)
In collaboration with Ph. Goldner and A. Ferrier (LCMCP ENSCP).

	Sample name	SiO_2, % mol.	Al_2O_3, % mol.	Na_2O, % mol.	ASI Al/Na	
no Yb-clusters	***AS22***	**74**	**6**	20	0.3	+ 5% mass. Yb_2O_3
	AS23	**68**	**12**	20	0.6	
Yb-clusters	***AS24***	**62**	**18**	20	0.9	
	AS26	**58**	**22**	20	1.1	
	AS24_0	62	18	20		
	AS24_005					+ 0.05% mass. Yb_2O_3
	AS24_02					+ 0.2% mass. Yb_2O_3
	AS24_05					+ 0.5% mass. Yb_2O_3
	AS24_1					+ 1% mass. Yb_2O_3
	AS24_8					+ 8% mass. Yb_2O_3
	AS22_0	74	6	20		

gamma

For example, the cross-section for the production of the 472 keV Compton electron from the 661 keV gamma particle is about 10^{-26} cm^2. To compare this with the cross-section for the electrons, it can be multiplied by the Z of the target atom, but, even then the total cross-section for this process is 10^{-5} to 10^{-6} times the electron ionization cross-section (which is $\sim 10^{-19}$ to 10^{-20} cm^2) and 1

Furthermore, gamma particles can also cause atomic displacement, but, because the atoms are significantly heavier than electrons, the displacement cross-sections are substantially smaller than Compton scattering cross-sections. In addition, the energy transfer during such collisions is very small. For instance, Si, Na and O can receive a maximum energy of about 33, 40 and 58 eV from a 661 keV gamma particle. This is just barely more than the typical atomic displacement energies (20–30 eV).

Electron irradiation, 2.5 MeV, 25 MGy/h, 35°C (LSI, SIRIUS)

10^9 Gy en 24h

NEC Pelletron Accelerator

HC defects

Silicate with alkali

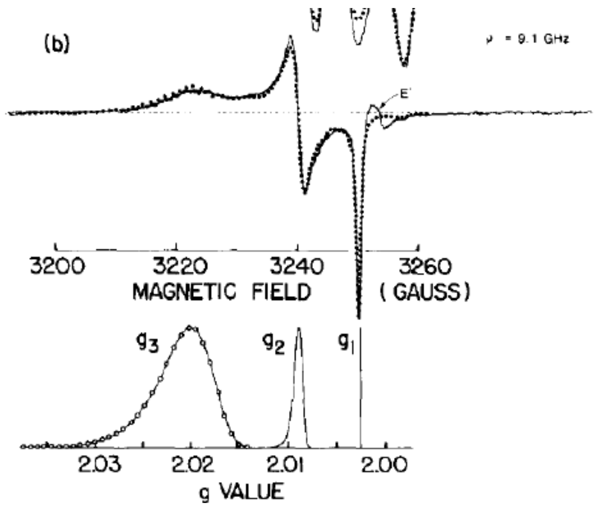

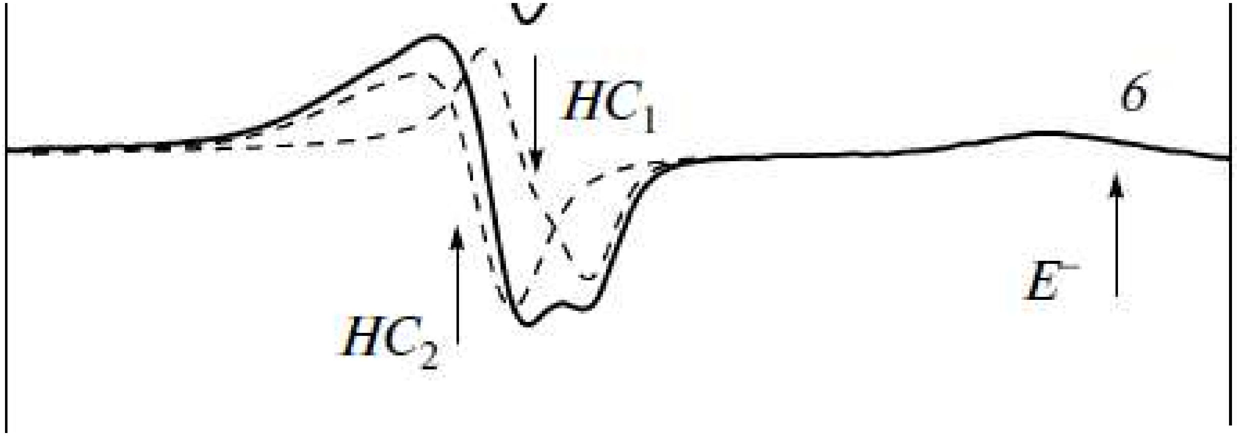

PHYSICS OF THE SOLID STATE Vol. 54 No. 9 2012

Parameter		HC_1	HC_2
$\langle g_1 \rangle$ a)		2.0026	2.0118
$\langle g_2 \rangle$ a)		2.0088	2.0127
$\langle g_3 \rangle$ a)		2.0213	2.0158
$\lvert A_1(^{29}Si) \rvert$	(G)	14.4	17.8
$\lvert A_2(^{29}Si) \rvert$	(G)	14.4	16.8
$\lvert A_3(^{29}Si) \rvert$	(G)	13	20
$A_{\parallel}(^{17}O)$ b)	(G)	−114	–
$A_{\perp}(^{17}O)$ b)	(G)	+12	–
ΔH_{pp}(Lorentzian)	(G)	0.4	c)
Measurement temp.	(°C)	+150	−30

D.L. Griscom / ESR studies of trapped hole centers

HC2

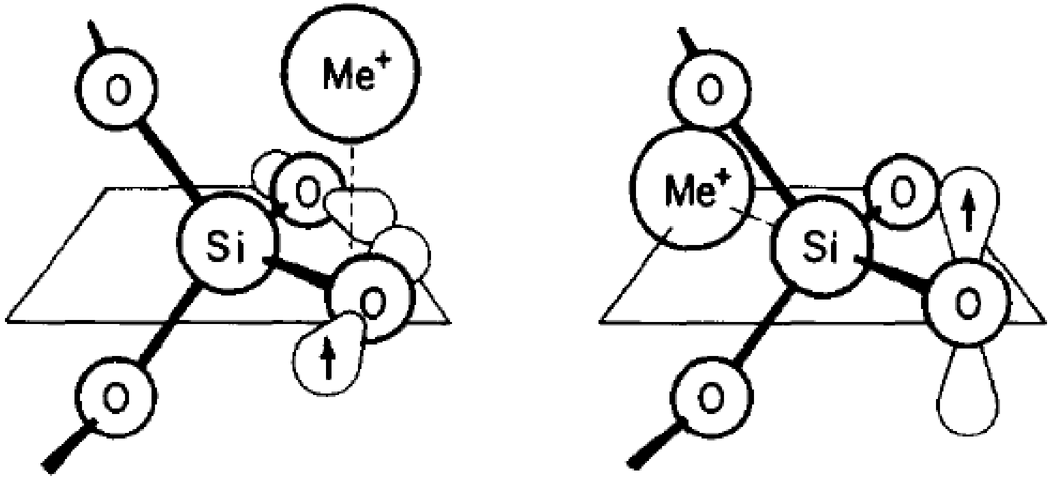

D.L. Griscom / ESR studies of trapped hole centers

HC1

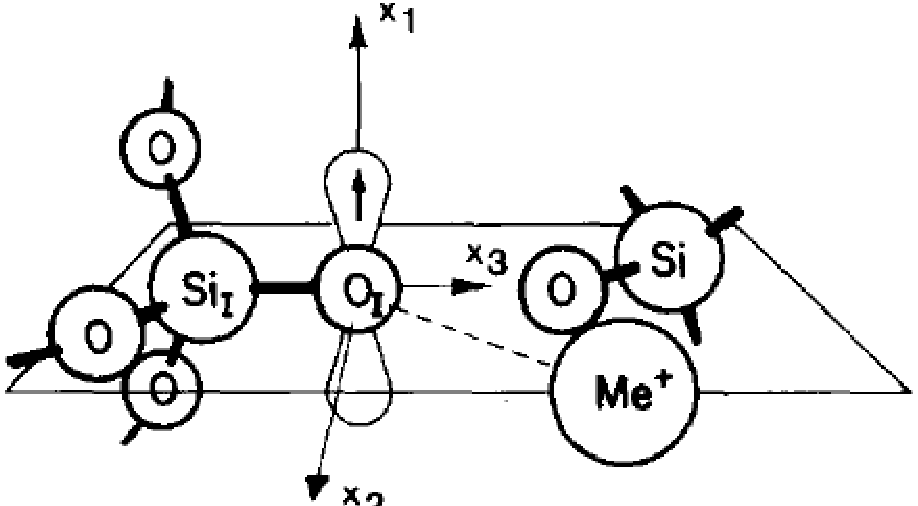

AlOHC

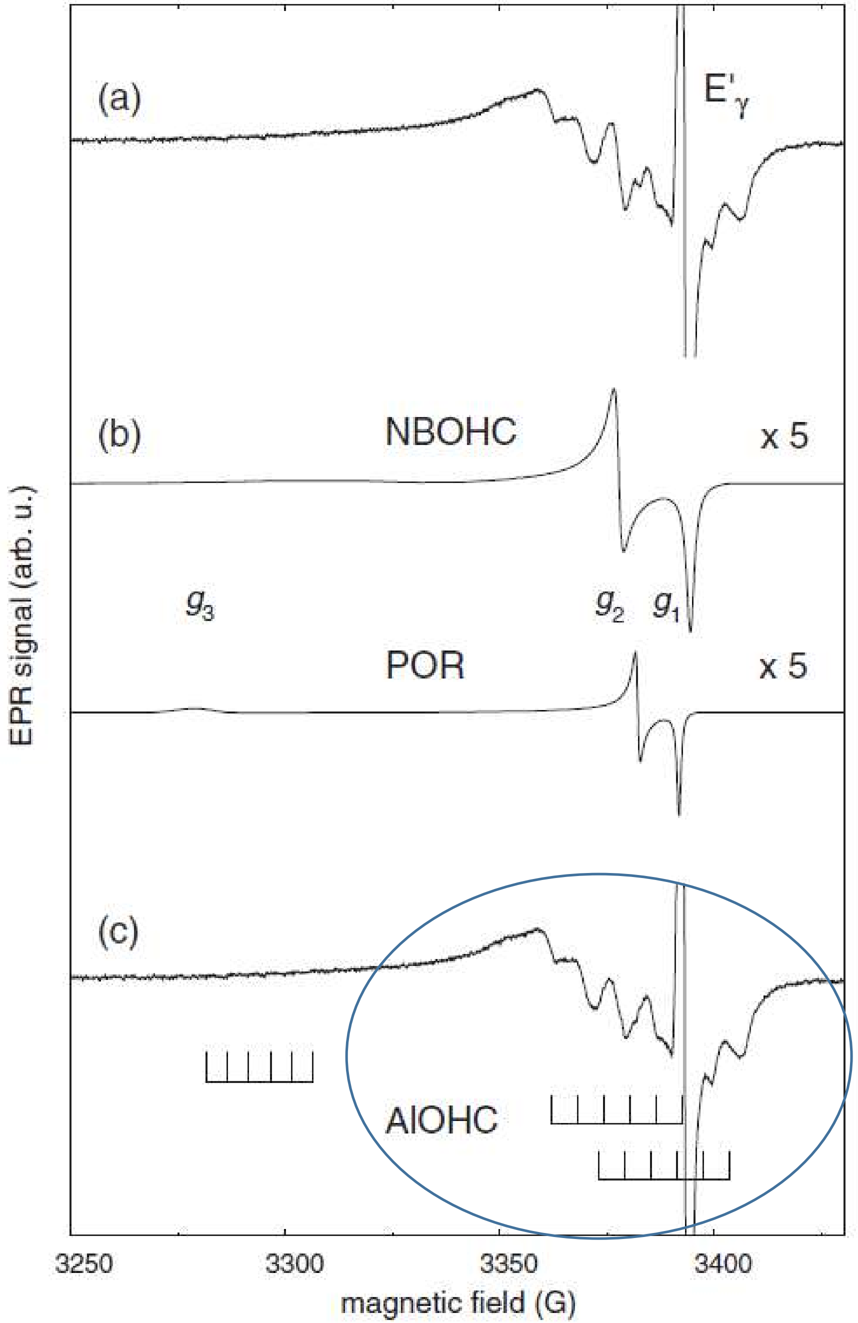

structure